Scattering Properties of Polyacrylamide Gels and Their Relation to Protein Electrophoretic Migration

by

Laurel A. Cook

Submitted to the
Department of Nuclear Engineering
in partial fulfillment of the requirements for the degrees of

Master of Science in Nuclear Engineering
and
Bachelor of Science in Physics

at the
MASSACHUSETTS INSTITUTE OF TECHNOLOGY
May 1994

Author .....
Department of Nuclear Engineering
May 18, 1994

Certified by .....
S. H. Chen, Thesis Supervisor
Professor of Nuclear Engineering

Accepted by .....
Aron M. Bernstein
Chairman, Undergraduate Thesis Committee

Accepted by .....
Allan Henry
Chairman, Committee on Graduate Students

Science

Scattering Properties of Polyacrylamide Gels and Their Relation to Protein Electrophoretic Migration

by

Laurel A. Cook

Submitted to the Department of Nuclear Engineering
on May 18, 1994, in partial fulfillment of the
requirements for the degrees of
Master of Science in Nuclear Engineering
and
Bachelor of Science in Physics

Abstract

The development of sodium sodecyl sulphate polyacrylamide gel electrophoresis (SDS-PAGE) is outlined to demonstrate the flexibility and importance of this technique to biomedical analysis. This development shows that there exists a surprising lack of knowledge surrounding the gel medium structure and exact mechanisms which allow SDS-PAGE to perform as well as it does. Electrophoresis with standard protein markers was performed on many polyacrylamide gels of differing polymer (T) and crosslinker (C) concentrations. The gels were characterized according to their electrophoretic performance in order to gain an intuitive knowledge for the electrophoretic technique. Small angle x-ray scattering (SAXS) was employed to measure an effective correlation length ξ' which described the effects of varying polymer (T) and crosslinker (C) concentrations on the effective pore size of the gels. The effective pore size relations developed from ξ' of the SAXS experiment were found to be consistant with the trends in gel performance during electrophoresis. This demonstrates the usefulness of SAXS in revealing structural information about the mechanisms of SDS-PAGE electrophoresis

Thesis Supervisor: S. H. Chen
Title: Professor of Nuclear Engineering

Acknowledgments

I wish to thank Professor Sow-Hsin Chen for acting as my supervisor and guiding me through my research experience at MIT. Special thanks goes to J. Kirsch for his personal support and sound advice on scientific and academic matters during the last four years.

I want to extend my personal gratitude to Jamie Ku and Daniel Lee for their support and advice during the last two years. Finally, I want to express my gratitude to the faculty and staff in the MIT Physics and Nuclear Engineering Departments who worked diligently with me to make this thesis possible.

Contents

List of Figures

List of Tables

Chapter 1

Historical Development of Electrophoresis

1.1 Background

Electrophoresis is one of the most important and extensively used methods in biochemical analysis today. It is a powerful tool capable of protein separation, molecular weight determination, and peptide mapping; all of which have contributed greatly to the determination of biological structures. The development of electrophoresis is spread out over nearly a century and is not the product of any one single development. Rather, electrophoresis is a technique which is continually expanding in influence and application.

Electrophoresis refers to a process by which a charged particle moves under the influence of an electric field. This travel may occur in a medium of which the most commonly used are solutions and gels. When traveling at constant velocity within a solution, a particle balances the frictional force of the medium f with an electrophoretic driving force. This electrophoretic driving force is the product of the effective charge on the particle Q and the potential gradient V. In a free solution the motion of the charged particle obeys Stoke's law such that

$$f = 6\pi r v \eta = QV \tag{1.1}$$

where r is the radius of the particle moving through a medium of viscosity η, with velocity v. In contrast, charged particles traveling in gels do not strictly obey Stoke's law because the frictional force itself is dependent on factors such as gel density and particle size.[2]

The electrophoretic mobility of a particular molecule in a medium under the influence of a potential gradient V is dependent on the particle's migration velocity, and is given by

$$m = d/tV \tag{1.2}$$

where m is the electrophoretic mobility of the molecule, d is the distance traveled by the molecule, and t is the time the potential gradient was applied to the gel. It is the differences in the mobilities of particles which allow the separation of mixtures for analytical and preparative purposes.[30] Depending on the type of separation desired in an electrophoretic operation, a gel and potential gradient may be selected to get a particular electrophoretic mobility from a sample of molecules. The type of potential gradient must be carefully selected because of possible heating effects. The higher the potential gradient applied to an electrophoretic system, the more heat that will be distributed into the gel or solution medium. The consequential heating of the system can change the characteristics of the electrophoretic medium and alter the expected molecule migration results.

Other complications arise due to the types of buffering systems used during electrophoretic migration through a medium. The buffering systems are present to inhance the mobilities and resolutions of molecules migrating in the electrophoretic medium. The charged molecules undergoing electrophoresis will have different disassociation constants (pK values) dependent upon the pH of the buffering system surrounding them. Thus, pH will affect the mobilities of samples. Another characteristics which will affect the mobilities of the samples is the ionic strength. The ionic strength of a buffering system determines the electrokinetic potential in which the sample molecules migrate. The ionic strength screens the net charge of the medium presenting a different effective charge to the sample molecules.

It is found that the electrophoretic mobility of a molecule is inversely proportional to the square root of the ionic strength. Thus, the lower the ionic strength of the buffering system, the higher the rate of migration through the medium. In contrast, higher ionic strengths decrease the rates of migration, but increase the sharpness of zones in a separation. Although higher ionic strength buffers seem appealing as far as resolution is concerned, the increase of ions in the buffering system also increases its conductivity. Undesirable heating effects will occur at a lower potential gradient than would in a lower ionic strength gel/buffer system because of this increased conductivity. Consequently, a balance must be reached between the ionic strength and applied voltage of the gel/buffer system.

It is demonstrated that the way in which ions travel during electrophoresis is affected by many numerous factors including gel density, potential gradient applied, and buffering system characteristics. All these variables make electrophoresis a complicated procedure to manipulate. However, it is exactly these factors that make the electrophoretic method so adaptable. Variations of these elements and others make electrophoresis one of the most valuable techniques for separation processes in biomedical technologies.

1.2 Development of Moving Boundary and Zone Electrophoresis

There are two categories of electrophoresis, moving boundary and zone electrophoresis. Moving boundary electrophoresis is based on the premise that similar molecules have charge properties which are similar. Therefore, similar molecules will move together, and different molecules will move apart during electrophoresis causing boundaries between the regions of different molecules. The first successful attempt at developing an electrophoretic separation method for proteins was accomplished by Tiselius in 1937.[78]

Tiselius used a moving boundary technique in a solution medium. The technique allowed initial sharp boundaries to be formed[79, 78], and offered thermostatic con-

trol to reduce convectional boundary disturbances produced by heating effects of the applied voltage.[69, 85] The method also featured large electrode vessels with reversible electrodes and an optical system to follow the movement of the boundaries. Tiselius' method seemed promising, but realistically moving boundary electrophoresis required expensive, complicated equipment that made it impractical for use as a regular laboratory technique.

Zone electrophoresis makes use of charged particles' abilities to migrate in a solid or gel medium as separate zones dependent upon their individual characteristics.[70] Zone electrophoresis is much more approachable in the laboratory environment than is moving boundary electrophoresis. Zone electrophoresis is theoretically capable of completely separating all proteins with different characteristics, and the separating capabilities of zone electrophoresis have been studied in several different mediums (both solution and gel in nature).

Zone electrophoresis appeared on the scene in 1952 when two techniques were suggested[47, 46]. Neither of these methods produced the resolving power achieved by Tiselius' method, and it was not until 1955 that Smithies proposed a zone electrophoresis method with promising results. The technique had advantages over moving boundary electrophoresis such as "freedom from qualitatively important boundary anomalies"[73], possibilities of separating via electrophoresis discrete proteins as compared to regions of proteins, and adapting to smaller sample quantities. Smithies made use of a starch gel as a supporting medium[73] in contrast to Tiselius' solution based electrophoresis.

The starch gel combined the advantages of starch-grain methods with the convenience of staining detection from filter-paper electrophoresis. Conveniently, the starch gel method was not subject to the limitations of filter-paper electrophoresis caused by absorption effects and large widths in application of samples to the paper.[47] As a matter of fact, the starch gel had comparable if not improved resolving power over Tiselius' solution electrophoresis method if the sample were placed in a narrow enough zone, and also there was an increased sharpening of the bands due to the lower ionic strength of the starch gel buffering system. Most importantly, the samples separated

according not only to electrophoretic mobility, but also according to size. The gel medium allowed for greater resolution of different species as Smithies had hoped.

1.3 Polyacrylamide Gels Used as a Medium for Electrophoresis

The introduction of starch gels spawned experimentation with other types of gels as supporting mediums for zone electrophoresis. Although starch gels worked well to separate molecules according to size, they degraded while in contact with electrophoretic samples. Starch gels were also limited in the pore sizes available for electrophoresis. A different species of starch had to be used to get a gel with a different pore size. Another gel system which would be less interactive with the protein samples and which had an easier method for varying pore size (other than growing gel from different species) was extremely attractive.

In 1959, Raymond and Weintraub introduced polyacrylamide gel as a stable, versatile medium for zone electrophoresis. The gelling agent present in polyacrylamide gel was named Cyanogum and the gel was formed by the polymerization cross-link reaction between acrylamide and N,N'-methylenebisacrylamide (BIS). The best gel for electrophoresis was found to have a Cyanogum concentration of 3 to 5 percent in the presence of acid or alkaline buffers (0.3M to 0.01M). The gel itself was a clear, flexible, stable and insoluble in water[64]. Raymond and his colleagues continued to improve the method of polyacrylamide gel electrophoresis (PAGE). In 1960, Raymond and Wang found that polyacrylamide gels were superior to starch gels in their physical properties. The polyacrylamide gels could be prepared more easily than starch gels, and they provided better defined, reproducible patterns. In addition, recovery of protein samples from the polyacrylamide gels was easier than from starch gels.[65, 62]

In 1962 a polyacrylamide gel apparatus was produced by the E-C Apparatus Corporation of Swathmore, Pennsylvania[63]. This was the first vertical slab gel apparatus. This apparatus is shown in figure 1.1. The apparatus had a vertical gel cell attached to upper and lower buffer chambers, and there were water cooling

channels running along the wall of the gel chamber.[61]

Other groups also contributed significantly to the development of the PAGE method. In 1962, Chang *et al.* prepared a sample of soluble *Neurospora crassa* resolving twenty-five bands of the mutant strain in polyacrylamide gel. They initially tried filter-paper electrophoresis resolving only six to eight bands, and then starch gels resolving eighteen bands. Their work highlighted the advantages of polyacrylamide gels as an electrophoretic medium. Their ability to separate twenty-five bands also demonstrated the need for completely solubilized samples as a method for further resolution.[15] Increasing the number of sample constituents solubilized prior to electrophoresis, increased the number of constituents resolved by electrophoresis. Also, during this time, Davis and Ornstein contributed to the PAGE method through their development of improved buffer systems with better resolution capabilities.[20]

Pore size effects on electrophoretic mobility and on the separation of proteins were not investigated until 1962. Raymond and Nakamichi noticed that changes in the polymer concentration of polyacrylamide gels altered the locations and resolution of protein bands during electrophoresis. They theorized that these effects were due to the changes in pore size that are connected to the polymer concentration of the gels[63]. The next year, Hjerten proved that protein migration in polyacrylamide gels not only depended on the charge and molecular size of the protein, but also on the pore size of the gel[39]. Ornstein estimated the dependence of the effective pore size on gel concentration using a simple cubic lattice model. His findings predicted an average pore size of about 50 Angstroms for a gel with monomer concentration 7.5%. Ornstein then chose a sample of proteins (those outlined in table 1.1) and predicted that such a pore size would inhibit the passage of "fibrogen, β_1 lipo-protein (and perhaps the α_2 macroglobulin)."[56, 325] All the other proteins in the sample were predicted to travel with no more difficulty than they would if traveling in a solution-type medium. His expectations were corroborated and so pore size could be easily varied via the monomer conentration of the polyacrylamide gels. Polyacrylamide gels of various pore sizes were being prepared by varying the monomer concentration as soon as 1964[81].

From 1964 to 1966 PAGE applications grew to include discontinuous electrophoresis. Jovin *et al.* developed an apparatus suitable for preparative, temperature-regulated PAGE in a discontinuous buffer system[43]. The term preparative implies two features: resolution of a material within a specific load range, and convenient elution of fractionated components. Their apparatus fulfilled both of these requirements. Sample volume limits required samples of at least 1 mL in volume, and the mechanical stability of the gel column depended upon the adherence of the gel to the glass wall and upon the rigidity of the gel. Smithies modified the vertical slab gel apparatus to perform a similar kind of preparative, discontinuous electrophoresis[24, 74]. Smithies apparatus allowed for the recovery of up to seventy percent of the protein sample from the electrophoresis apparatus. During this two year period many other apparatuses were developed for use in polyacrylamide gel electrophoresis, and the PAGE method had many notable successes including use as a molecular sieve for intercellular particles.[40]

1.4 The Introduction of Sodium Dodecyl Sulphate into Polyacrylamide Gel Electrophoresis

Maizel was the first to use sodium dodecyl sulfate (SDS) in connection with polyacrylamide gel electrophoresis in 1966[49]. SDS is a negatively charged surfactant with a hydrophobic head group and a hydrophillic tail group. Maizel used SDS to disassociate the Adenoviruses he was studying[49]. The use of SDS was only briefly mentioned in the paper, but the presence of SDS in his sample preparation allowed him to produce electropharograms of quality equal to those obtained by more labor intensive manual sectioning processes. The impact of SDS disassociation on polyacrylamide gel electrophoresis did not become obvious until after 1970.

Higher resolution of normal serum proteins via PAGE techniques were apparent in 1967 due to the works of Raymond and Weintraub[64], and Davis and Ronstein[20]. Also, modifications to discontinuous electrophoresis protocols allowed for the use of 22 mm gels which are desirable for preparative electrophoresis[60]. Preparative

electrophoresis was modified to allow the loading of one gram samples of proteins (previous limitations for loading were 50 mg)[41]. During this period, in addition to new PAGE apparatuses being developed[23, 28, 84, 11], gel slicing[9, 32] and preservation[72] techniques were developed for polyacrylamide gels.

In 1967, through the earlier vertical PAGE work of Raymond and Weintraub[64], an important procedure for measuring the molecular weight of proteins based on the weights of known sample proteins from polyacrylamide gel electrophoresis was developed[87]. The ratio of the mobilities of known proteins in gels of two differing polymer concentrations to the log of their molecular weights were used to set up calibration curves[87]. From these calibration curves crude determinations of unknown proteins' molecular weights could be made. A year later, another method based on the same premise established molecular weight measurements with a precision of $\pm 4\%$[38]. This new method plotted "the molecular weights of well-known proteins against the slope of the line resulting from the log of the relative protein mobility *versus* the acrylamide gel concentration."[70, 228] These important methods were perfected and give accurate results[58, 10].

In 1967, an attempt was made to develop concentration-gradient gel electrophoresis, which would enable the separation of a full mixture of proteins as they gradually traveled through a gel of constantly varying pore size.[50] This work finally had its first success in 1968 when a pore-size gradient gel separated a sample of highly concentrated proteins into bands.[27] This success fathered the perfection of a pore-size gradient method which used a gradient of different concentration polyacrylamide gels ranging 5% to 20%.[71] Another variation in PAGE techniques led to the use of mixed acrylamide and agrose gels as mediums with even better resolutions than those obtained in pore-size gradient acrylamide gels.[66]

The use of SDS complexes in the disassociation of protein samples was again investigated in 1968 by Shapiro, Vinuela, and Maizel. They discovered that the molecular sizes of polypeptides could be estimated by the relative mobilities of their SDS-complexes on polyacrylamide gels. They developed an expedient method for electrophoresis; it was versatile but flawed.[68] However, they found an almost linear

relation between the mobilities of the proteins and their molecular weights with few deviations. These results were repeatable but not completely explained. Their results suggested "that SDS minimizes the native charge differences and that all proteins migrate as anions as the result of complex formation with SDS.'[40] The flaws were corrected by 1969, and the method was successful in estimating molecular weights with an accuracy of at "least 10%".[83] Further improvements in that same year increased accuracy to $\pm 6\%$.[26]

When Sodium dodecyl sulfate (SDS) is added to a protein sample, its hydrophobic head group binds to the protein molecule causing the protein to unfold. The hydrophillic tail group then allows the protein to be dissolved in water and become independent from the other proteins in the sample. The result is a fully soluble protein sample. The proteins now associated with the negatively charged SDS molecules will travel towards the positive electrode when an electric field is placed across a gel during electrophoresis. SDS allows for the complete separation of proteins according to their size, independent of their normal configurations and solubilities in water.[1] The SDS surfactant is one of the most powerful compounds in use in biochemical analysis, and the procedures it makes possible are strongly dependent on its disassociating abilities.

In 1972, the SDS-PAGE method had been corrected through the use of reducing agents to yield more accurate molecular weight determinations.[34] Earlier SDS-PAGE experiments had been done without regard for the reduction of the protein aggregates and had given false values for molecular weights[34] Also later in 1972, human serum was separated by SDS-PAGE resulting in the resolution of twice as many proteins as had been separated previously.[13] Molecular weight determinations on the human serum were validated by another research group[4], and confidence in the SDS-PAGE method grew.

SDS-PAGE grew from isolated use into a very widely popular laboratory tool within a couple of years. Parts of the SDS-PAGE method were modified and applied to other electrophoretic methods. Isoelectric focusing of SDS-solubilized protein samples was explored.[54] Optimal results were achieved when the sample protein in SDS

solution was dialyzed against a large excess of 10 M urea to remove as much of the SDS as possible prior to focusing. Low molecular weight (in the range 1,000 to 12,000 Daltons) SDS-solubilized protein samples were separated using an SDS-PAGE technique.

The SDS-PAGE method was nearly perfected by 1975. Modifications to the procedure included eliminating SDS from the gel and buffer solutions used during electrophoresis limiting its presence to that in the protein sample alone.[75] Results were comparable to those found in systems which contained SDS throughout the entire system. Another modification eliminated the need for staining the gel after electrophoresis by cooling it to 0-4° C in order to see the opaque (white) bands of protein.[82] Also, another technique which eliminated SDS in favor of sodium octylbenzene-*p*-sulphonate was developed,[80] but not widely used. SDS-PAGE remained limited, but it had become the most powerful protein separation method of the time.

1.5 Development of Two-dimensional Polyacrylamide Gel Electrophoresis Techniques

Two-dimensional gel electrophoresis developed as the demands placed on electrophoresis became greater. In samples containing a large number of different proteins (greater than 50), one dimensional SDS electrophoresis would yield separations with overlapping lines of similar molecular weight proteins.[70] Thus, the addition of a further separation based on some criterion other than molecular weight was desirable. The most advanced two-dimensional gel electrophoresis methods call for the initial separation of protein samples based on their isoelectric points, and then another separation based on their molecular weights.

The first steps toward two-dimensional electrophoresis in a polyacrylamide gel medium were taken by Margolis and Kenrick in 1969. They used a low concentration polyacrylamide gel to perform first discontinuous electrophoresis, and then gel gradient electrophoresis.[51] The separations achieved were only slightly better than those obtainable with one-dimensional SDS-PAGE. In 1970, researchers introduced a more

effective two-dimensional PAGE method for separating mixtures of ribosomes.[44] Although its uses were limited, it was widely used over the next five years.

1972 saw the introduction of a two-dimensional PAGE technique for the separation of complex RNA mixtures.[25] DeWachter and Fiers first performed a separation in an polyacrylamide acid gel containing a large concentration of urea; while the second stage was performed in a high concentration (20%) polyacrylamide gel buffered at pH 8. 1973 saw the development of another two-dimensional PAGE technique by Orrick *et al.* which was capable of separation of extracted rat liver into nearly one hundred proteins.[57] In 1974 the separation of ribosomal proteins was improved upon when DeWachter and Fiers modified their original two-dimensional PAGE technique. The first stage used a 4% polyacrylamide gel in 8M urea at pH 5 for the separation. The second stage was a molecular weight separation SDS-PAGE technique.[53] The results were improved over the previous method. In the same year, Orrick improved the separation of rat liver proteins by modifying the first dimension of his method to include the reduction of the polyacrylamide concentration from 10% to 6%. His second dimension was changed from a 8 - 10% linear gradient polyacrylamide gel to a homogeneous 8% polyacrylamide gel. Again the resolution of the proteins was improved.

A powerful two-dimensional method was introduced by O'Farrel[55] in 1975. The first dimensional separation was performed in isoelectric focusing gels, where proteins were separated according to their isoelectric points. The second dimension was SDS-PAGE molecular weight separation in discontinuous polyacrylamide gel. The method was effective enough to separate proteins that differed in charge carrying groups by a single charge, and also effective enough to separate proteins that consisted of only 10^{-4} to 10^{-5} present in both dimensions.

1976 brought the development by Lambin *et al.* of an SDS-PAGE method suitable for the measurement of high molecular weight proteins. SDS-PAGE was performed on polyacrylamide gels with concentrations in the 20% to 30% range. The molecules were in the weight range of 10,000 to 1,000,000 Daltons and were separated with good resolution. 1977 witnessed the development of a micro-gel-electrophoresis technique

capable of analyzing protein levels as low as 10^{-9}g in a PAGE system.[18] This enabled the use of micro-samples for molecular weight analysis. Previous micro-gel systems in capillary tubes had required tedious handling with low resolution and reproducibility. The new micro-gel technique had resolution comparable to that of tube gels, with completion of gel preparation, electrophoresis, staining, and destaining of the sample in under six hours. SDS could be used with the system, and densiometry could be performed on the system using existing equipment.

O'Farrel's technique greatly increased the popularity of two-dimensional SDS-PAGE because with very few modifications it became useful in many different situations. As a matter of fact, O'Farrel's technique was in use less than one year after it was published. Modifications allowed the separation of *Escherichia coli* and *Salmonella typhimurium* cell envelopes. In addition, the procedure was modified to separate plasma membrane proteins from HeLa cells[29] and analyze the non-histone chromosomal proteins of HeLa cells.[59] Many rare (less than 10,000 copies per cell) components were detected in the cytoplasm which had not been previously observed. Subsequently, SDS was added to the sample preparation which increased the reproducibility and enhanced the patterns obtainable from the O'Farrel technique.[85] Further modifications used ultracentrifugation of the gel during the second dimension to reduce clogging at the top of the isoelectric focusing gel.

In 1979 a differential two-dimensional PAGE technique was developed for peptide mapping of heterogeneous protein samples.[12] Denatured and reduced proteins were separated on a SDS-polyacrylamide gel slab in the first stage. The second stage submitted each separated protein to partial proteolysis thus resolving them into a characteristic pattern of peptides via a stacking technique. As many as twenty proteins could be analyzed at once using this technique. From 1980 to 1982, double isotope labeling using ^{3}H and ^{14}C began developing[16] as well as the use of the minislab apparatus.[19]

In 1984, Hodges and Hirata[42] demonstrated that heating the protein samples in the SDS buffer prior to performing electrophoresis hydrolyzed the peptide backbone of the proteins. Many more spots are resolved in the gel when the samples

are hydrolyzed prior to electrophoresis. These spots have a greater intensity after the gel is silver stained. Similarly, Cleveland *et al.* found an increased intensity in protease electrophoretic samples after partial hydrolysis of the samples.[17] Unfortunately, Rittenhouse and Marcus[67] showed that "heating polypeptides to 110° C in SDS buffer prior to electrophoresis preferentially cleaved the aspartyl-protyl peptide bond."[70, 245] Even though Rittenhouse and Marcus performed their analysis on fructose-1,6-bisphosphatase, the cleavage mechanism resulted in discernibly different PAGE patterns than the patterns produced by non-hydrolyzed protein samples containing no aspartyl-prolyl peptide bonds. The success of hydrolysis in the protein sample preparation found by Hodges and Hirata or Cleveland may be due to this cleavage.

In 1983 Tijssen and Kurstak developed a method for simultaneous peptide mapping from proteins in a mixture via a two-dimensional SDS-PAGE technique.[77] The inconsistencies in previous[12, 48] peptide mapping methods inspired this work. First, they separated the peptides by SDS-PAGE. Second, they embedded a strip of the SDS-PAGE gel in the stacking component of a second gel system which is loaded with proteolyitc enzymes. This technique may be performed in a modified Laemmli[77] gel system as well. It has the advantages of good resolution without isotope labeling, elimination of purification steps (and the associated losses) and no special two-dimensional equipment needed.

1.6 Electrophoresis Today

More recently people have returned to look at the exact mechanisms which allow SDS-PAGE to function as it does. Guo (1991)[35] studied the structure of SDS-protein complexes in solution using small angle neutron scattering (SANS). He concluded that the structure had the form of a "polymer like object consisting of micelle-like SDS clusters formed along the flexible unfolded polypeptide chain." He then drew an analogy between the reptation theory applied to electrophoresis of charged polymers in gels, reformulating the theory of mobility of protein-SDS complexes in SDS-PAGE.

Guo successfully described the experimental mobility-molecular weight relationship for the migration of standard proteins in SDS-PAGE.

SDS-PAGE continues in development today, but it is by far one of the most widely used tools in the biomedical field. It is now well established in basic protocols. This work began with Tiselius' success with an electrophoretic separation in 1937. It benefitted greatly with the introduction of polyacrylamide gel as an electrophoretic medium (Raymond and Weintraub) in 1959. Finally, with Maziel's introduction of SDS for protein denaturing in 1966, the basics of the modern SDS-PAGE technique was developed.

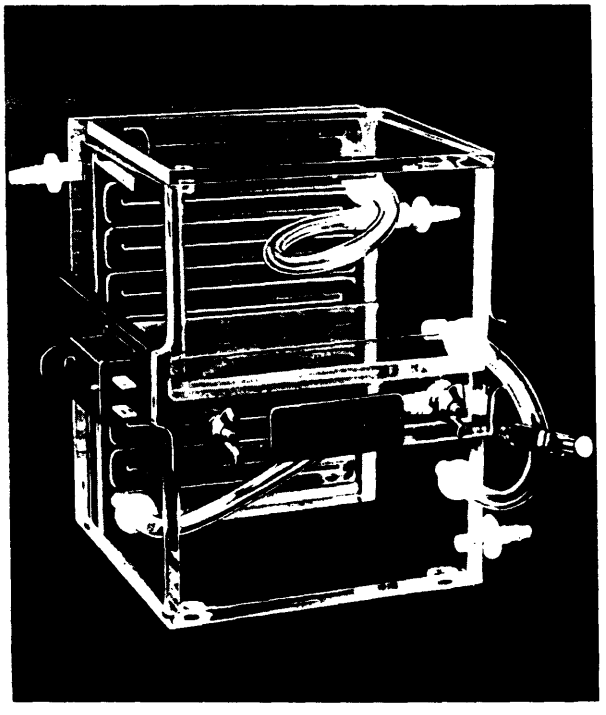

Figure 1-1: Electrophoresis apparatus produced by the E-C Apparatus Corporation of Swathmore, PA in 1962.

Protein	Mobility, m_w	Molecular weight	Length	Diameter
Albumin	−6.1	69,000	150	38
Transferrin	−3.3	90,000	190	37
β_1 lipoprotein	−3.0 (approx.)	1,300,000	185	185
γ globulin	−1.0 (approx.)	156,000	235	44
Fibrinogen	−2.1	400,000	700	38
α_2 macroglobulin	−4.2	850,000	—	—

* Data from Oncley[17] and Schultz.[18] m_w in mobility units, length and diameter in Angstrom units. 1 mobility unit = 10^{-5} cm.^{2}/volt-sec. Approximate mobilities for 0°C.

Table 1.1: Proteins used by Ornstein to demonstrate how pore size in polyacrylamide gels may be tailored to the dimensions of the molecule which will be separated.

Chapter 2

Characterization of Polyacrylamide Gels via Electrophoresis

2.1 Background

2.1.1 T%, C%, and Pore Size of Polyacrylamide Gels

The polyacrylamide gel is formed through the vinyl polymerization of acrylamide monomers (CH_2=CH-CO-NH_2) into polyacrylamide chains with the inclusion of crosslinking chains of bisacrylamide (CH_2=CH-CO-NH-CH_2-NH-CO-CH=CH_2) to form a three dimensional network as shown in figure 2.1.[3, 6] There are two concentrations which characterize a polyacrylamide gel; they are termed T% and C%. T is the percentage weight of total monomer (acrylamide and bisacrylamide) per 100 ml of water (i.e. weight per volume percent). C is the weight of crosslinker (bisacrylamide) divided by the total weight of monomer (acrylamide plus bisacrylamide). The concentration of acrylamide in the gel determines the average polymer chain length while the bisacrylamide concentration determines the extent of crosslinking in the gel. Therefore, the T% and C% concentrations are important in determining gel characteristics such as gel density, mechanical strength, elasticity, and pore size.

By varying the T% and C% of a gel, the characteristics of the gel medium used in electrophoresis may be adjusted to give better resolution. When a particle is passing through a gel medium, it is hindered in its passage by its size relative to the pore size of the gel. This sieving effect is in addition to the charge effects the particle will experience in the potential gradient applied during electrophoresis. The relation of pore size to the concentrations of gel constituents has been studied through gel chromatography experiments by Fawcett and Morris (1966). They found that with a fixed proportion of bisacrylamide (fixed C) "the pore size varied inversely with and approximately linearly to the total monomer concentration T."[3, 7] These results pointed toward a minimum pore diameter for a fixed T with C equal to about 5%. Later work has demonstrated that for T values higher than 15%, the value of C required for minimum pore diameter is influenced by the value of T itself.[52, 33, 14]

Due to pore size effects and their relation to T and C concentrations in a gel medium, electrophoresis for a particular sample will proceed differently in gels with differing T and C concentrations. The electrophoresis results for a particular protein sample in different T% and C% gels may or may not resolve all constituents of the sample. The band patterns of a broad range of different molecular weight protein must be explored in order to determine T% and C% ranges which are useful as gel mediums for electrophoresis.

2.1.2 Discontinuous Gel Electrophoresis (Laemmli Method)

The most widely used method for discontinuous gel electrophoresis is that of Laemmli (1970). This procedure involves the denaturing of the protein samples with sodium dodecyl sulphate (SDS). SDS is present in the buffering system as well as in the protein samples themselves. The Laemmli procedure is designated as a discontinuous electrophoresis method because of its buffering system. A discontinuous buffer system uses buffers of different pH and composition to create a discontinuous pH, and thus a voltage gradient within the gel. The discontinuous gel system has the advantage that it concentrates the proteins in a sample into a narrow band; therefore, dilute samples may be used in discontinuous electrophoresis.

The sample passes first through a stacking gel that has a large pore size (usually a monomer concentration near T=5%). The stacking gel buffer contains chloride ions that act as leading ions during electrophoresis. The stacking buffer also contains glycine ions that act as trailing ions during electrophoresis. The chloride ions have a higher mobility in the gel than do the sample proteins, while the glycine ions have a lower mobility in the gel than do the sample proteins. The leading ion leaves a zone of reduced conductivity between itself and the trailing ion. The higher voltage gradient in the zone between the ions allows the sample proteins to travel faster and stack together into a narrow band between the zones of ions.

After the sample proteins pass through the stacking gel, they enter the resolving or separating gel. The resolving gel has a smaller pore size (monomer concentrations usually between 7.5% and 20%), a higher pH, and a higher salt concentration than does the stacking gel. The glycine ions migrate past the sample proteins in the resolving gel. The presence of a denaturing agent (about 0.1/SDS) in the resolving gel allows the proteins to be separated according to their molecular weight. If there is no denaturing agent present, the sample proteins are separated according to molecular size, shape, and charge.

2.2 Sample Preparation

The protocols for making the gels were modified versions of the standard Laemmli protocols with discontinuous buffer system for minigel apparatus published in the 1991 book of *Current Protocols in Immunology.*[31] Sample preparation for polyacrylamide stacking and resolving gels involved the making of several stock solutions. The acrylamide, N,N'-methylenebisacrylamide (BIS), tetraethylenediamine (TEMED), and ammonium persulfate (APS) used in the sample preparations were all of electrophoresis purity, while all other chemicals were of analytical grade.

The following stock solutions of acrylamide/bisacrylamide were made: T=40% with differing crosslinking concentrations of (a) C=1.25%, (b) C=2.5%, (c) C=5.0%, and (d) C=10%. Also made were solutions of 4 $\times$ Tris $\cdot$ Cl/SDS, pH 6.8 solution (0.5

M Tris · Cl containing 0.4% SDS); and 4 × Tris · Cl/SDS, pH 8.8 solution (1.5 M Tris · Cl containing 0.4% SDS). All stock solutions were filtered through a 0.45-μm filter and stored at 4 ° C.

Each gel was cast using a Protean II minigel casting stand (BIO-RAD) with glass plates separated by 0.75 mm spacers. First, the separating gel solution was prepared according to the recipies outlined in Table 2.1. Prior to the addition of the accelerator (APS) and the initiator (TEMED), the solutions were degassed under vacuum. After the solutions were degassed, APS and TEMED were added. The solutions were gently swirled, and pipetted into the glass plate sandwich to a height of ~11 cm. A small layer of deionized water was placed on top of the separating gel to speed polymerization. Polymerization was complete within 30 minutes, and the separating gel was then rinsed briefly with deionized water to wash off any unpolymerized solution which may have remained on the surface of the gel.

The stacking gel was then prepared according to the directions in Table 2.1. Again the solution was degassed prior to the addition of APS and TEMED. The stacking gel solution was then pipetted on top of the separating gel until its level was about 1 cm below the top of the glass plate sandwich. A 0.75-mm Teflon comb was then inserted into the layer of stacking gel solution, with care taken not to trap any air bubbles under the comb teeth. The stacking gel polymerized within 45 minutes.

After the stacking gel had polymerized, the comb was carefully removed and the gel wells were washed with deionized water to remove unpolymerized acrylamide solution. The gel sandwiches were then attached to the upper buffer chamber and immersed in the lower buffer tank. The upper and lower buffer chambers were filled with 1 × SDS/electrophoresis buffer solution containing Tris base, 0.19 Molar glycine, and 3.47×10^{-3} Molar SDS with a pH of 8.3.

2.3 Electrophoresis

SDS-PAGE broad range molecular-weight standards (product number: 161-0317) were purchased from BIO-RAD. This standard protein sample contained a set of nine

pre-stained proteins with molecular weights ranging from 1600 Daltons to 205,000 Daltons. The specific proteins present in the sample are found in Table 2.2. These standards were denatured in SDS and found in such quantities to yield "bands of equal intensity on SDS polyacrylamide gels run according to Laemmli."[8, 7]

Eight μl of prestained (Coomassie blue) SDS-PAGE broad range molecular markers were placed into two of the wells in each sample gel. The cover was then placed on the electrophoresis apparatus and the electrodes were connected to a high voltage power supply. The high voltage was raised to 200 V. The gels remained at 200 V for 20 to 40 minutes until the protein markers had either achieved a good resolution in the gel, or it had been determined that the sample gel would not adequately resolve the protein marker bands.

The voltage was then lowered and turned off, and the upper gel chamber was removed from the apparatus. After the excess buffer solution was drained, the gels were rinsed in deionized water. The gels were then removed from the sandwiched plates by carefully sliding one of the spacers out from the edge of the glass plates and using it to lever the plates apart. With the gel sitting on one plate, a corner was sliced off to mark lane orientation for the electrophoresis run. The gel with the separated molecular markers was then placed in a solution of (fixing solution makeup-need to look this up too). The methacylic solution fixed the protein markers and allowed the gel to be stored in an air-tight plastic sleeve for mobility measurements.

2.4 Electrophoresis Results and Gel Characterization

The results of the electrophoresis runs are pictured in figure 2.2. The broad range markers were resolved to varying degrees in the different gels. When bands of proteins are clearly visible and distinct within the electrophoresed gel, accurate results may be expected from molecular weight determinations of sample proteins. The T=5% gels, for all cross-linking (C) concentrations, did not resolve any of the protein markers. These gels are suitable for use as stacking gels in electrophoresis because they allow

the entire protein sample to move together in a band. This property may enable the use of more dilute samples which may then be concentrated in a narrow band as it migrates through the T=5% gel. The resolution of the single band in the T=5% gels is narrower in the C=2.5% and C=5% gels than in the C=1.25% and C=10% gels. This indicates that the crosslinking concentrations of 2.5% and 5% are preferable to the other crosslinking concentrations for use in stacking gel.

In contrast to the T=5% gels, the T=10%, 15%, 20%, and 30% all resolved some of the protein bands. As mentioned before, the broad range molecular markers used in this electrophoresis were of weights ranging from 6,500 to 200,000 daltons. Table 2.3 contains information on the number of bands and molecular weight ranges visibly separated in each gel. Although the T=30% gels resolved 6 or 7 different proteins each, the distance over which the protein bands span in the gels was between 1.5 and 8 mm, as compared to a span of 13 to 47 mm in the other resolving gels. Also, the T=30% gels only resolved bands for proteins with molecular weights over 20,000 daltons. In this sense, the T=30% gels are not the most desirable gels for resolving proteins with molecular weights lower than 21,500 daltons, and they are not an ideal medium for molecular weight determination of unknown proteins because the electrophoresis will not be completed in a short time so that the gels will not degrade due to heating effects in the minigel apparatus. The T=30% gels may work well for molecular weight determinations in a larger water-cooled version of the electrophoresis apparatus used in this experiment.

All the other T=10%, 15%, and 20% gels resolved proteins of molecular weight greater than 21,500 daltons. In addition, (T=20%, C=1.25%), (T=15%, C=1.25%), and (T=15%, C=5%) resolved proteins down to 14,400 daltons, but by far the best resolution for the molecular markers used in the experiment was achieved in the (T=15%, C=2.5%) gel where all 9 proteins (down to molecular weight 6,500 daltons) were visibly resolved. These gels are therefore the T and C concentration which may be used to determine the molecular weight of an unknown weight sample protein because they offer resolution over a large range of possible molecular weights.

A gel will work well for molecular weight determination if in addition to good visual

resolution, the calibration curve from known protein markers is well defined within the gel. A general scaling relation connecting the protein mobility μ (or the relative mobility R_f) to molecular weight M_w can be derived. Assuming the polypeptide chain (protein) is only allowed to move along its own contour, one may develop a simple relation between mobility and molecular weight:

$$\mu = \frac{A}{M_w} \tag{2.1}$$

where the constant $A = (Q/3\xi)(g/d)$ depends only on the gel concentration. Q is the total effective charge of the protein-SDS complex, ξ is the frictional coefficient of the protein-SDS complex in the gel medium, g is a parameter dependent on the effective pore size of the gel or the gel concentration, and d is the distance migrated by the protein during electrophoresis.[35] It has been found that this relation is true only for intermediate gel concentrations using proteins with weights over 20,000 daltons. There are considerable deviations from the $\mu \sim M_w^{1.0}$ behavior in low and high gel concentrations. Only the high molecular weight proteins follow equation (2.1) and the resolution of separating low molecular weight proteins becomes poor. It has been concluded that as the gel concentration decreases, the effective pore size of the gel increases, and thus the assumption of no lateral movement during the migration of the SDS-protein complex becomes invalid. While in the low concentration range (near T=5%) gels the effective pore size causes deviations, in the high concentration range (T$\geq$15%) a relation of the form $\mu \sim M_w^{-a}$ in which a >1.0 depends on the gel concentration causes deviation. No theory for the high concentration deviations is available at this time. Therefore, the relation in equation (2.1) is only valid over a limited range of molecular weights near T=10%. At T=10%, a plot of the logarithm of the molecular weight versus the logarithm of the relative mobility may be used to calibrate the electrophoresed gel.[35] For a broader range of molecular weights and gel concentrations, a plot of the logarithm of the molecular weight versus the relative mobility of protein markers will yield a curve that may be used to determine the unknown molecular weights of sample proteins.[36] This is the standard protocol for

molecular weight determinations most used today.

Mobility of a protein in a gel is determined by

$$\mu = \frac{d}{tE} \tag{2.2}$$

where d is the distance traveled by the protein in time t, and E is the voltage difference between the two electrodes of the apparatus. For prestained protein standards such as were used in this experiment, the excess Commasie blue dye in the electrophoresed sample has a higher mobility than do the prestained proteins. Therefore, the dye will be the bottom most band in a column, and the relative mobility R_f of the proteins with respect to the dye may be determined by

$$R_f = \frac{\mu_{protein}}{\mu_{dye}} = \frac{d_{protein}}{d_{dye}} \tag{2.3}$$

where $\mu_{protein}$ and μ_{dye} are the mobilities of the protein and the dye respectively, and $d_{protein}$ and d_{dye} are the distances traveled by each. From this relation, the relative mobilities R_f of the resolved proteins in each sample gel were calculated.

To help determine the quality of each gel as a medium for electrophoresis, calibration curves were constructed and the χ^2 value for each curve was calculated. The χ^2 value for a curve fit to a data set is a measure of the "goodness of fit." χ^2 is the ratio of the estimated variance in the fitted curve s^2, to the parent variance of the experimental data σ^2.

$$\chi^2 = \frac{s^2}{\sigma^2} \tag{2.4}$$

If the curve adequately describes the data, the parent variance and the estimated variance should be the same, and the χ^2 value will be equal to 1. If the fitting function does not describe the data, then the deviations will be larger and the estimated variance s^2 will be too large, resulting in a χ^2 value that is larger than 1. If the χ^2 value is less than 1, it does not indicate an improvement in fit. Calculating a χ^2 less than one is simply a consequence of the fact that there exists an uncertainty in the determination of s^2. From this it is apparent that the best fit curve for the calibration

data will have a $\chi^2 \sim 1$. If a χ^2 of 1 is untenable for a curve and data set, then the best fit will be that which results in a χ^2 that is close to 1.

As mentioned before, a plot of the logarithm of the molecular weight versus the relative mobility of protein markers will give a calibration curve for a gel which is used to determine the molecular weight of an unknown protein. The calibration curves for the gels are shown in figure 2.3, and the χ^2 values for each fit are presented in table 2.4. It was not possible to calibrate the T=5% gels because they do not behave as resolving gels in this experiment. For determining the molecular weight of an unknown protein sample, the χ^2 values for the gel calibrations suggest that all of the T=10% and T=15% gels will work well. At first glance the T=30% gels would seem to have the best calibration curves overall, but because these gels do not spread the molecular markers over a very large distance, error in position of the unknown and the possibility for severe diffusion effects make molecular weight determination with the T=30% gels impractical in a mini-gel apparatus.. As for the T=20% gels, the χ^2 values imply that they may be useful but not as reliable as the T=10% and T=15% gels.

To sum up, the T=5% gels may be characterized as stacking gels because they do not resolve the molecular markers, but they do allow the protein sample to migrate into a narrow band so that dilute protein samples may be used. The T=30% gels have excellent calibration curves, but the mobilities of molecular markers in T=30% gels are not as easily measured as they are in other gels because of the narrow range which the markers migrate within the T=30% gel. The T=20% gels offer better range than the T=30% gels, but their resolutions and calibration curves are not as good as those found in the T=10% and T=15% gels. By far the best resolution, resolving protein markers from the full range of 6,500 to 200,000 daltons was the T=15%, C=2.5% gel which also had an excellent calibration curve with χ^2=1.09.

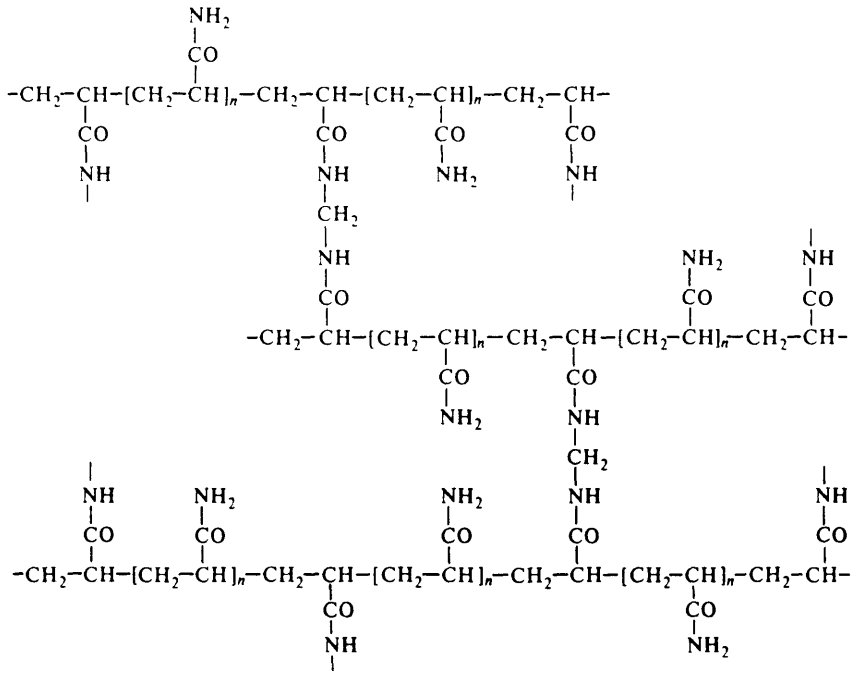

Figure 2-1: Structure of polyacrylamide gel matrix formed by copolymerization of acrylamide monomer and N,N'-methylenebisacrylamide cross-linking agent.

(a)

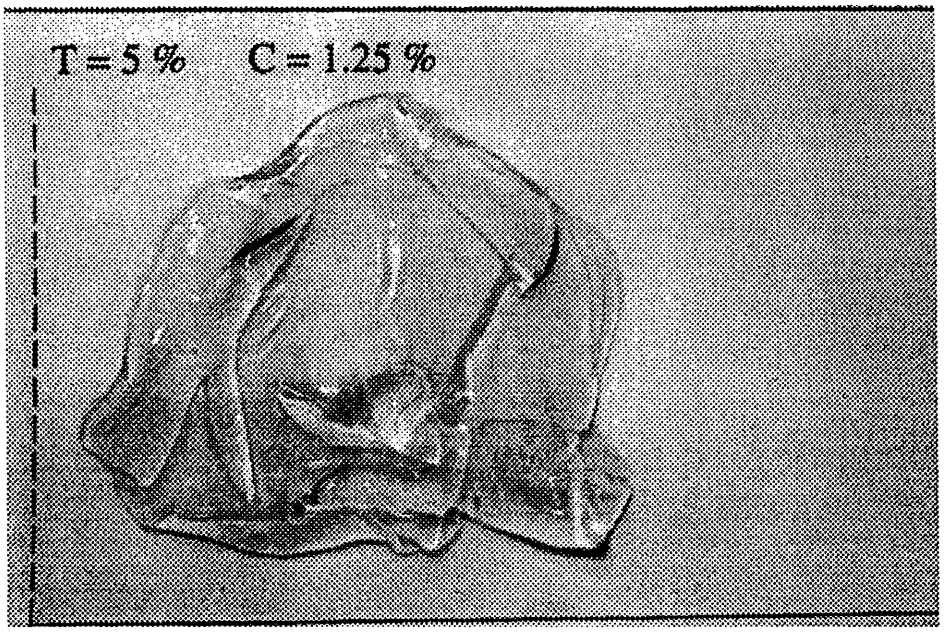

(b)

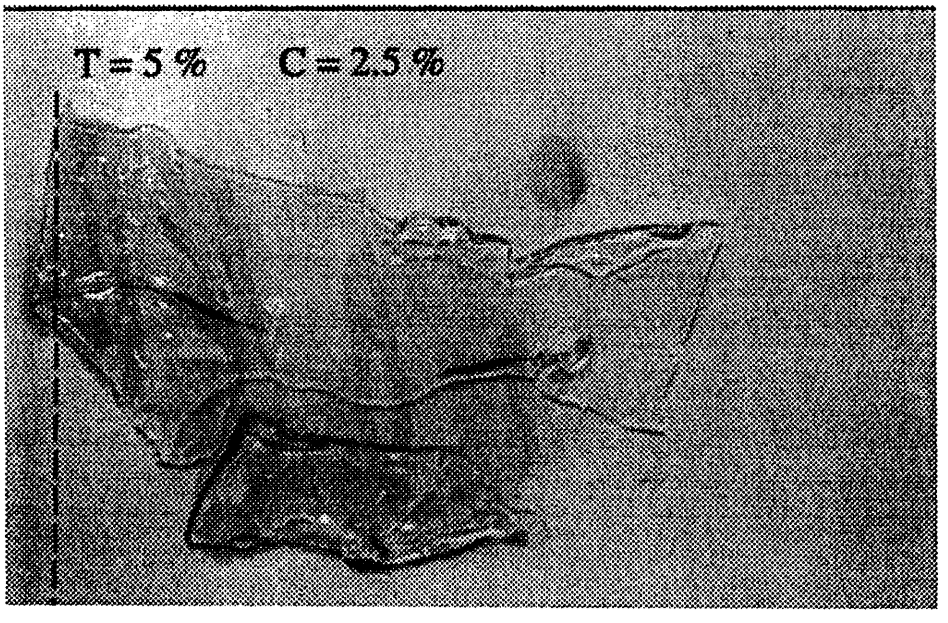

Figure 2-2: The electrophoresis gels that were run with molecular markers.

(c)

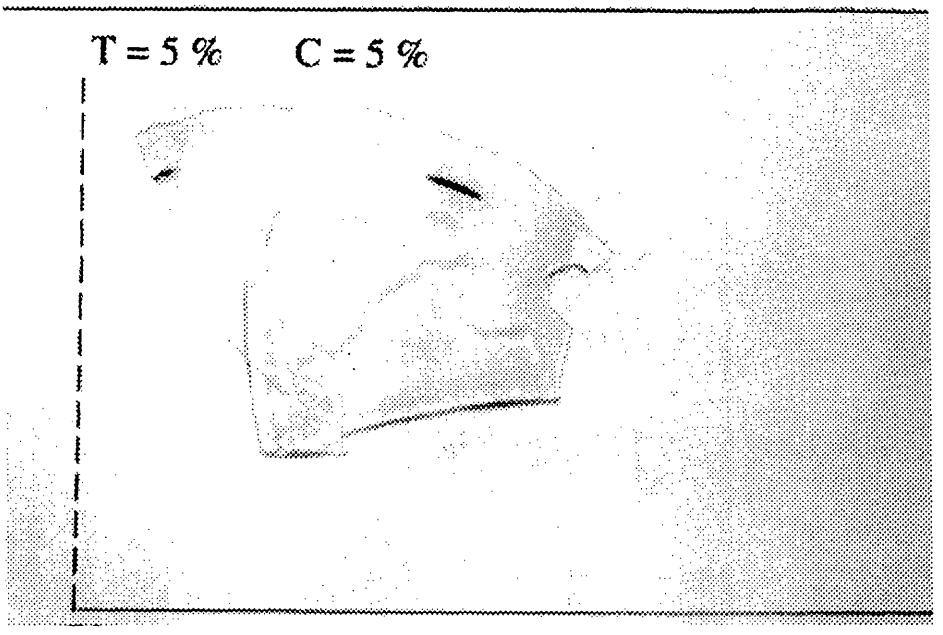

(d)

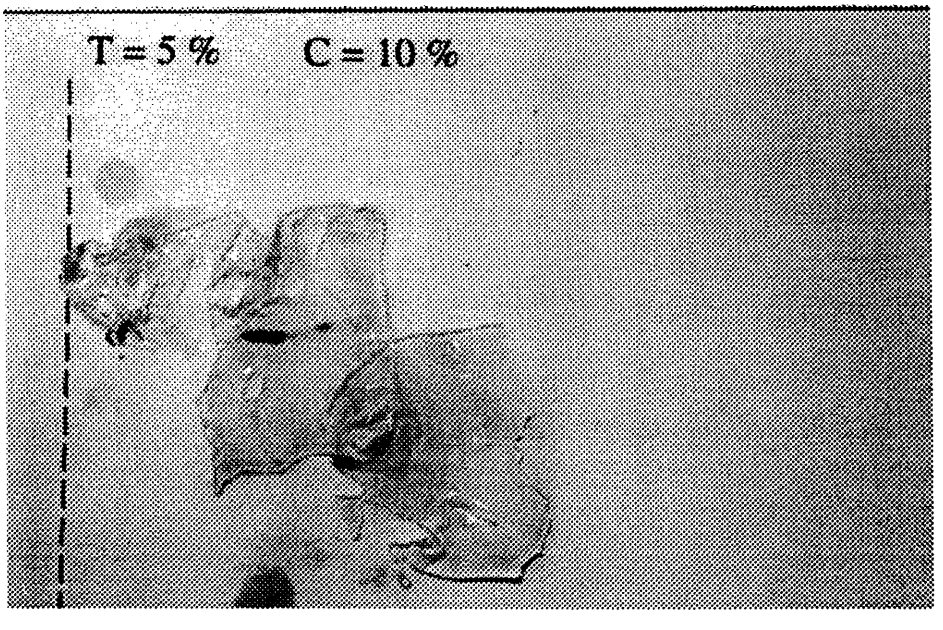

(e)

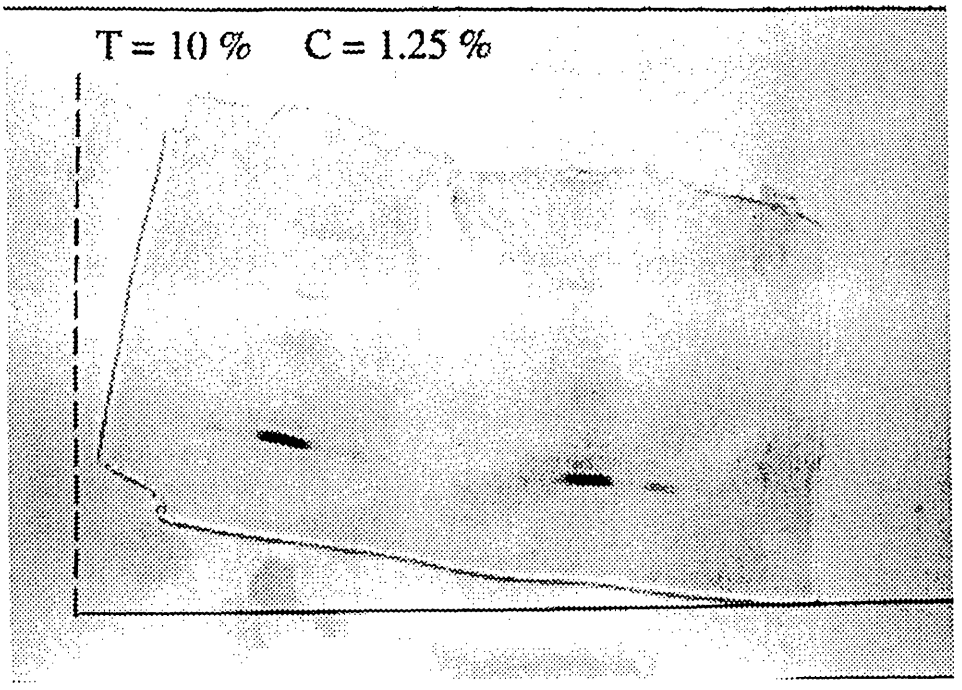

(f)

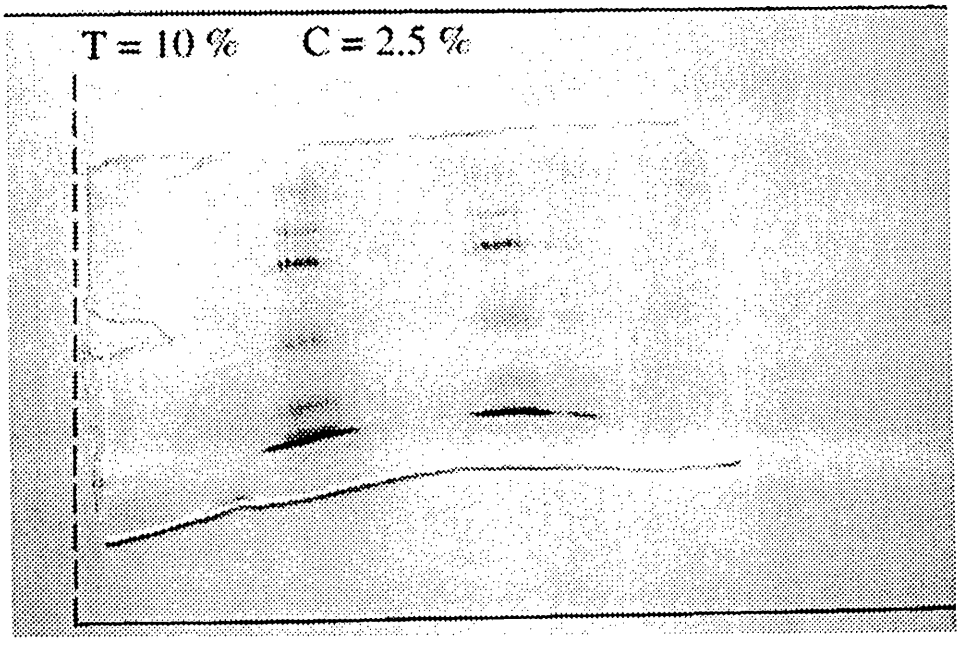

(g)

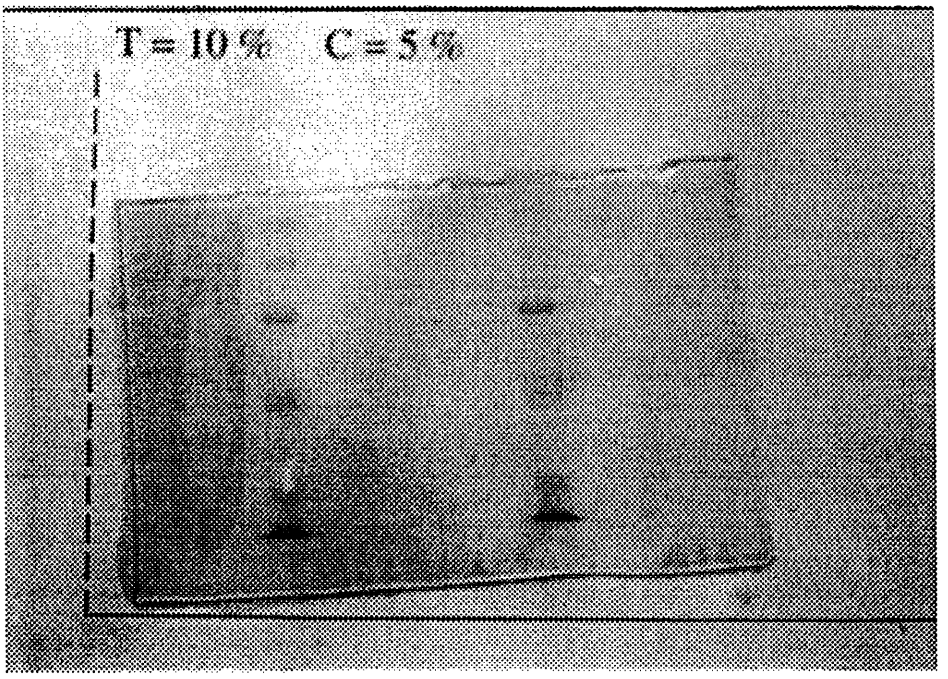

(h)

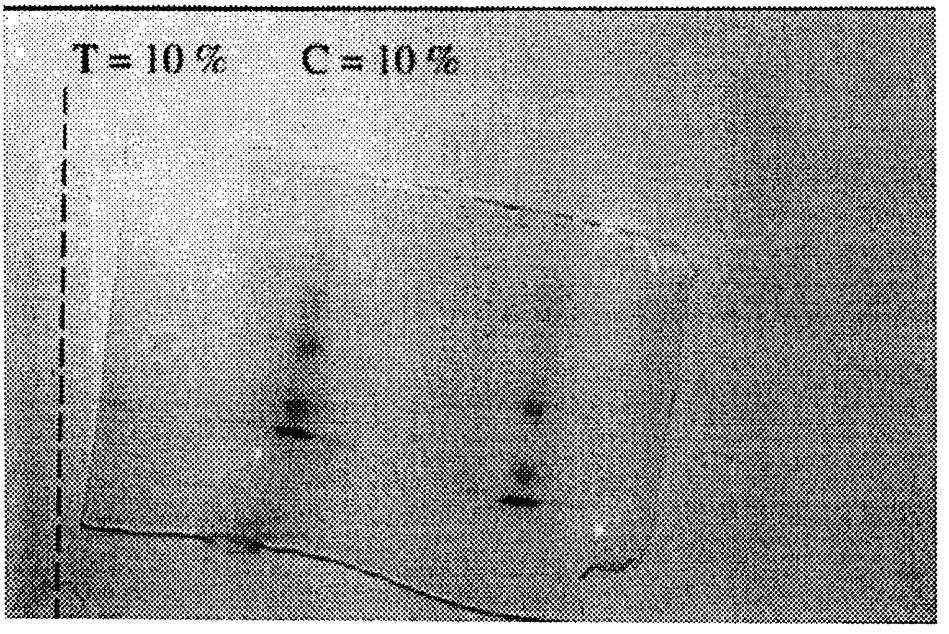

(i)

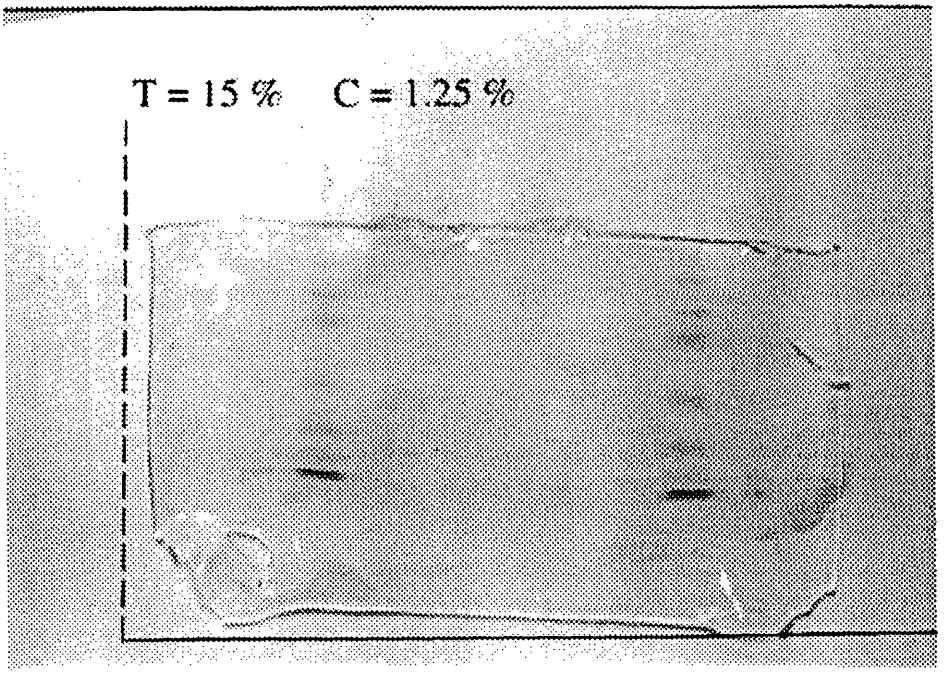

(j)

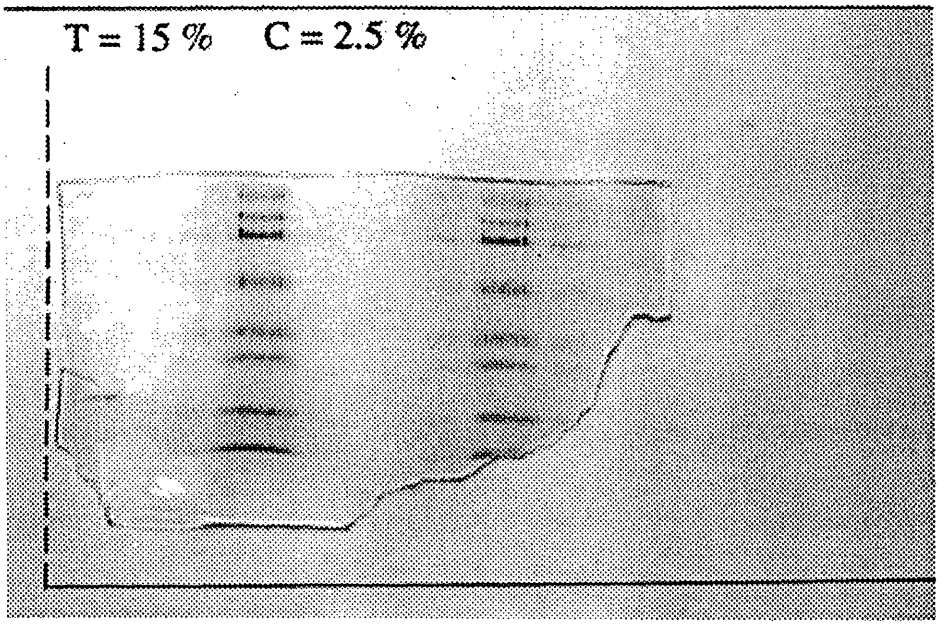

(k)

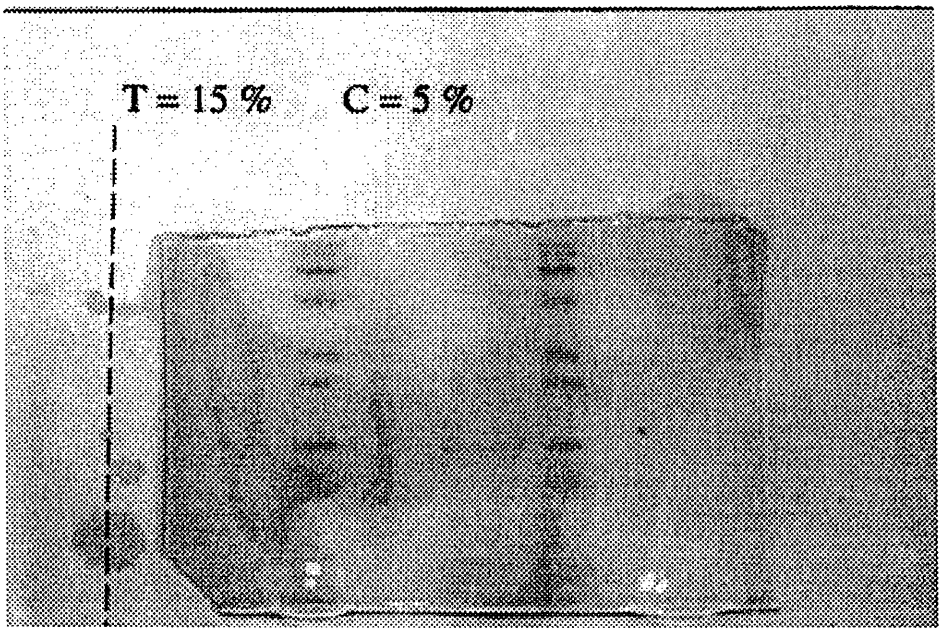

(l)

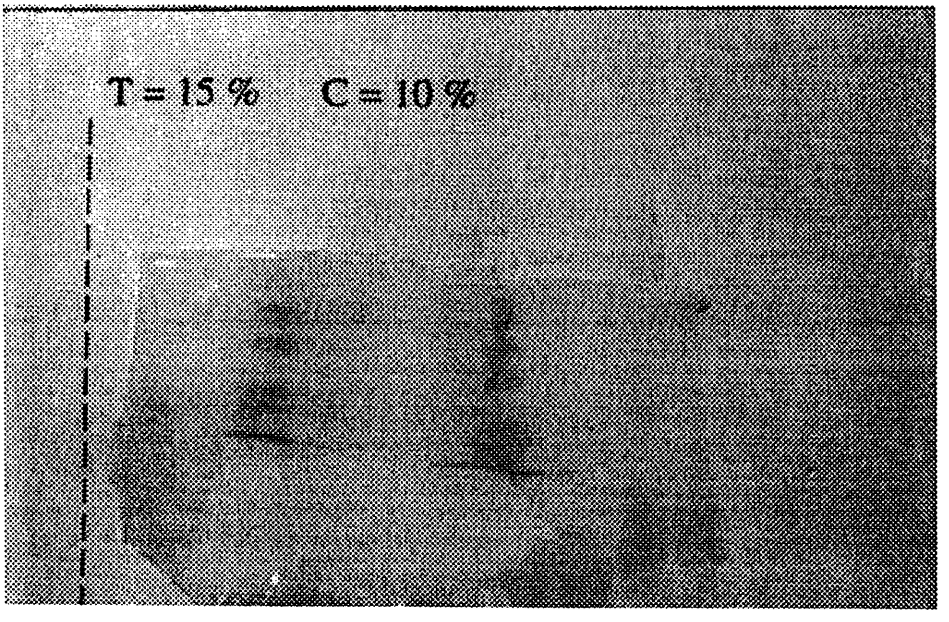

(m)

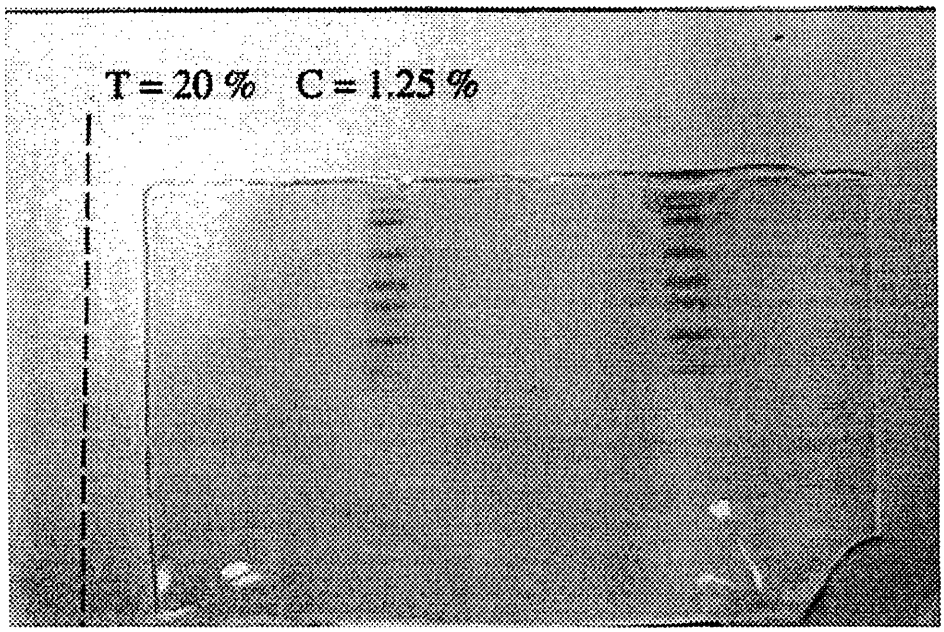

(n)

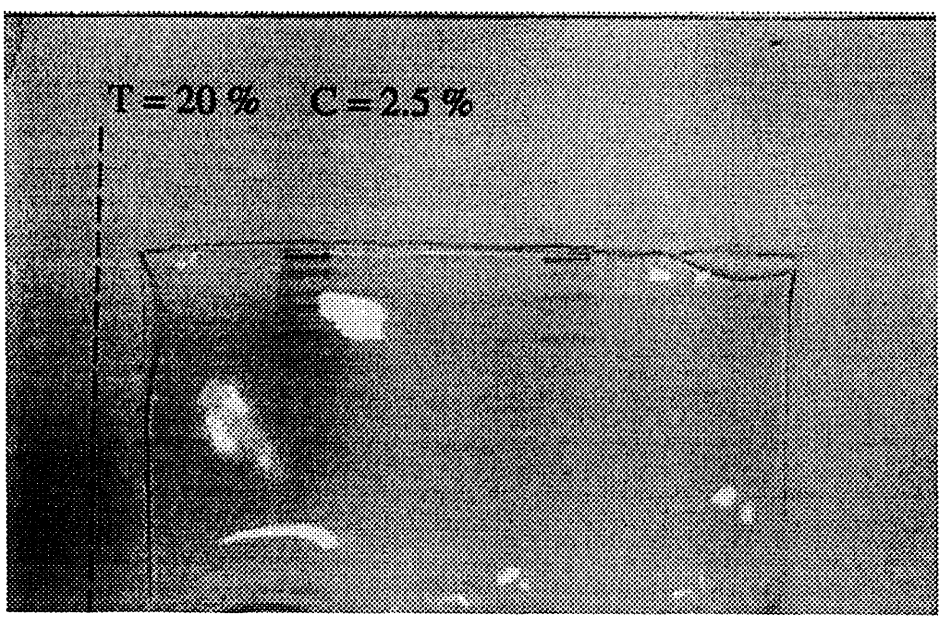

(o)

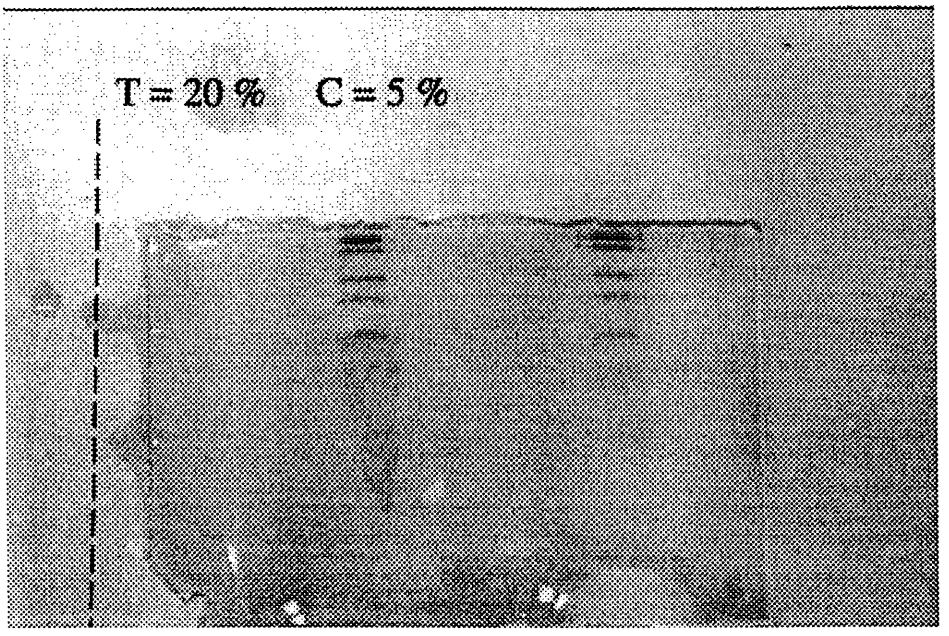

(p)

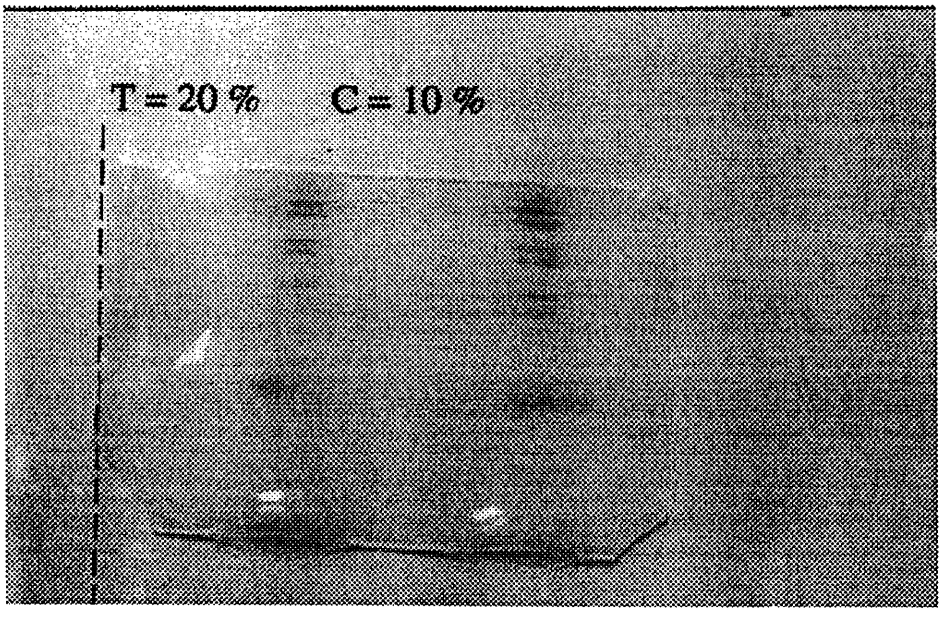

(q)

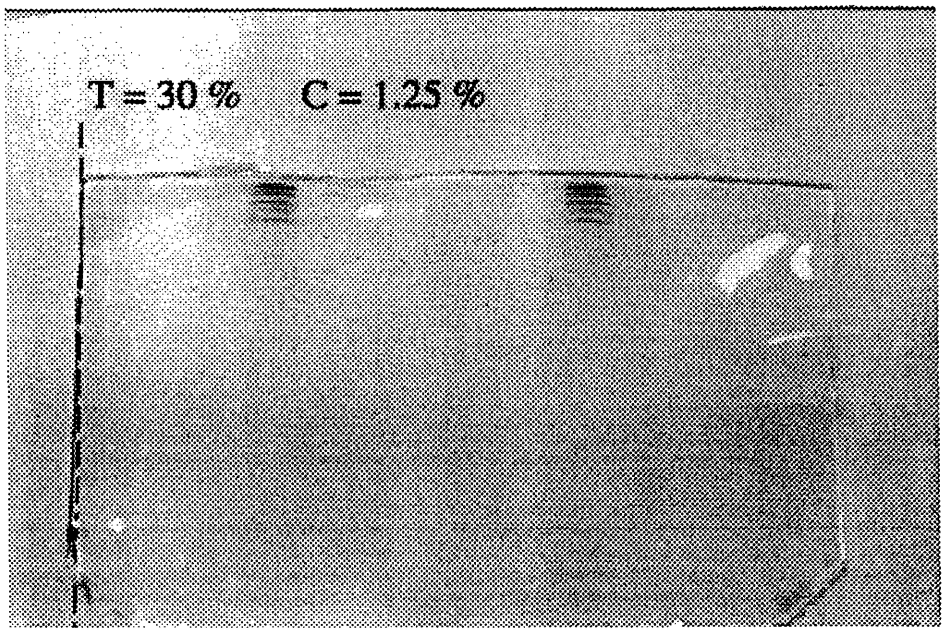

(r)

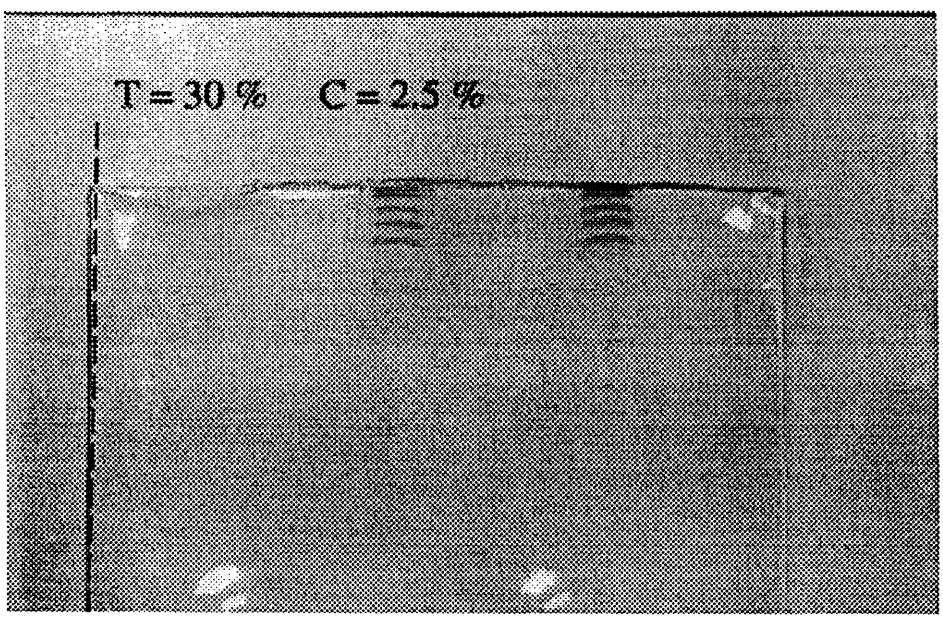

(s)

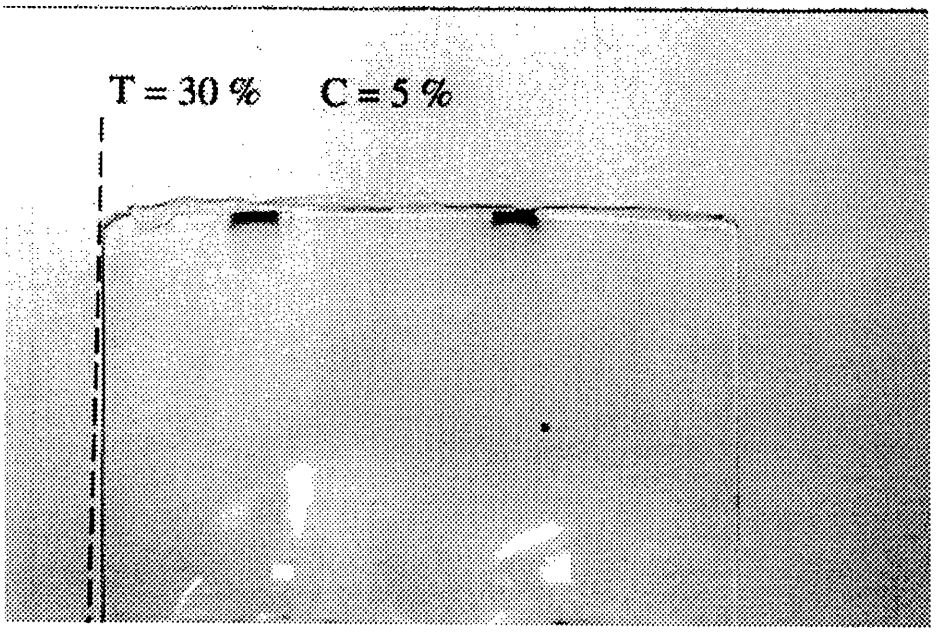

(t)

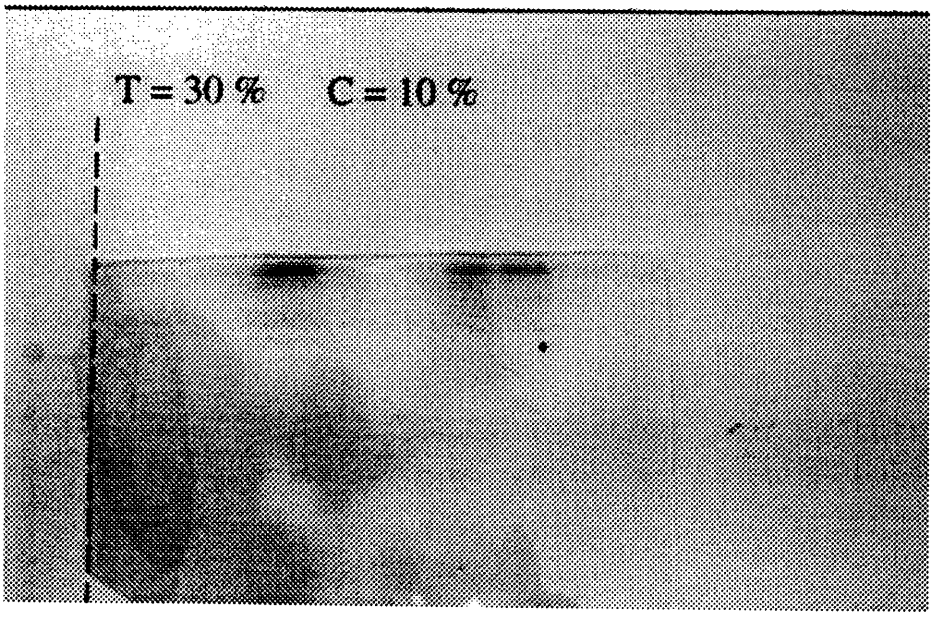

(a)

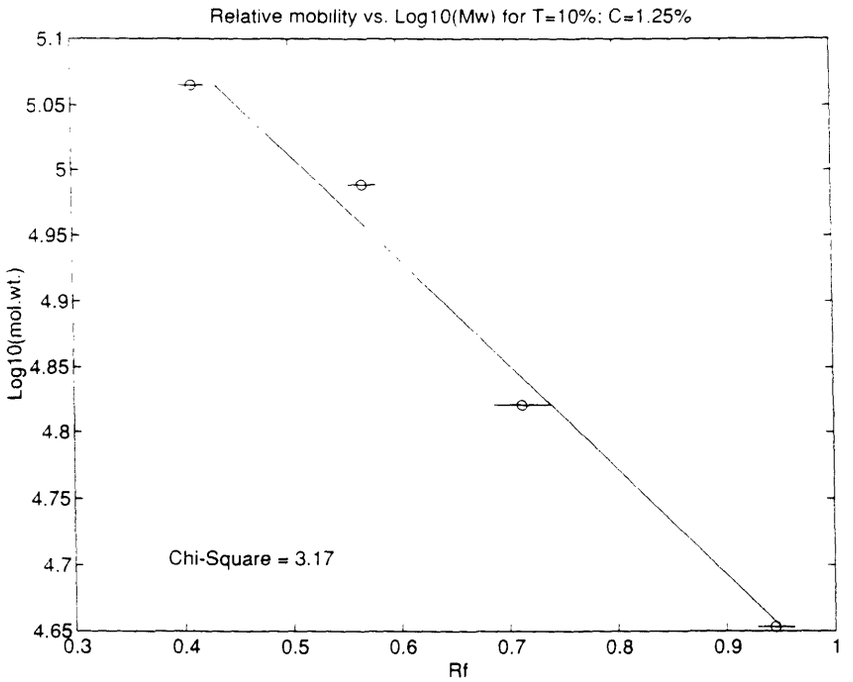

(b)

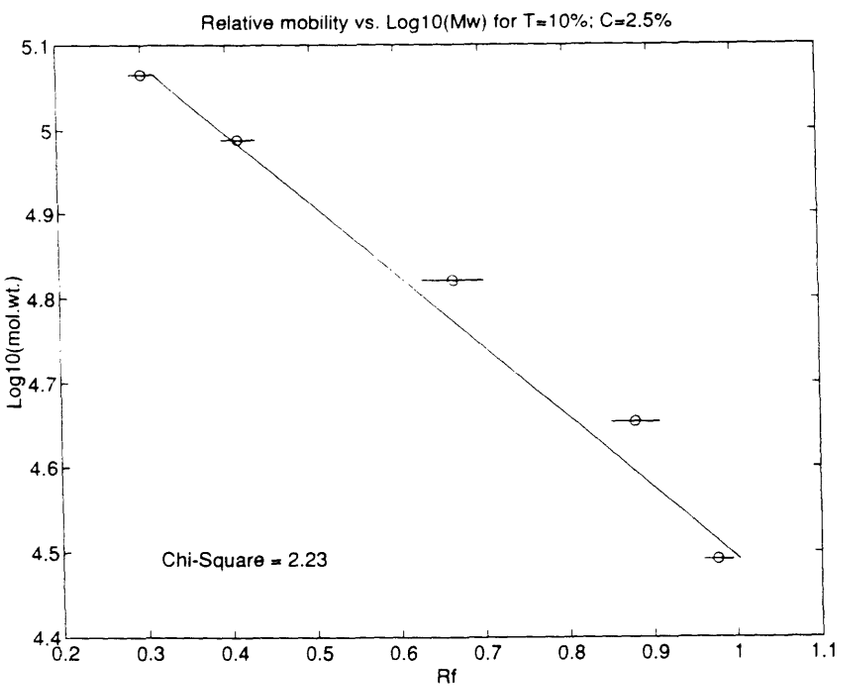

Figure 2-3: The calibration curves resulting from mobility measurements of braod range molecular markers in each gel sample.

(c)

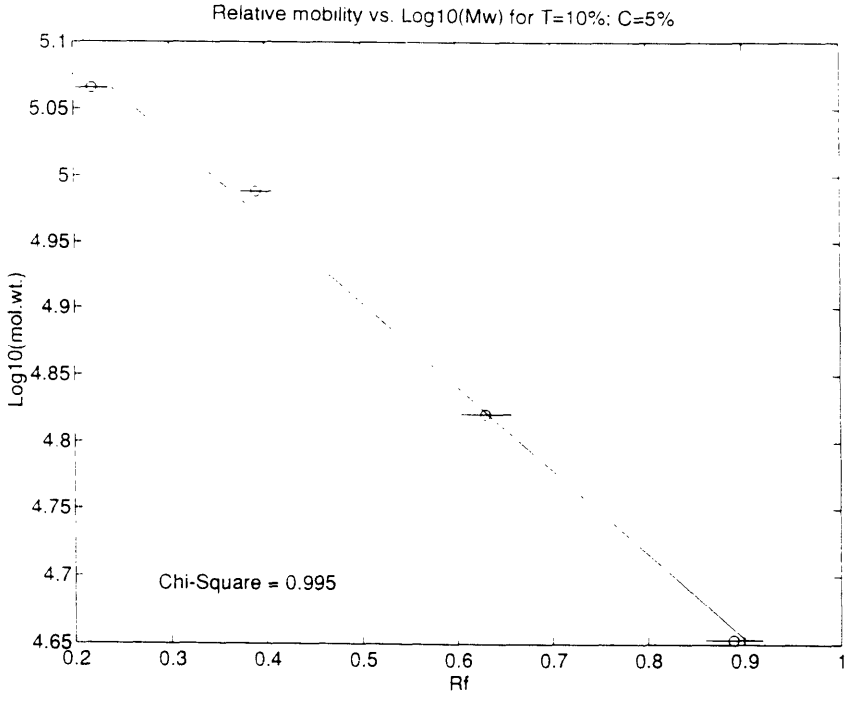
Relative mobility vs. Log10(Mw) for T=10%; C=5%
Log10(mol.wt.)
Rf
Chi-Square = 0.995
5.1
5.05
5
4.95
4.9
4.85
4.8
4.75
4.7
4.65
0.2
0.3
0.4
0.5
0.6
0.7
0.8
0.9
1

(d)

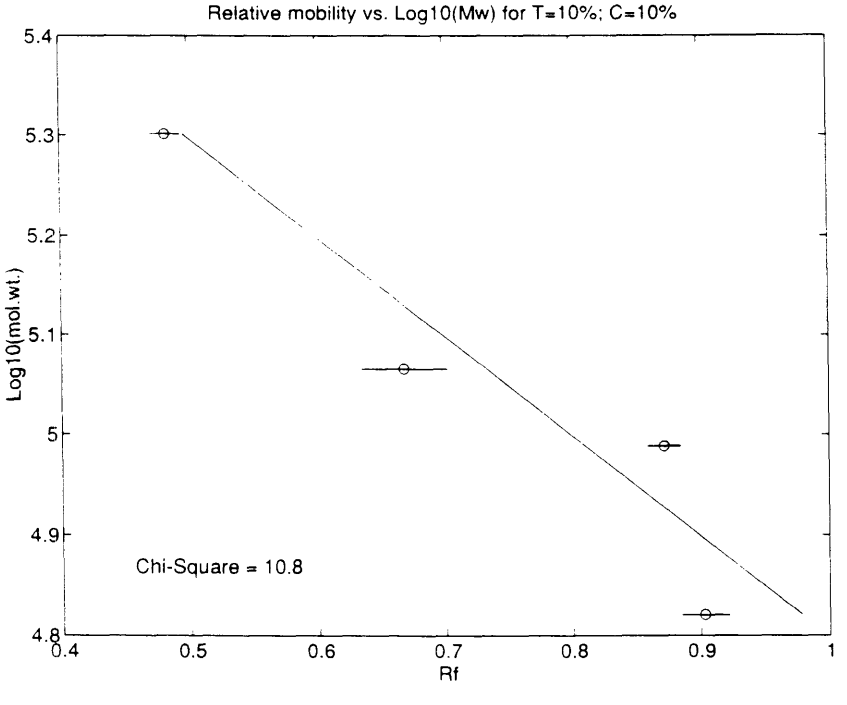
Relative mobility vs. Log10(Mw) for T=10%; C=10%
Log10(mol.wt.)
Rf
Chi-Square = 10.8
5.4
5.3
5.2
5.1
5
4.9
4.8
0.4
0.5
0.6
0.7
0.8
0.9
1

(e)

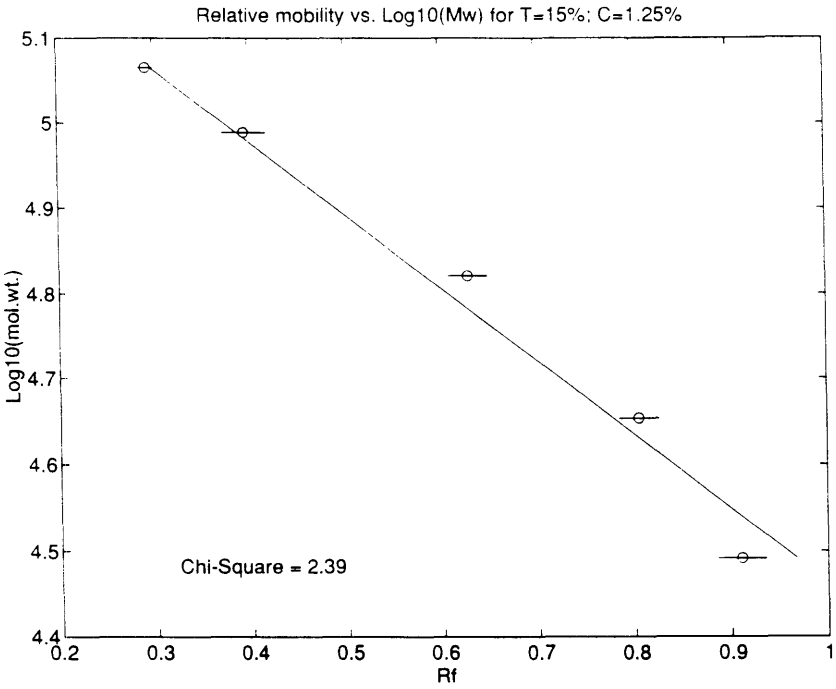
Relative mobility vs. Log10(Mw) for T=15%; C=1.25%
Log10(mol.wt.)
Rf
Chi-Square = 2.39
5.1
5
4.9
4.8
4.7
4.6
4.5
4.4
0.2
0.3
0.4
0.5
0.6
0.7
0.8
0.9
1

(f)

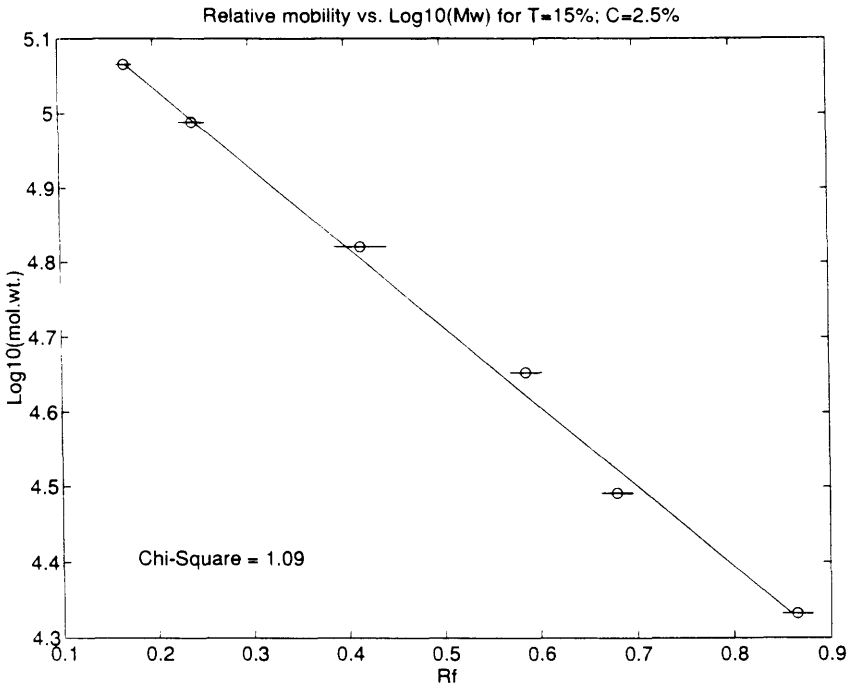
Relative mobility vs. Log10(Mw) for T=15%; C=2.5%
Log10(mol.wt.)
Rf
Chi-Square = 1.09
5.1
5
4.9
4.8
4.7
4.6
4.5
4.4
4.3
0.1
0.2
0.3
0.4
0.5
0.6
0.7
0.8
0.9

(g)

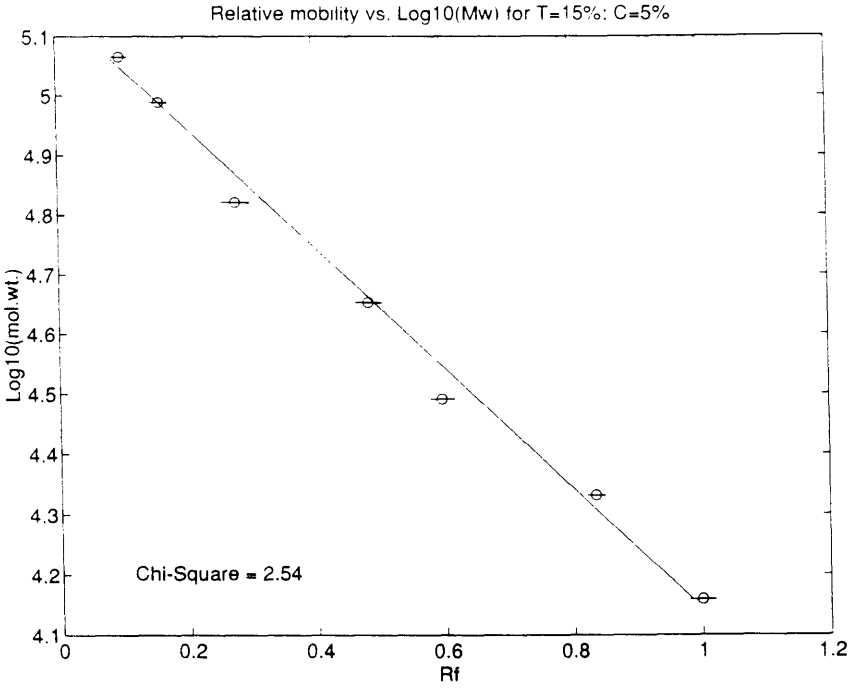
Relative mobility vs. Log10(Mw) for T=15%; C=5%
Log10(mol.wt.)
Rf
Chi-Square = 2.54
5.1
5
4.9
4.8
4.7
4.6
4.5
4.4
4.3
4.2
4.1
0
0.2
0.4
0.6
0.8
1
1.2

(h)

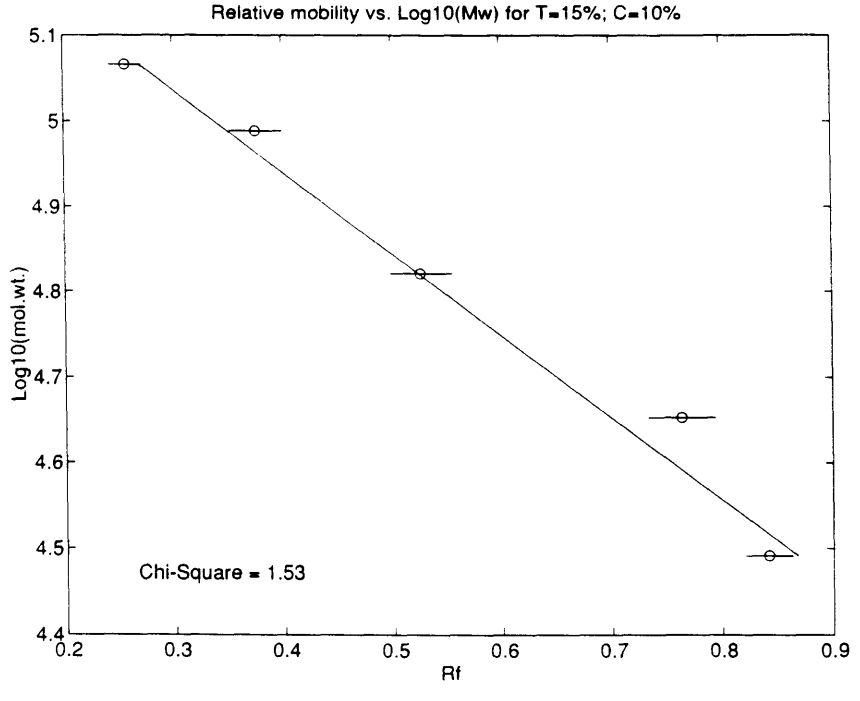
Relative mobility vs. Log10(Mw) for T=15%; C=10%
Log10(mol.wt.)
Rf
Chi-Square = 1.53
5.1
5
4.9
4.8
4.7
4.6
4.5
4.4
0.2
0.3
0.4
0.5
0.6
0.7
0.8
0.9

(i)

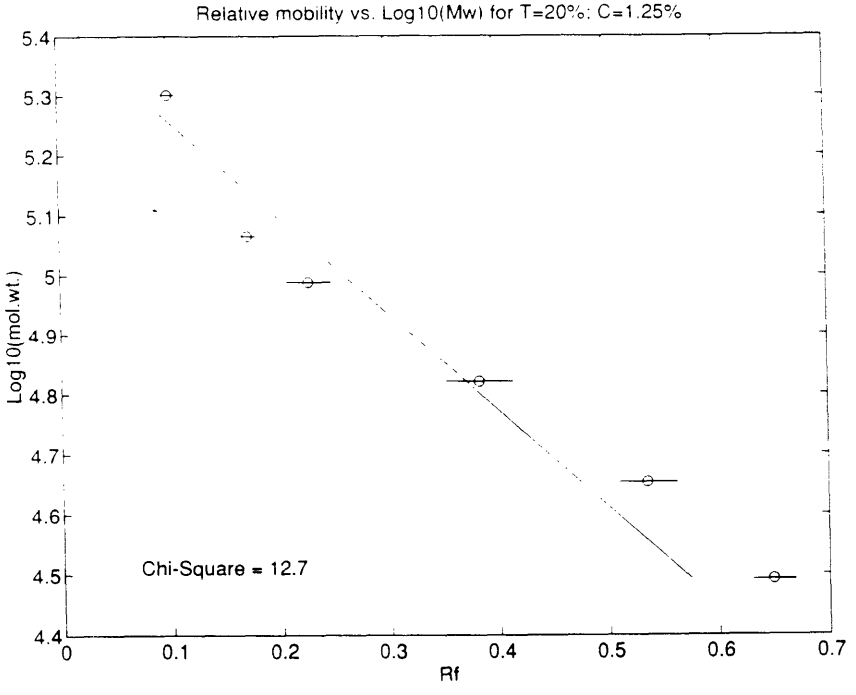
Relative mobility vs. Log10(Mw) for T=20%; C=1.25%
Log10(mol.wt.)
Rf
Chi-Square = 12.7
5.4
5.3
5.2
5.1
5
4.9
4.8
4.7
4.6
4.5
4.4
0
0.1
0.2
0.3
0.4
0.5
0.6
0.7

(j)

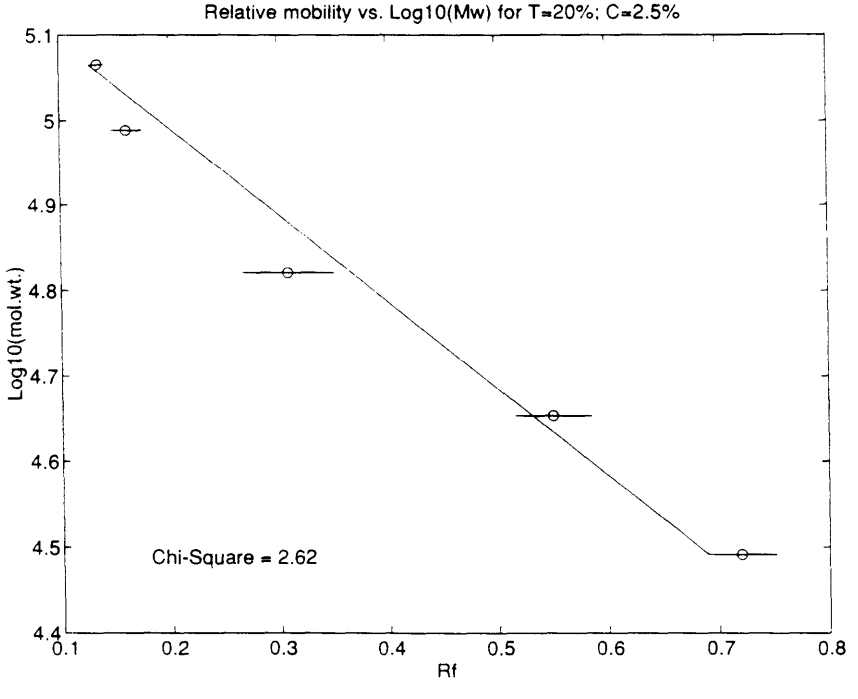
Relative mobility vs. Log10(Mw) for T=20%; C=2.5%
Log10(mol.wt.)
Rf
Chi-Square = 2.62
5.1
5
4.9
4.8
4.7
4.6
4.5
4.4
0.1
0.2
0.3
0.4
0.5
0.6
0.7
0.8

(k)

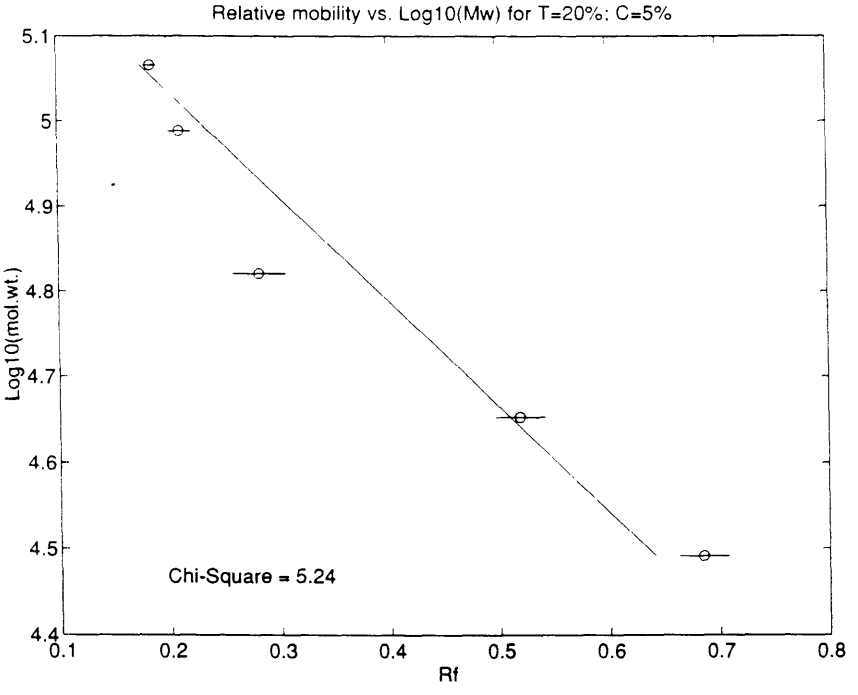
Relative mobility vs. Log10(Mw) for T=20%; C=5%
Log10(mol.wt.)
Rf
Chi-Square = 5.24
5.1
5
4.9
4.8
4.7
4.6
4.5
4.4
0.1
0.2
0.3
0.4
0.5
0.6
0.7
0.8

(l)

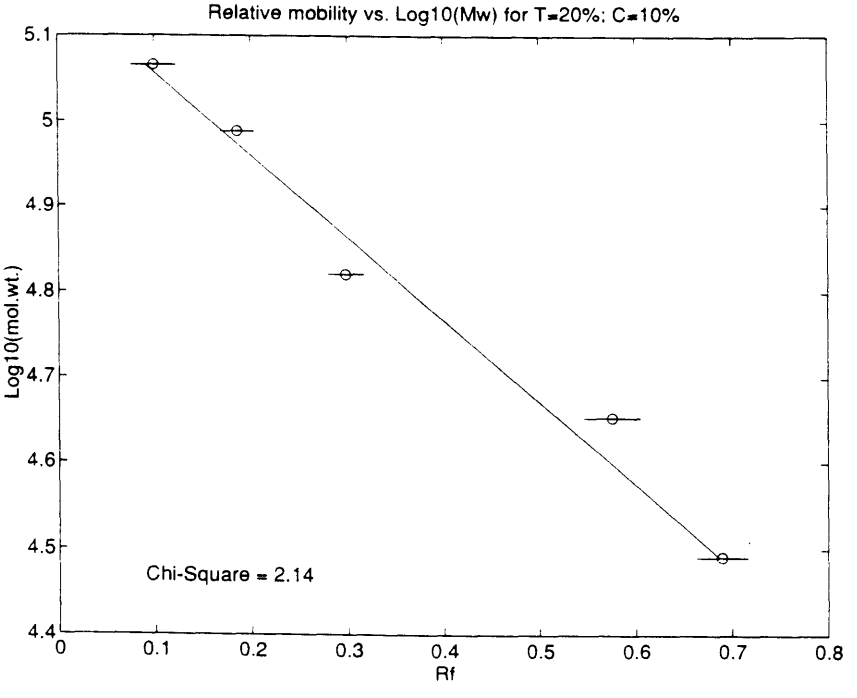
Relative mobility vs. Log10(Mw) for T=20%; C=10%
Log10(mol.wt.)
Rf
Chi-Square = 2.14
5.1
5
4.9
4.8
4.7
4.6
4.5
4.4
0
0.1
0.2
0.3
0.4
0.5
0.6
0.7
0.8

(m)

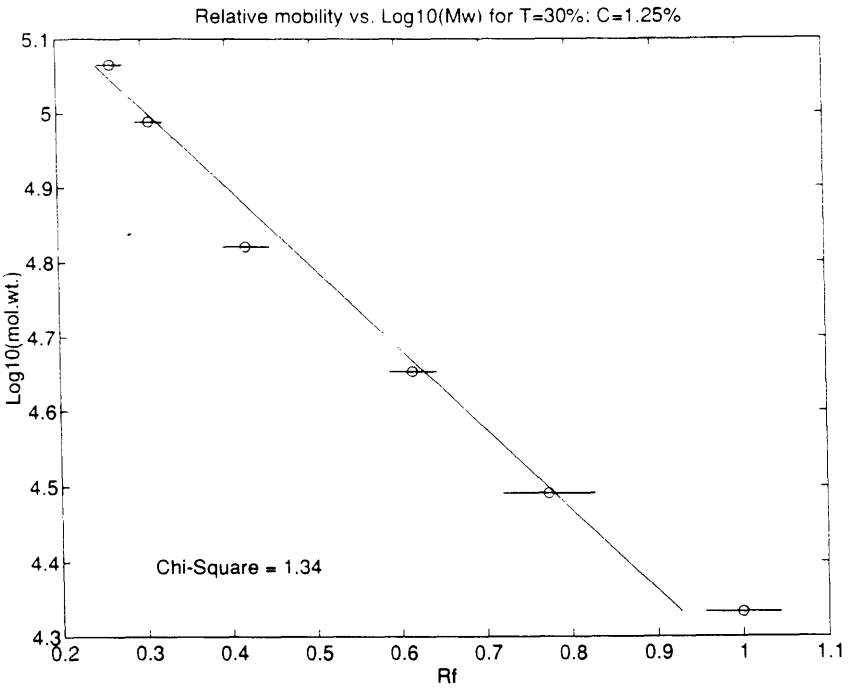
Relative mobility vs. Log10(Mw) for T=30%; C=1.25%
Log10(mol.wt.)
Rf
Chi-Square = 1.34
5.1
5
4.9
4.8
4.7
4.6
4.5
4.4
4.3
0.2
0.3
0.4
0.5
0.6
0.7
0.8
0.9
1
1.1

(n)

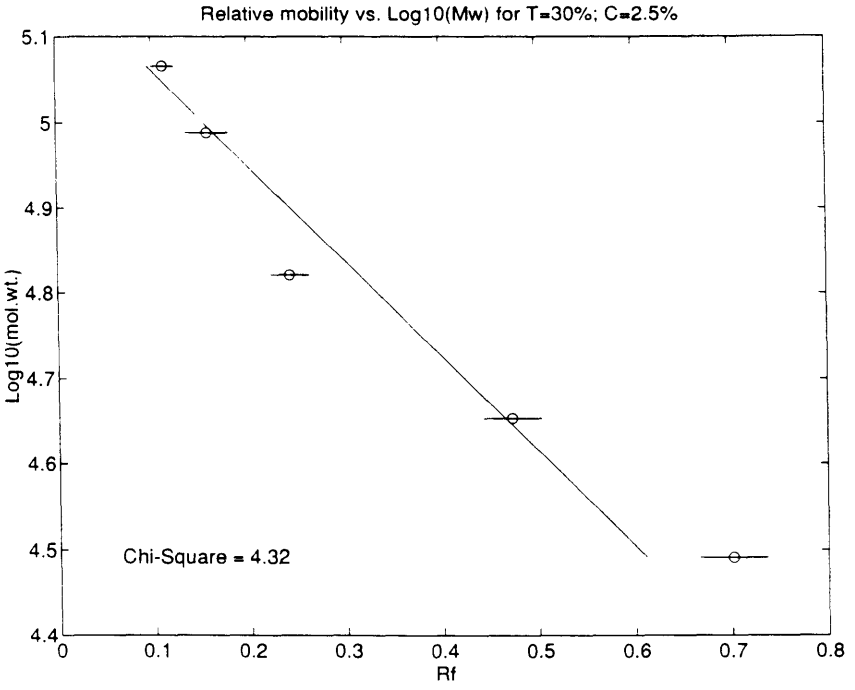
Relative mobility vs. Log10(Mw) for T=30%; C=2.5%
Log10(mol.wt.)
Rf
Chi-Square = 4.32
5.1
5
4.9
4.8
4.7
4.6
4.5
4.4
0
0.1
0.2
0.3
0.4
0.5
0.6
0.7
0.8

(o)

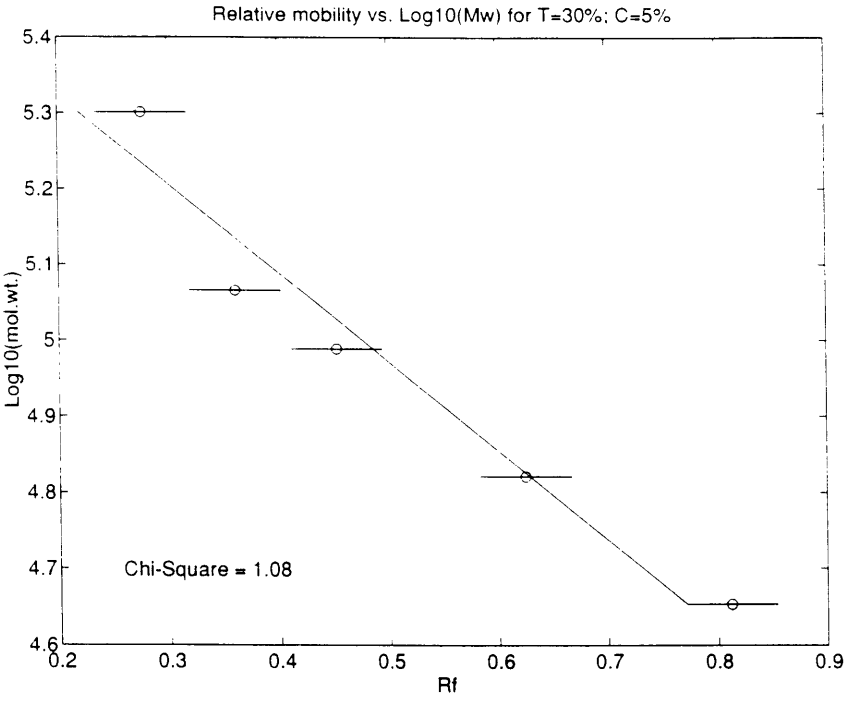
Relative mobility vs. Log10(Mw) for T=30%; C=5%
Log10(mol.wt.)
Rf
Chi-Square = 1.08
5.4
5.3
5.2
5.1
5
4.9
4.8
4.7
4.6
0.2
0.3
0.4
0.5
0.6
0.7
0.8
0.9

(p)

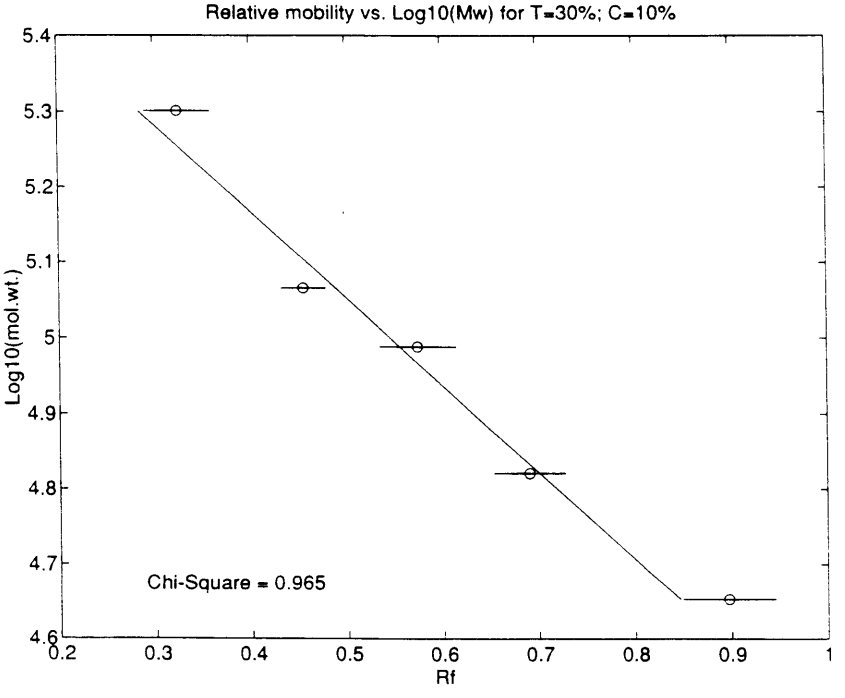
Relative mobility vs. Log10(Mw) for T=30%; C=10%
Log10(mol.wt.)
Rf
Chi-Square = 0.965
5.4
5.3
5.2
5.1
5
4.9
4.8
4.7
4.6
0.2
0.3
0.4
0.5
0.6
0.7
0.8
0.9
1

Table 8.4.1 Recipes for Polyacrylamide Separating and Stacking Gels[a]

SEPARATING GEL

Stock solutions	Final acrylamide concentration in the separating gel (%)[b]									
	5	6	7	7.5	8	9	10	12	13	15
30% acrylamide/ 0.8% bisacrylamide	2.50	3.00	3.50	3.75	4.00	4.50	5.00	6.00	6.50	7.50
4× Tris·Cl/SDS, pH 8.8	3.75	3.75	3.75	3.75	3.75	3.75	3.75	3.75	3.75	3.75
H_2O[c]	8.75	8.25	7.75	7.50	7.25	6.75	6.25	5.25	4.75	3.75
10% ammonium persulfate[d]	0.05	0.05	0.05	0.05	0.05	0.05	0.05	0.05	0.05	0.05
TEMED	0.01	0.01	0.01	0.01	0.01	0.01	0.01	0.01	0.01	0.01

Preparation of separating gel

In a 25-ml sidearm flask, mix 30% acrylamide/0.8% bisacrylamide solution, 4× Tris·Cl/SDS, pH 8.8 (see reagents, below), and H_2O. Degas under vacuum 10 to 15 min. Add 10% ammonium persulfate and TEMED. Swirl gently to mix. Use immediately.

STACKING GEL

In a 25-ml sidearm flask, mix 0.65 ml of 30% acrylamide/0.8% bisacrylamide, 1.25 ml of 4× Tris·Cl/SDS, pH 6.8 (see reagents, below), and 3.05 ml H_2O. Degas under vacuum 10 to 15 min. Add 0.025 ml of 10% ammonium persulfate and 0.005 ml TEMED. Swirl gently to mix. Use immediately. Failure to form a firm gel usually indicates a problem with the persulfate, TEMED or both.

REAGENTS USED IN GELS

30% acrylamide/0.8% bisacrylamide

Mix 30.0 g acrylamide and 0.8 g *N,N'*-methylene-bisacrylamide in a total volume of 100 ml H_2O. Filter the solution through a 0.45-μm filter and store at 4°C in the dark. 2× crystallized grades of acrylamide and bisacrylamide are recommended. Purchase as such or prepare as described in Reagents and Solutions. Discard after 30 days, since acrylamide gradually hydrolyzes to acrylic acid and ammonia.

CAUTION: *Acrylamide monomer is neurotoxic. Mask should be worn when weighing acrylamide powder. Gloves should be worn while handling the solution, and the solution should not be pipetted by mouth.*

4× Tris·Cl/SDS, pH 6.8 (0.5 M Tris·Cl containing 0.4% SDS)

Dissolve 6.05 g Tris base in 40 ml H_2O. Adjust to pH 6.8 with 1 N HCl. Add H_2O to 100 ml total volume. Filter the solution through a 0.45-μm filter, add 0.4 g SDS, and store at 4°C.

4× Tris·Cl/SDS, pH 8.8 (1.5 M Tris·Cl containing 0.4% SDS)

Dissolve 91 g Tris base in 300 ml H_2O. Adjust to pH 8.8 with 1 N HCl. Add H_2O to 500 ml total volume. Filter the solution through a 0.45-μm filter, add 2 g SDS, and store at 4°C.

[a] These recipes produce 15 ml of separating gel and 5 ml of stacking gel, which are adequate for a gel of dimensions 0.75 mm × 14 cm × 14 cm. These recipes are based on the SDS (denaturing)-discontinuous buffer system of Laemmli (1970).

[b] Units of numbers in table body are milliliters. The percentage of acrylamide in separating gel depends on the molecular size of the protein being separated. See annotation to step 3, first basic protocol.

[c] All reagents and solutions used in this protocol must be prepared with distilled deionized water.

[d] Best to prepare fresh.

Table 2.1: Recipies for Polyacrylamide Separating and Stacking Gels taken from *Current Protocols in Immunology* (1991)

Protein Molecular Weights (daltons)

Protein	Molecular Weight	Low Range	High Range	Broad Range
Myosin	200,000		X	X
ß-galctosidase	116,250		X	X
Phosphorylase b	97,400	X	X	X
Serum albumin	66,200	X	X	X
Ovalbumin	45,000	X	X	X
Carbonic anhydrase	31,000	X		X
Trypsin inhibitor	21,500	X		X
Lysozyme	14,400	X		X
Aprotinin	6,500			X

Table 2.2: Proteins found in molecular marker standard sample

	C=1.25%	C=2.5%	C=5%	C=10%
T=10%	7 bands 200,000 to 21,500	7 bands 200,000 to 21,500	7 bands 200,000 to 21,500	5 bands 200,000 to 45,000
T=15%	8 bands 200,000 to 14,400	9 bands 200,000 to 6,500	8 bands 200,000 to 14,400	7 bands 200,000 to 21,500
T=20%	8 bands 200,000 to 14,400	7 bands 200,000 to 21,500	7 bands 200,000 to 21,500	7 bands 200,000 to 21,500
T=30%	7 bands 200,000 to 21,500	7 bands 200,000 to 21,500	6 bands 200,000 to 31,000	6 bands 200,000 to 31,000

Table 2.3: Number of bands and corresponding weight ranges (given in daltons) resolved in the different gel samples.

	C=1.25%	C=2.5%	C=5%	C=10%
T=10%	3.17	2.23	0.995	10.8
T=15%	2.39	1.09	2.54	1.53
T=20%	12.7	2.62	5.24	2.14
T=30%	1.34	4.32	1.08	0.965

Table 2.4: ξ'^2 values for linear fit.

Chapter 3

SAXS Experiment

3.1 Background

X-ray scattering yields information about the electron distribution of a material, and thus the atomic positions within the material. Small angle x-ray scattering (SAXS) gives structural information in the range of 1-1,000 nm. Most SAXS work is done with CuK_α line having a wavelength of 0.154 nm; or in terms of energies, it contains photons of energy 8.04 keV. The scattered x-ray is denoted by $\vec{Q}$ where

$$\vec{Q} = \frac{4\pi}{d} \sin\theta \tag{3.1}$$

where 2θ is the scattering angle.

The amplitude of the x-ray beam in the direction of $\vec{Q}$ is given by

$$A(\vec{Q}) = \int \rho(\vec{r}) \exp(-i4\pi^2 \vec{r} \cdot \vec{Q}) d\vec{r} \tag{3.2}$$

where $\rho(\vec{r})$ is the electron density, and the amplitude $A(\vec{Q})$ is in electron units (on a relative scale in comparison to the amplitude of scattering from a single electron in the same direction). The intensity $I(\vec{Q})$ is given by

$$I(\vec{Q}) = \mid A(\vec{Q}) \mid^2 = A(\vec{Q})A^*(\vec{Q}) \tag{3.3}$$

The amplitude of scattering resulting from all electrons in an atom is the atomic scattering factor f of that atom. Its magnitude depends on the direction of scattering. At $\vec{Q} = 0$ (scattering in the forward direction), all scattering waves simply add together and the atomic scattering factor f is equal to the atomic number Z. As the scattering angle 2θ deviates from zero, the phases of the scattered waves from different electrons begin to differ, and consequently, the magnitude of f is a steadily decreasing function of 2θ.

$\rho(\vec{Q})$ may be factored into groupings of electrons, each group belonging to an electron

$$A(\vec{Q}) = \sum_{n=1}^{N} f_n \exp(-i4\pi\vec{Q} \cdot \vec{r}_n) \tag{3.4}$$

where f_n and r_n are the atomic scattering function and the position vector of the n^{th} atom. Squaring eqn (3.4), the scattering intensity $I(\vec{Q})$ may be written as

$$I(\vec{Q}) = \sum_{n=1}^{N} \sum_{m=1}^{N} f_n f_m \exp(-i4\pi\vec{Q} \cdot \vec{r}_{nm}) \tag{3.5}$$

where $\vec{r}_{nm} = \vec{r}_m - \vec{r}_n$ is the vector pointing from atom n to atom m. Collecting terms for which n and m refer to the same atom

$$I(\vec{Q}) = \sum_{n=1}^{N} f_n^2 + \sum_{n\neq} \sum_{m} f_n f_m \exp(-i4\pi\vec{Q} \cdot \vec{r}_{nm}) \tag{3.6}$$

and if the sample contains only one type of atom,

$$\frac{I(\vec{Q})}{Nf^2} = 1 + \frac{1}{N} \sum_{n\neq} \sum_{m} \exp(-i4\pi\vec{Q} \cdot \vec{r}_{nm}) \tag{3.7}$$

If the amplitude $A(\vec{Q})$ could be full determined, an inverse Fourier transform of equation (3.2) would yield the electron-density distribution $\rho(\vec{r})$. What is found experimentally is $I(\vec{Q})$. From $I(\vec{Q})$ one may obtain the modulus of $A(\vec{Q})$ but not its phase. This phase problem inhibits the ability to gain information on the structure by means of x-ray diffraction. However, valuable information may be gained from a direct analysis of $I(\vec{Q})$. For instance, Fourier inversion of equation (3.7) where the

distribution of interatomic vectors $\vec{r}_{nm}$ is obtained. Therefore, with some knowledge of the physics of a particular material, the scattering intensity $I(\vec{Q})$ may be used to determine structural information about that material.

3.2 Sample Preparation

Samples were made from electrophoresis purity acrylamide, N,N'-methylethylenebisacrylamide (BIS), ammonium persulfate (APS), and tetraethylenediamine (TEMED). All other chemicals were of analytical grade. The gel solutions were made according to the proportions outlined in table 3.1, and were degassed under vacuum for 15 - 20 minutes. The initiator and accelerator constituents of the gels were kept separate from the acrylamide solutions until just prior to injection into the sample cells.

The sample cells for the small angle x-ray experiment (SAXS) were aluminum boxes with 0.110 mm thick Kapton windows into which solutions may be injected. The gel solutions were injected via syringe into the sample cells shortly after the addition of accelerator (APS) and initiator (TEMED). In this way, the gels had just begun to polymerize and the solutions were not too viscous to manipulate in this manner. The sample cells were then fully sealed vacuum tight. The gel was then left undisturbed for 30 minutes in the sample cell and allowed to complete polymerization. The completed sample cells contained gels that were about 1 cm thick and which could be mounted onto sample wheels in sets of 4 to be x-ray scattered.

3.3 SAXS Apparatus and Experiment

The small angle X-ray scattering experiments were performed on the 10-m SAXS facility in the National Center for Small Angle Scattering Research (NCSAR) at Oak Ridge National Laboratory. The ORNL 10-m SAXS camera (shown in figure 3.1) utilizes a 12 kW Rigaku rotating anode x-ray source producing a CuK_α line with wavelength $\lambda = 1.54$ $\AA$. The Cu K_β radiation was removed from the incident beam via Bragg reflection from a hot-pressed pyrolytic graphite crystal monochromator.

The X-ray generator was kept at a power level of 40 kV/100 mA throughout the entire course of the experiment.

The apparatus may be adjusted to cover the Q range of $3 \times 10^{-3} \leq Q \leq 0.5\mathring{A}^{-1}$ which corresponds to angle range of 0.043 deg $\leq 2\theta \leq$ 7.15 deg. The sample to detector distances are 1.0, 1.5, 2.0, ..., 5 m allowing for the selection of different specific Q ranges within the maximum range stated above. The maximum flux at the sample is 10^8 photons per second per irradiated area (typically 2-mm diameter sample area). The sample to detector distance selected for the experiments was 2.115 meters. This corresponds to a Q range of $0.008\mathring{A}^{-1} \leq Q \leq 0.261\mathring{A}^{-1}$.

The collimation system is optimized subject to the constraint of having a 0.5 mrad resolution. This resolution meets the requirement that the beam not have a diameter larger than 1 mm at the speciman position. The collimation was achieved by a circular 1mm aperture at the source and a 1×1 mm ^{2} square aperture at the sample position. The two-dimensional detector is made up of 100 by 100 wires placed 2 mm apart in both the x and y directions. It is a 20×20 cm^2 position-sensitive proportional counter filled with Xe gas and quenched with CO_2. The active area is divided into a 64×64 array of 3.125×3.125 mm^2 virtual pixels.

A beam stop was placed in the center of the beam path to absorb the major part of the incident, undiffracted X-rays (so as not to overload the counter system). Scattering signals from the samples were collected for times between one and three hours. The raw data were corrected for dark current, cosmic radiation, empty sample cell scattering, sample transmission, and then normalized by the number of incident X-rays counted by a scintillation detector located just downstream of the source slit and monochromator. Variations in pixel detection efficiency of the detector were corrected by measuring the diffraction pattern of the ^{55}Mn K-shell fluorescene from a 10 μCi ^{55}Fe source which undergoes β^+-decay. The diffraction is isotropic and should register properly in all the detector sights; thus, the detector efficiency may be corrected.

3.4 Method of Data Analysis

3.4.1 Large Q

The large Q data was fit to a form of the Tuebner-Strey model which has been successfully employed in the study of microemulsions. The scattering intensity as shown by Debye is

$$I(Q) = (\Delta\rho)^2\phi_p(1-\phi_p)\int_0^\infty dr 4\pi^2 \frac{\sin Qr}{Qr}\Gamma_D(r) \tag{3.8}$$

$$= (\Delta\rho)^2\phi_p(1-\phi_p)S(Q) \tag{3.9}$$

where $\Gamma_D(r)$ is the Debye correlation function found by Teubner and Strey for a bicontinuous structure as being

$$\Gamma_D(r) = \exp(-r/\xi)\left(\frac{\sin kr}{kr}\right) \tag{3.10}$$

This correlation function was derived by Teubner and Strey[76] from a consideration of a Landau expansion of the free energy functional of a microemulsion system. The Teubner-Strey model yields two length scale parameters which are used to interpret distances between domains in a material. In equation (3.10), $k = 2\pi/d$, where d is the inter-pore distance and ξ is the coherence length which measures the extent of order from a central point.

The structure factor derived from the Teubner-Strey model is

$$S(Q) = \frac{8\pi\xi^3}{(k^2\xi^2+1)^2 + 2(1-k^2\xi^2)\xi^2Q^2 + Q^4} \tag{3.11}$$

For the large Q region because of the predicted domain size of the gel structure from electrophoresis analysis, the Q^4 term in the structure factor is negligible. The remaining terms represent a Lorentzian form

$$S(Q) = \frac{I_L(0)}{(1+Q^2\xi'^2)} \tag{3.12}$$

where

$$I_L(0) = \frac{8\pi\xi^3}{(k^2\xi^2+1)^2} \tag{3.13}$$

and

$$(\xi')^2 = \left[\frac{2(1-k^2\xi^2)}{(k^2\xi^2+1)^2}\right](\xi)^2 = \alpha(\xi)^2 \tag{3.14}$$

The asypmtotic region in the large Q range yields a straight line, corresponding to the Lorentzian form

$$I_L(Q) - C = \frac{I_L(0)}{(1+Q^2\xi'^2)} \tag{3.15}$$

where ξ' is the effective correlation length of the polymer density fluctuations in the gel and C is the background. In the small Q range, $(I(Q) - C)$ deviates from the Lorentzian form. The Lorentzian form for large Q may be factored to yield the relation

$$I_L(Q) - C = \frac{I_L(0)}{Q^2\xi'^2}\left(\frac{1}{1+\frac{1}{Q^2\xi'^2}}\right) \tag{3.16}$$

which for large Q is

$$I_L(Q) - C = \frac{I_L(0)}{Q^2\xi'^2}\left(1 - \frac{1}{Q^2\xi'^2}\right) \tag{3.17}$$

It is easy to see then that a linear fit to the data of the form

$$I(Q) = \frac{A}{Q^4} + \frac{B}{Q^2} + C \tag{3.18}$$

will give coefficients A and B whose ratio is equal to

$$\frac{B}{A} = -\frac{1}{\xi'^2} \tag{3.19}$$

The effective correlation length for the gel may be easily determined and may be used as a measure of the effective pore size of the gel.

When speaking of polymer networks, it is also instructive to consider the scattering results obtained from polymer chains. At large angles, the scattering of polymer

chains obeys a law of the form

$$I(Q) = kQ^{-1/\nu} \tag{3.20}$$

where $I(Q)$ is the intensity of the scattering function given as a function of the modulus of the scattering vector $Q = (4\pi/\lambda_o)\sin(\theta/2)$, where λ_o is the wavelength of the X-ray, and ν is the swelling exponent defined by the relation $R \sim N^\nu$ between the size R of the chain and the number N of units. k is a prefactor to be determined later. The relation defined by equation (3.20) holds regardless of the architecture of the molecule.[22]

A linear Gaussian chain demonstrates this behavior well because the scattering intensity is directly proportional to the structure factor $I(Q) = \bar{b}^2\phi S(Q)$, where ϕ is the polymer volume fraction and $\bar{b}^2$ is the contrast factor. Debye has calculated the structure factor of a Gaussian chain as[21]

$$S(Q) = NP(Q) = \frac{2}{\lambda^2 N}(\lambda N - 1 + exp(-\lambda N)) \tag{3.21}$$

where λ is defined as $Q^2b^2/6$. $P(Q)$ is the form factor normalized to unity when Q=0, and b^2 is the mean square of the statistical element. At large wave vectors (large Q), the structure factor decays as $S(Q) = 2/\lambda$.

Scattered intensity is usually displayed as a Zimm[86] plot ($1/I(Q)$ plotted against Q^2 or λ) or as a Kratky[45] plot ($Q^2I(Q)$ or $\lambda I(Q)$ plotted against Q^2 or λ). In these representations, large Q data follows the behavior outlined by equation (3.20) allowing the verification of the exponent ν and the length b of the statistical element, either from the slope of the asymptote (Zimm plot) or from the intercept of the horizontal asymptote (Kratky plot). The behavior in the low Q range relays information about the radius of gyration and the molecular weight.

When the size of the polymer is small, X-ray experiments give access to both the initial and asymptotic parts of the curve. However when the polymer is large (having a radius of gyration greater than 500Å), experimental constraints make the low Q range inaccessible. Experiments are then limited to the asymptotic tail of the

scattering curve (large Q data).

Networks and gels are one such category of substances having large structures which many times limit experiments to the high Q range because of the difficulties surrounding low Q measurements. This makes it interesting to study the tail of the scattering curve in more detail. For a Gaussian chain, an expansion of equation (3.20) to the next order gives

$$S(Q) = \frac{2}{\lambda} - \frac{2}{N\lambda^2} \tag{3.22}$$

Using a Zimm representation for the data, the molecular weight of the chain may be determined from the intercept of the asymptote with the horizontal axis. If the polymer is polydisperse, then this yields the number-average molecular weight rather than the weight-average as in the Guinier[6] range.

Benoit, Joanny, Haziioannou, and Hammouda[5] generalized this idea of high Q range analysis and applied it to more complex situations than the simple Gaussian chain. They considered the cases of branched chains, chains with excluded volume, polydisperse systems, chains submitted to a unidirectional force as in an extended rubber sample, and block copolymers in a molten phase. They concluded that the first correction to the asymptotic behavior of the structure factor of polymers at large Q does indeed give important information. Their corrections (determined for the above mentioned systems) most times depended only on the local architecture of the chain. In addition, the corrections did not depend on the size of the molecules as long as the small-scale structure remained constant.

In all cases, their corrections produced a form for the large Q structure factor $S(Q)$ given by:

$$S(Q) = \frac{A}{\lambda} + \frac{B}{\lambda^2} \tag{3.23}$$

where A and B do not depend on the size of the molecule, and where once again $\lambda = Q^2b^2/6$. The coefficient A characterizes the length of the statistical element. For a linear chain B gives the number-average degree of polymerization. For branched polymers without loops, B depends mainly on the number of statistical elements between two cross-links or one cross-link and one end. Finally, if the polymer is suffi-

ciently long, B gives the number-average degree of polymerization of these branches. A and B may be determined from a linear fit to the asymptotic large Q data.

More specifically, Benoit *et al.* developed the general equation for scattering from branched polymers. A polymer is made of s branches each with the same length n for a total of $N = sn$ monomers. A polymer chain is defined as running between two cross-links or between one cross-link and one end. Each chain has c cross-links of functionality f, where f is the number of branches starting from each cross-link. There are no ring structures and the chains are Gaussian; therefore, the chain structure is that of a Bethe lattice or a Cayleigh tree, and there is only one way to travel along the chain between points.

They calculated to show that the structure factor resulting from a large Q expansion of the Debye relation for Gaussian chain in a network is given by

$$S(Q) = \frac{2}{\lambda} + \frac{cf(f-1)}{sn\lambda^2} - \frac{2}{n\lambda^2} \tag{3.24}$$

The inverse used to plot in the Zimm representation is

$$\frac{1}{S(Q)} = \frac{\lambda}{2} - \frac{1}{4n}\left[\frac{cf(f-1)}{s} - 2\right] \tag{3.25}$$

Two interesting cases which apply to polymer networks are firstly the situation where there are chains with no loops, and secondly the situation where the entire network is completely crosslinked in a gel. For the case of chains with no loops; if there is only one cross-link of functionality f, there are f branches in the molecule. For every new cross-link, $(f-1)$ branches are added to the molecule. In a molecule with c cross-links, there are $f + (c-1)(f-1) = c(f-1) + 1$ branches, and thus

$$s - 1 = c(f-1) \tag{3.26}$$

Substituting this relation into equations (3.24) and (3.25)

$$S(Q) = \frac{2}{\lambda} - \frac{1}{n\lambda^2}\left[\frac{cf(f-1)}{s} - 2\right] \tag{3.27}$$

$$\frac{1}{S(Q)} = \frac{\lambda}{2} - \frac{1}{4n}\left[f - 2 - \frac{f}{s}\right] \tag{3.28}$$

These formula may be checked in known limiting cases. For example, consider a linear chain of s blocks with junctions of functionality 2, the Debye formula is then recovered.

An interesting note is the fact that because there is branching in the system, the second term in equation (3.28) is negative (except for three-arm star structure for which it would be zero). The structure factor $S(Q)$, and therefore the intensity profile $I(Q)$, will have a negative intesection with the horizontal axis in the Zimm representation; and in the Kratky plot, the curve reaches its asymptote from above. This has been frequently observed on multi-arm stars and networks.

In contrast to a model having chains without loops, a completely crosslinked gel with c crosslinks each of functionality f will have $s/2$ branches:

$$cf = 2s \tag{3.29}$$

Substituting this relation into equation (3.24) and (3.25)

$$S(Q) = \frac{2}{\lambda} + \frac{2(f-2)}{n\lambda^2} \tag{3.30}$$

$$\frac{1}{S(Q)} = \frac{\lambda}{2} - \frac{1}{2n}(f-2) \tag{3.31}$$

Because this relation is for a fully crosslinked chain, the functionality f must always be greater than 2. This implies that in equation (3.30) the second term must always be positive for a completely crosslinked gel.

3.4.2 Absolute Intensity, $S(Q)$

The absolute scattering intensity $s(Q)$ of a scattering sample is directly proportional to the measured scattering intensity $I(Q)$ through the relation

$$S(Q) = \frac{I(Q) - bgd}{< \eta^2 >} \tag{3.32}$$

where *bgd* is the scattering intensity background due to atomic scale density fluctuations and $< \eta^2 >$ is the invariant. The invariant $< \eta^2 >$ is defined by the integral of the scattering intensity over all values of Q, which for an isotropic system is

$$< \eta^2 >= \frac{1}{2\pi^2} \int_0^\infty Q^2 I(Q) dQ \tag{3.33}$$

The invariant is related to the scattering length densities of the two phases (water ρ_w and polymer ρ_p) and to the volume fraction ϕ_p of the polymer by the relation:

$$< \eta^2 >= (\Delta\rho)^2 \phi_p (1 - \phi_p) \tag{3.34}$$

where $(\Delta\rho)^2 = (\rho_w - \rho_p)^2$.

3.5 Results and scussion

3.5.1 Large Q

In the large Q region, the gel sample intensity profiles $I(Q)$ were fitted with a function of the form

$$I(Q) = \frac{A}{Q^4} + \frac{B}{Q^2} + C \tag{3.35}$$

where the constant term C was added to correct for background intensity that remained after the raw data had been reduced. These large Q fits are shown in figure 3.2. From these fits, the coefficients A and B were determined for each gel sample. The ratio of B/A is related to the effective correlation length ξ'

$$\frac{B}{A} = -\frac{1}{\xi'^2} \tag{3.36}$$

The resulting values for the ξ' are shown in table 3.2.

A comparison of effective correlation length ξ' change with increasing polymer concentration T, holding the total crosslinker concentration C constant is shown in figure 3.3. For a constant C at low concentrations (C<20%), the ξ' decrease with

increasing monomer concentration. The effective correlation length ξ' may be interpreted as an effective pore size. The distance over which order may be found in low concentration gel is an effective measure of the pore size because the order will not exist far beyond the first neighboring structure. Therefore, as more monomer is added, the network becomes a denser, more disordered mesh and the effective pore size decreases.

A comparison of effective correlation length ξ' change with increasing crosslinker concentration C, holding the total monomer concentration T constant is shown in figure 3.4. For a constant T, the effective correlation length ξ' increases with increasing crosslinker concentration C, and even has a negative value for T=15%, C=20%. This negative value is permitted by the Teubner-Strey model used because α from the relation $(\xi')^2 = \alpha(\xi)^2$ is allowed to have both positive and negative values. If ξ' is considered as an effective pore size in this instance, then the pore size will be increasing with increasing C. Hecht *et. al.*(1985)[37] studied structural inhomogeneities in the range of 2.5-2500$\AA$ in polyacrylamide gels using light, x-ray, and neutron scattering. They found that the pore size of the gels at a fixed T, increased with increasing bisacrylamide content. They concluded that the structure of the polymer chains was profoundly changed by bisacrylamide, tending to form chains with higher electron density with a greater number of monomers per unit length. They suggested that (as a result of increasing bisacrylamide content) the singly stranded structure prevalent in the polymer solution was replaced by denser bundles of fibers bound together by bisacrylamide (see figure 3.5 (a) and (b)) Thus, denser bundles of chains were formed between crosslinks. In compensation, average spacing between the chains increased strongly.

The interpretation presented by Hecht *et. al.*(1985) is not consistant with what is seen in electrophoretic results. As seen in chapter 2, the mobilities of the molecular markers decreased as the crosslinking concentration was increased, indicating a decrease in effective pore size. As the gel becomes more highly crosslinked, the effective correlation length ξ' may be interpreted as a long range coherence length. When the crosslinker concentration at a fixed T goes up, the gel topology changes

and becomes more ordered. In this way, the interpretation of ξ' as an effective pore size is disallowed for the specific case of studying crosslinker effects alone rather than total monomer concentration. With ξ' interpreted as a long range correlation length, it is observed that the gel pore size will decrease as ξ' increases.

3.5.2 Absolute Scattering Intensity, $S(Q)$

Using equation (3.32), the absolute scattering intensities $S(Q)$ of the gels were determined. The invariant $< \eta^2 >$ was measured from the scattering intensity $I(Q)$ with background removed using relation (above). $< \eta^2 >$ was determined from the $I(Q)$ for the T=10%, C=5% gel. This gel had the most regular intensity profile with a good signal in the low Q range and did not suffer the noise in the lower Q range that many other intensity profiles did. The $I(Q)$ for T=10%, C=2.5% is shown in figure 3.6. $< \eta^2 >$ was determine by numerical integration in the lower Q range (using the trapezoidal method), and by a definite integration in the higher Q region.

$$< \eta^2 >= \int_0^{Q_{high}} Q^2 I(Q) dQ + \int_{Q_{high}}^{\infty} Q^2 I(Q) dQ \tag{3.37}$$

In the high Q range, $I(Q)$ is assumed to have a form

$$I(Q) = \frac{A}{Q^4} + \frac{B}{Q^2} + C \tag{3.38}$$

and as Q gets larger, the Q^4 term will dominate. Consequently in the calculation of the invariant, $I(Q)$ in the high Q part of the integration is assumed to have the form $I(Q) \sim A/Q^4$. By substitution into eqn (sds), the invariant may be calculated as

$$< \eta^2 >= \int_0^{Q_{high}} Q^2 I(Q) dQ + \frac{A}{Q_{high}} \tag{3.39}$$

$(\Delta\rho)^2$ was determined for the T=10%, C=2.5% sample using the relation found in equation (3.34) and knowledge of the volume fraction of polymer in the gel. The volume fraction ϕ are related to the T and C concentrations of the gels. The derivation of this relation is found in Appendix A. Because the electron density difference $(\Delta\rho)^2$

is a characteristic of the materials in the gel, it is the same for all the gels. From $(\Delta\rho)^2$ and the volume fractions of the other gel samples, all other invariants $< \eta^2 >$ were determined. Next, the background intensities determined in the large Q linear fits were subtracted from $I(Q)$, and then their difference was divided by the invariant $< \eta^2 >$ to find the absolute scattering intensity

$$S(Q) = \frac{I(Q) - bgd}{< \eta^2 >} \tag{3.40}$$

The absolute scattering intensity profiles for all gel samples are shown in figure 3.7. These $S(Q)$ may be fit to a function to give more information about the gel structure. Possible functions that may be fit to the $S(Q)$ are a Lorentzian (Appendix A.) which has been found to describe short range fluctuations in matter, and the Tuebnerstrey (Appendix A.) which has been used as a structural model for the analysis of microemulsions. These functions allow the interpretation of the gel network as consisting of two components (polymer chains and water), which have a correlation length associated with the size of the water domain. The interpretation of such a functional fit may yield further information about the pore size and other structural characteristics.

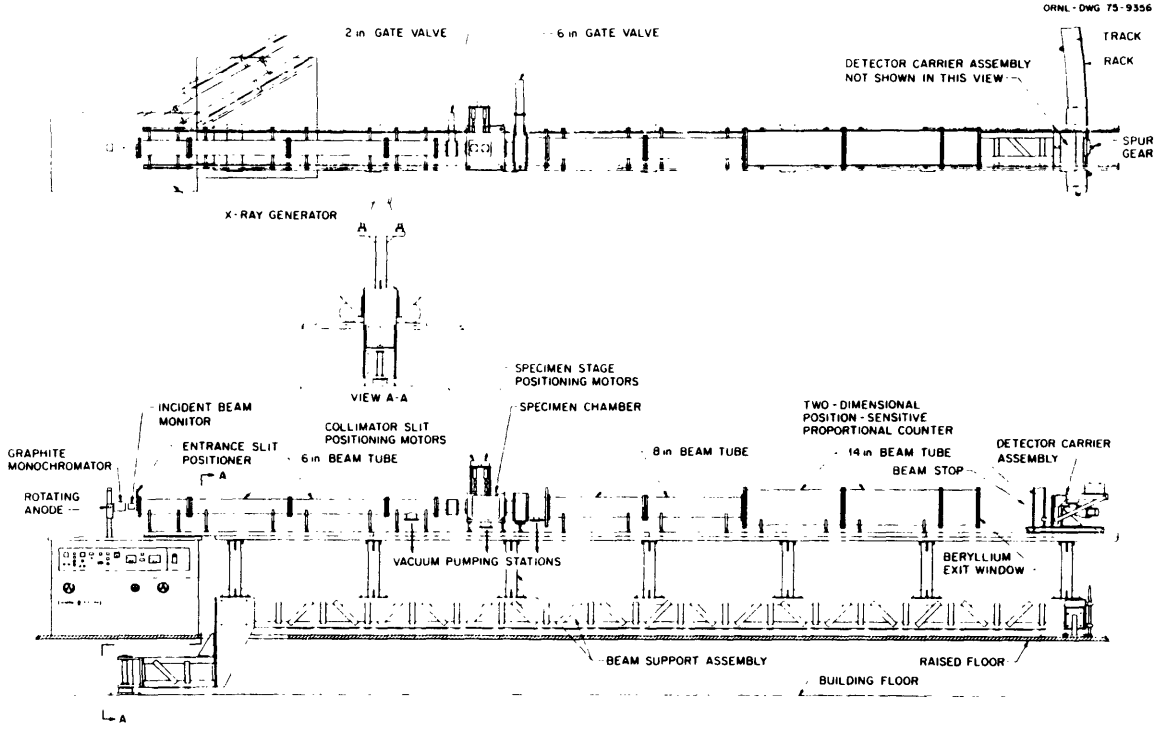

Figure 3-1: Schematic Drawing of the ORNL 10-m Small-Angle Y-Ray Scattering Camera.

(a)

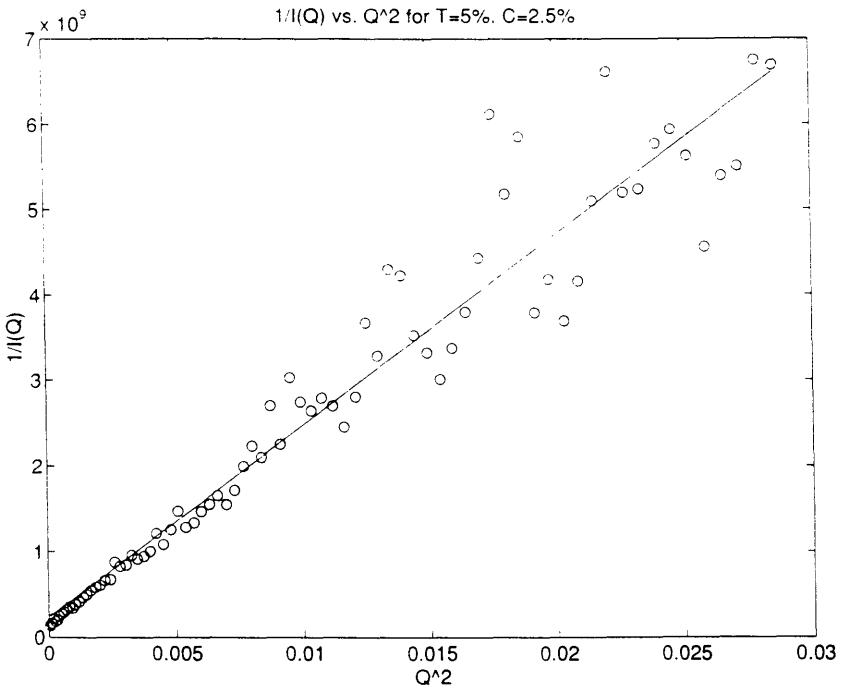

(b)

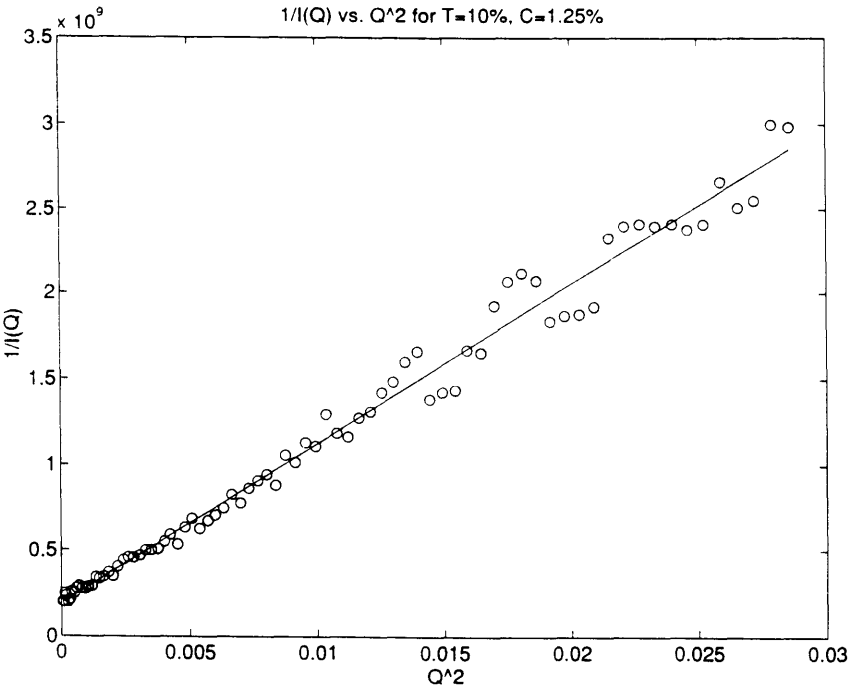

Figure 3-2: The large Q linear fits to $1/I(Q)$ vs. Q^2 plots of the data sets.

(c)

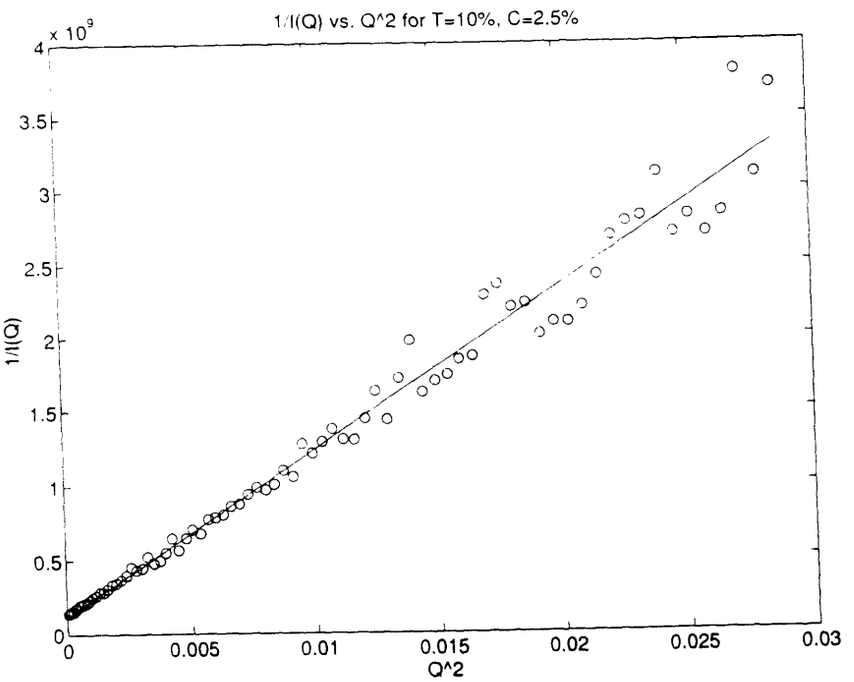
1/I(Q) vs. Q^2 for T=10%, C=2.5%
x 10^9
1/I(Q)
Q^2
0
0.5
1
1.5
2
2.5
3
3.5
4
0.005
0.01
0.015
0.02
0.025
0.03

(d)

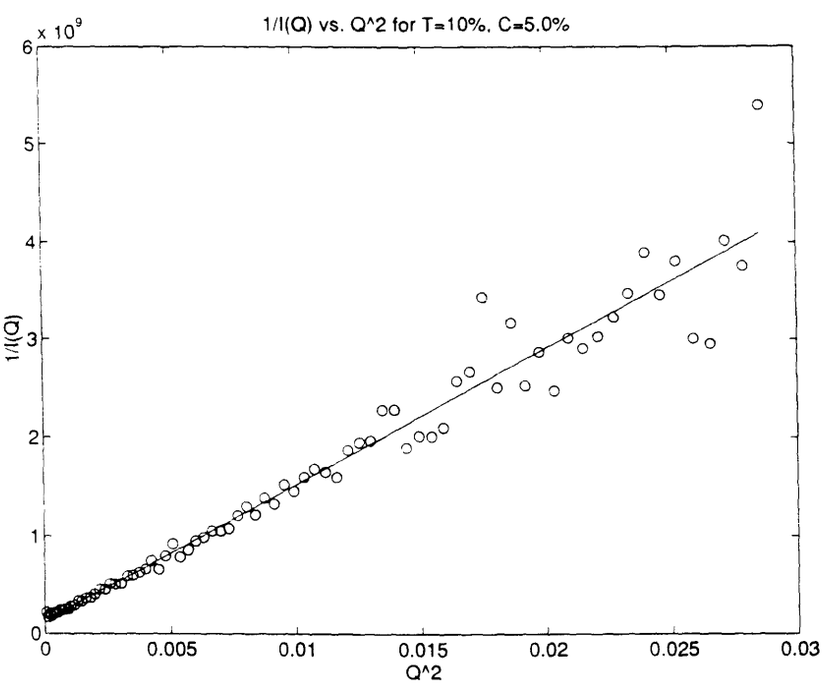
1/I(Q) vs. Q^2 for T=10%, C=5.0%
x 10^9
1/I(Q)
Q^2
0
1
2
3
4
5
6
0.005
0.01
0.015
0.02
0.025
0.03

(e)

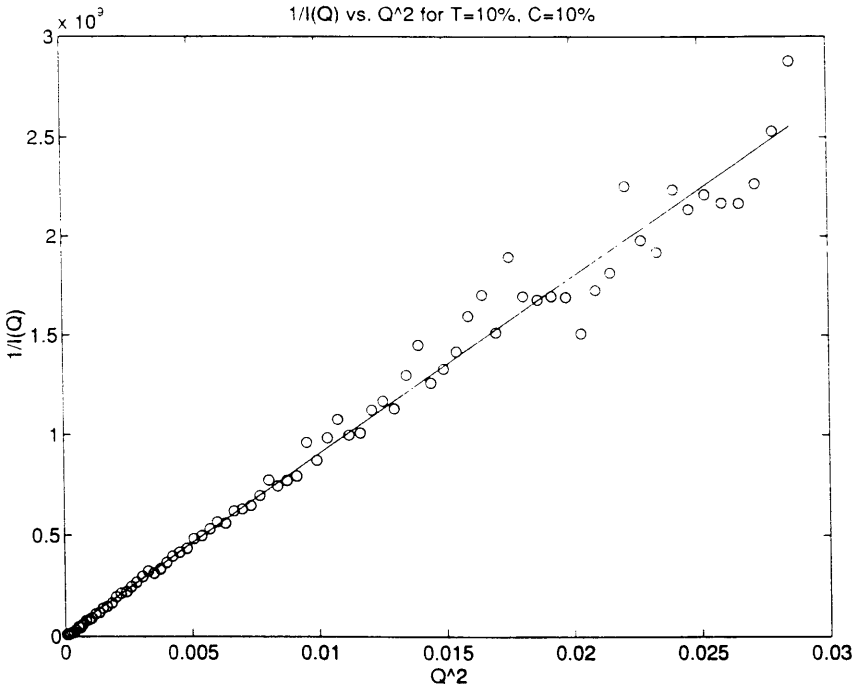
1/I(Q) vs. Q^2 for T=10%, C=10%
x 10^9
3
2.5
2
1.5
1
0.5
0
1/I(Q)
0
0.005
0.01
0.015
0.02
0.025
0.03
Q^2

(f)

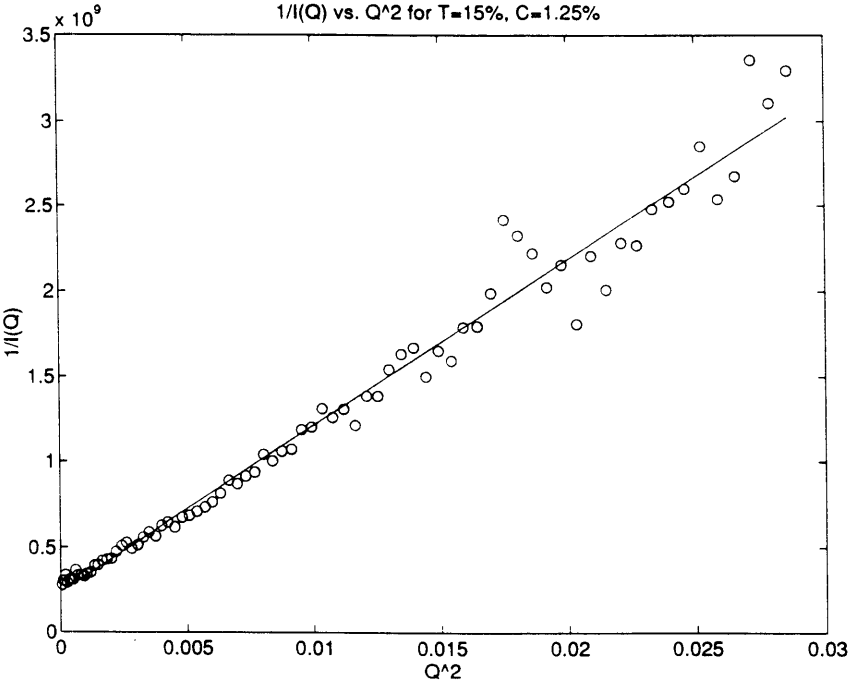
1/I(Q) vs. Q^2 for T=15%, C=1.25%
x 10^9
3.5
3
2.5
2
1.5
1
0.5
0
1/I(Q)
0
0.005
0.01
0.015
0.02
0.025
0.03
Q^2

(g)

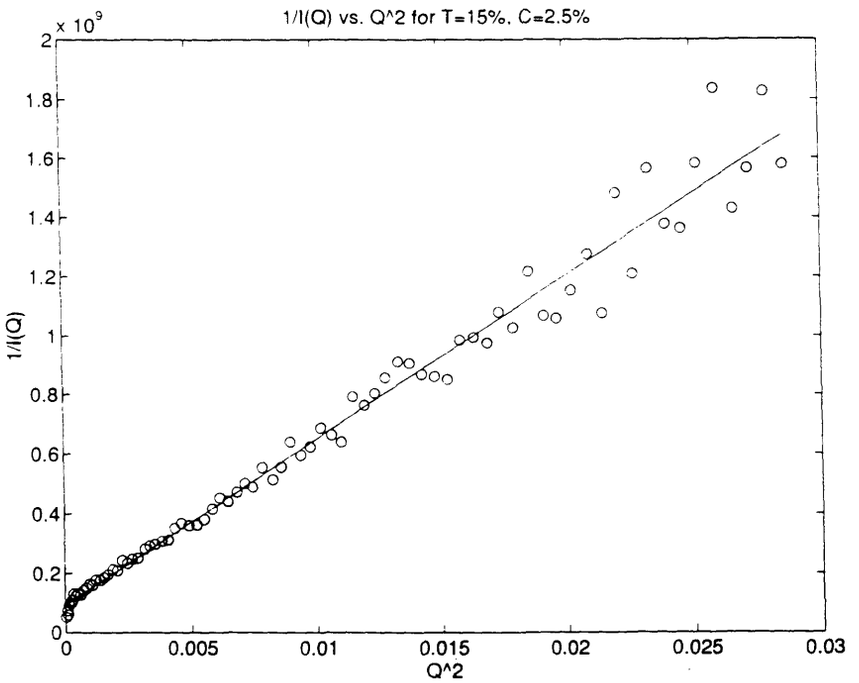
1/I(Q) vs. Q^2 for T=15%, C=2.5%
x 10^9
2
1.8
1.6
1.4
1.2
1
0.8
0.6
0.4
0.2
0
1/I(Q)
0
0.005
0.01
0.015
0.02
0.025
0.03
Q^2

(h)

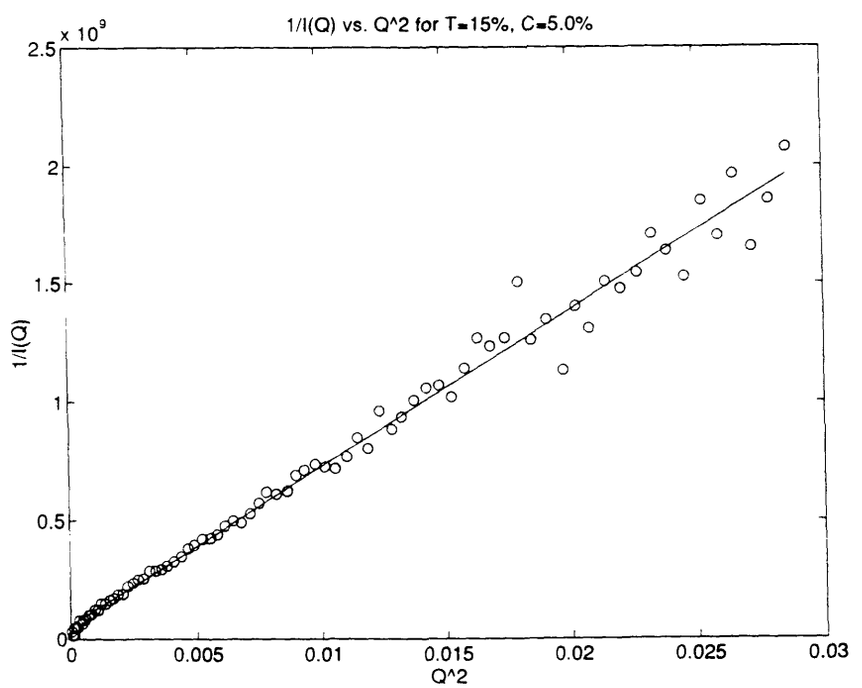
1/I(Q) vs. Q^2 for T=15%, C=5.0%
x 10^9
2.5
2
1.5
1
0.5
0
1/I(Q)
0
0.005
0.01
0.015
0.02
0.025
0.03
Q^2

(i)

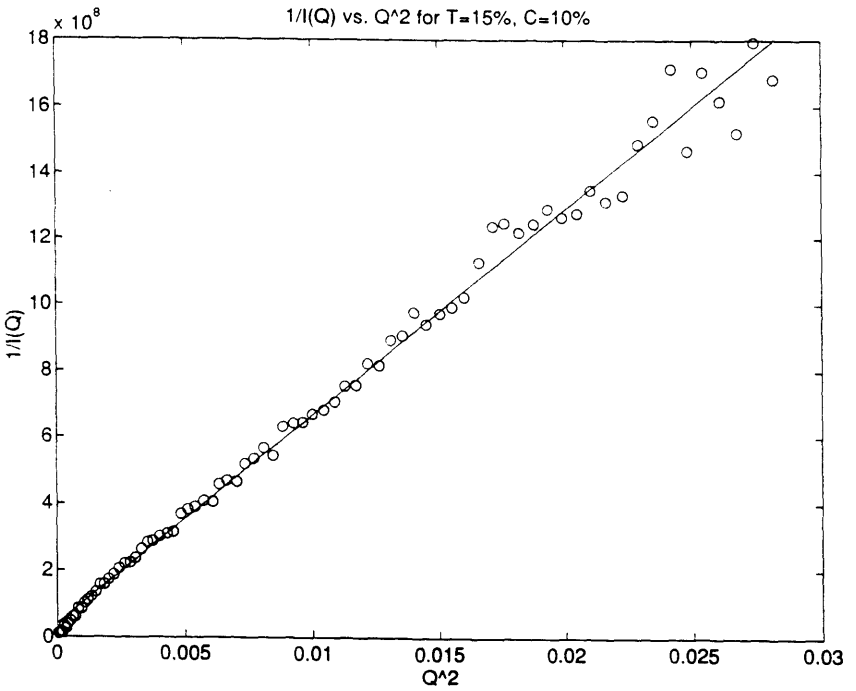
1/I(Q) vs. Q^2 for T=15%, C=10%
x 10^8
1/I(Q)
Q^2
0
2
4
6
8
10
12
14
16
18
0.005
0.01
0.015
0.02
0.025
0.03

(j)

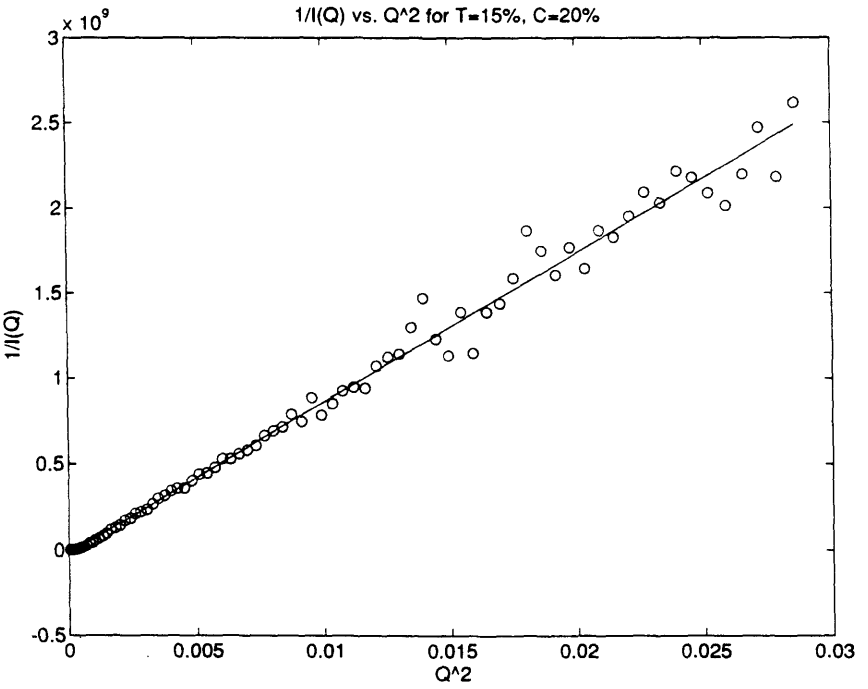
1/I(Q) vs. Q^2 for T=15%, C=20%
x 10^9
1/I(Q)
Q^2
-0.5
0
0.5
1
1.5
2
2.5
3
0.005
0.01
0.015
0.02
0.025
0.03

(k)

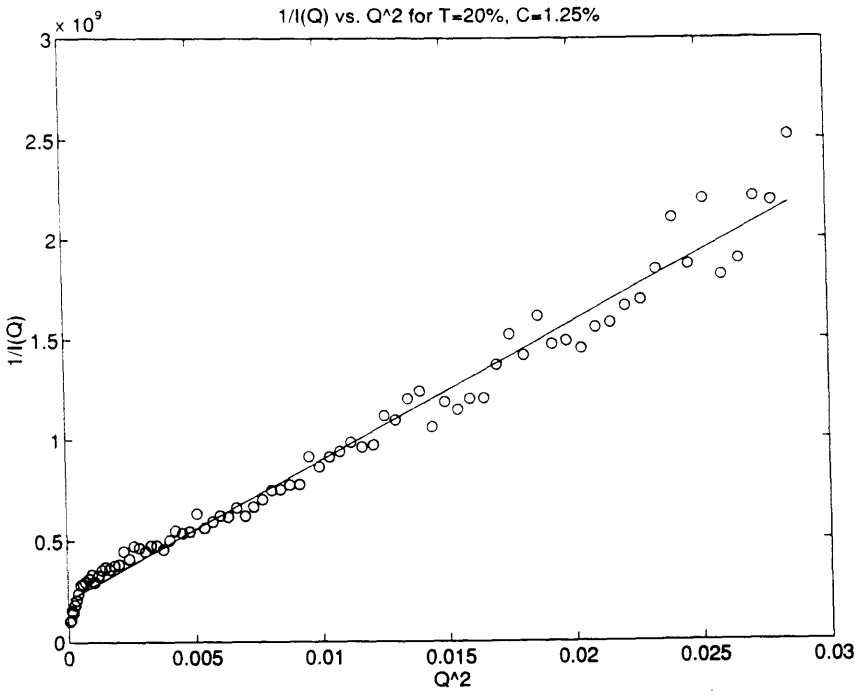
1/I(Q) vs. Q^2 for T=20%, C=1.25%
x 10^9
3
2.5
2
1.5
1
0.5
0
1/I(Q)
0
0.005
0.01
0.015
0.02
0.025
0.03
Q^2

(l)

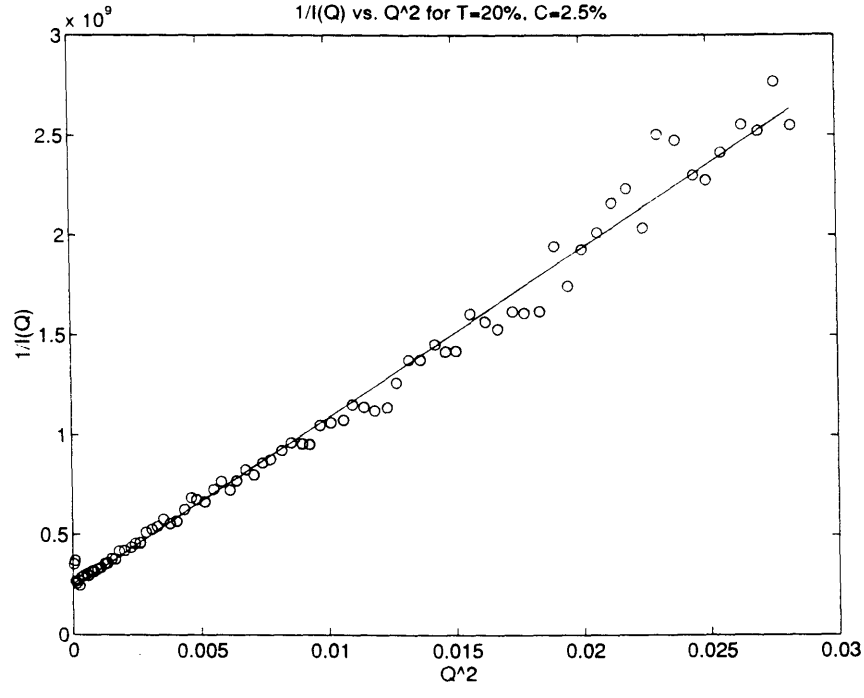
1/I(Q) vs. Q^2 for T=20%, C=2.5%
x 10^9
3
2.5
2
1.5
1
0.5
0
1/I(Q)
0
0.005
0.01
0.015
0.02
0.025
0.03
Q^2

(m)

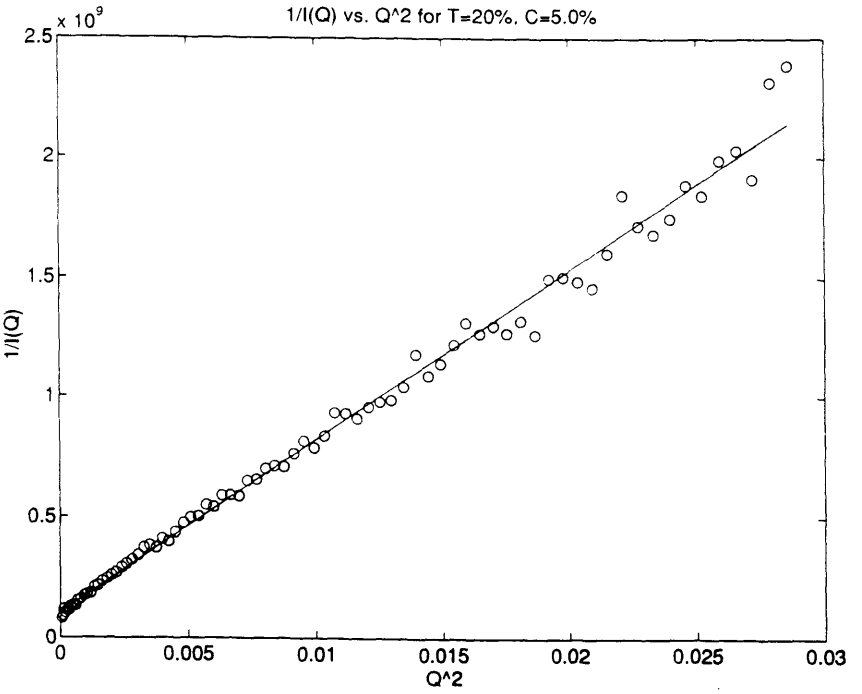
1/I(Q) vs. Q^2 for T=20%, C=5.0%
x 10^9
2.5
2
1.5
1
0.5
0
1/I(Q)
0
0.005
0.01
0.015
0.02
0.025
0.03
Q^2

(n)

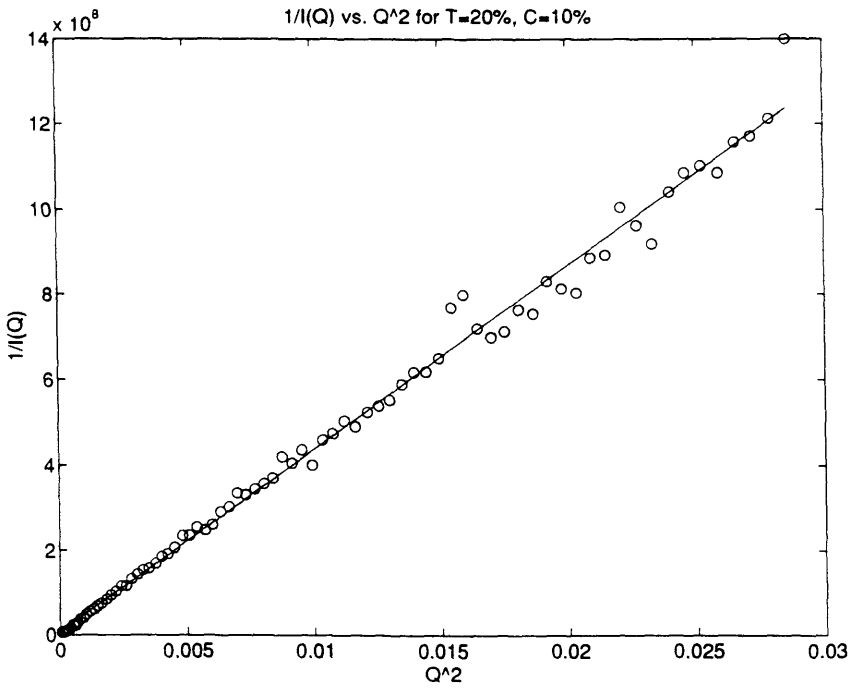
1/I(Q) vs. Q^2 for T=20%, C=10%
x 10^8
14
12
10
8
6
4
2
0
1/I(Q)
0
0.005
0.01
0.015
0.02
0.025
0.03
Q^2

(o)

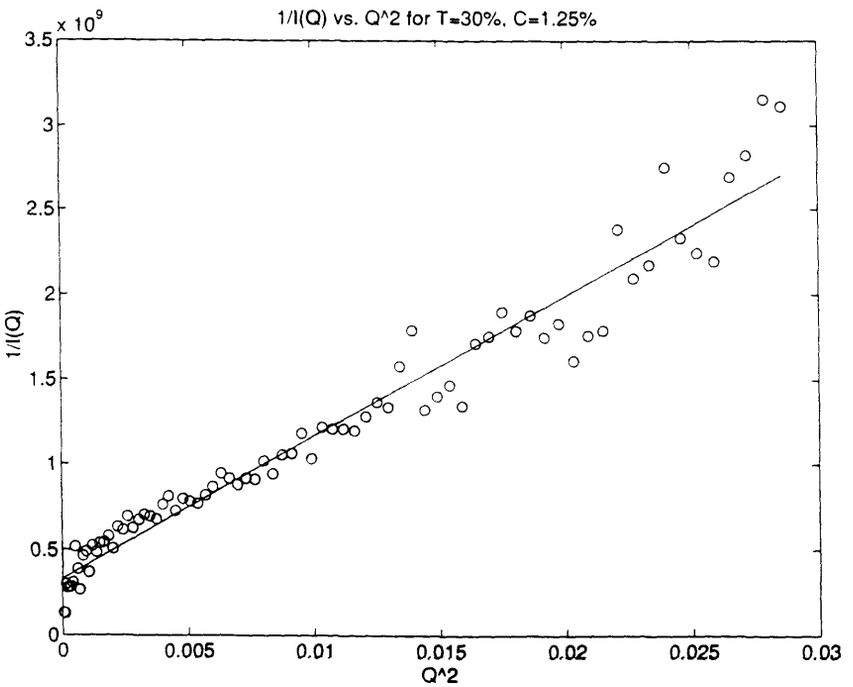
1/I(Q) vs. Q^2 for T=30%, C=1.25%
x 10^9
3.5
3
2.5
2
1.5
1
0.5
0
1/I(Q)
0
0.005
0.01
0.015
0.02
0.025
0.03
Q^2

(p)

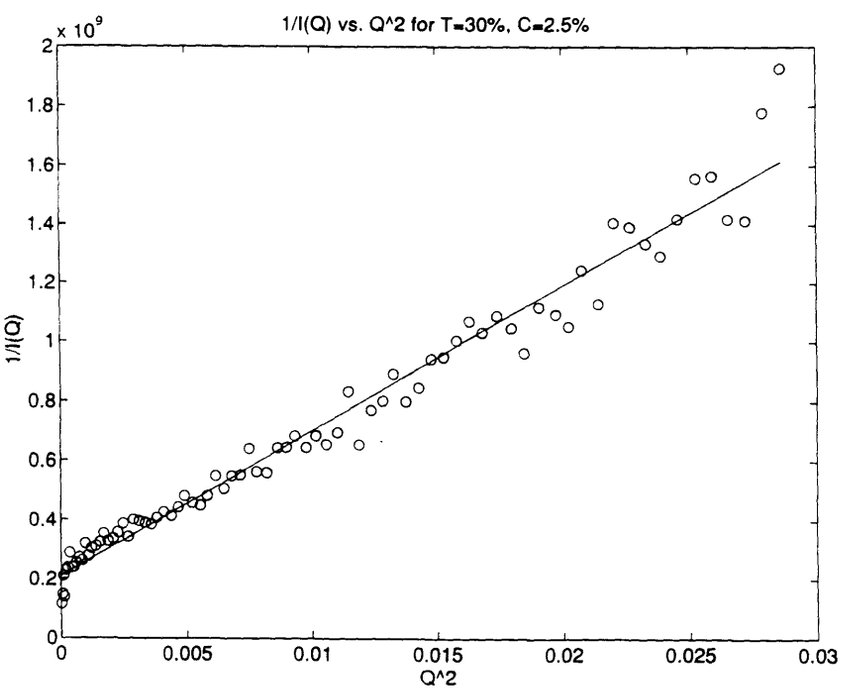
1/I(Q) vs. Q^2 for T=30%, C=2.5%
x 10^9
2
1.8
1.6
1.4
1.2
1
0.8
0.6
0.4
0.2
0
1/I(Q)
0
0.005
0.01
0.015
0.02
0.025
0.03
Q^2

(q)

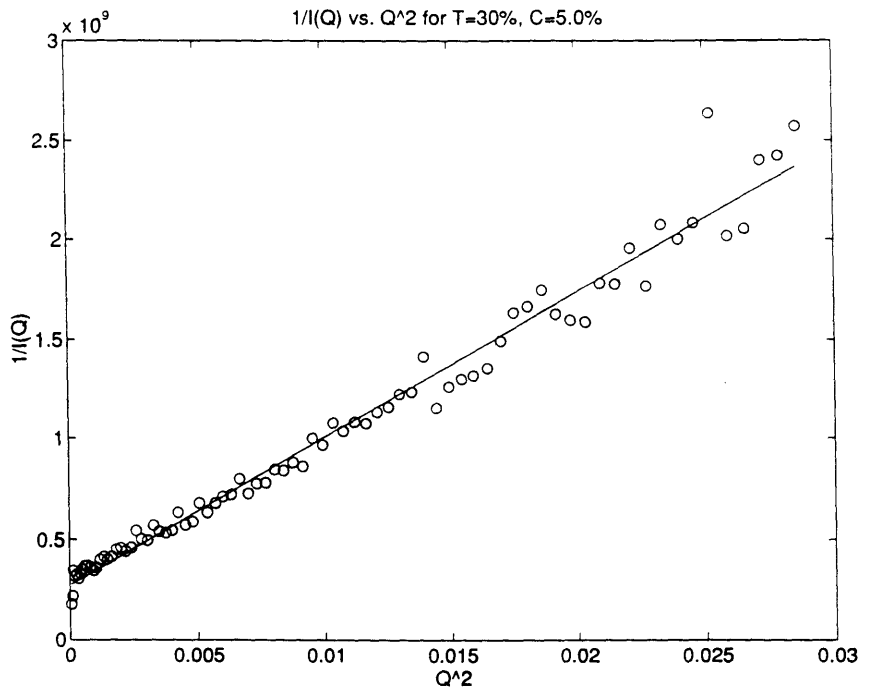
1/I(Q) vs. Q^2 for T=30%, C=5.0%
x 10^9
3
2.5
2
1.5
1
0.5
0
1/I(Q)
0
0.005
0.01
0.015
0.02
0.025
0.03
Q^2

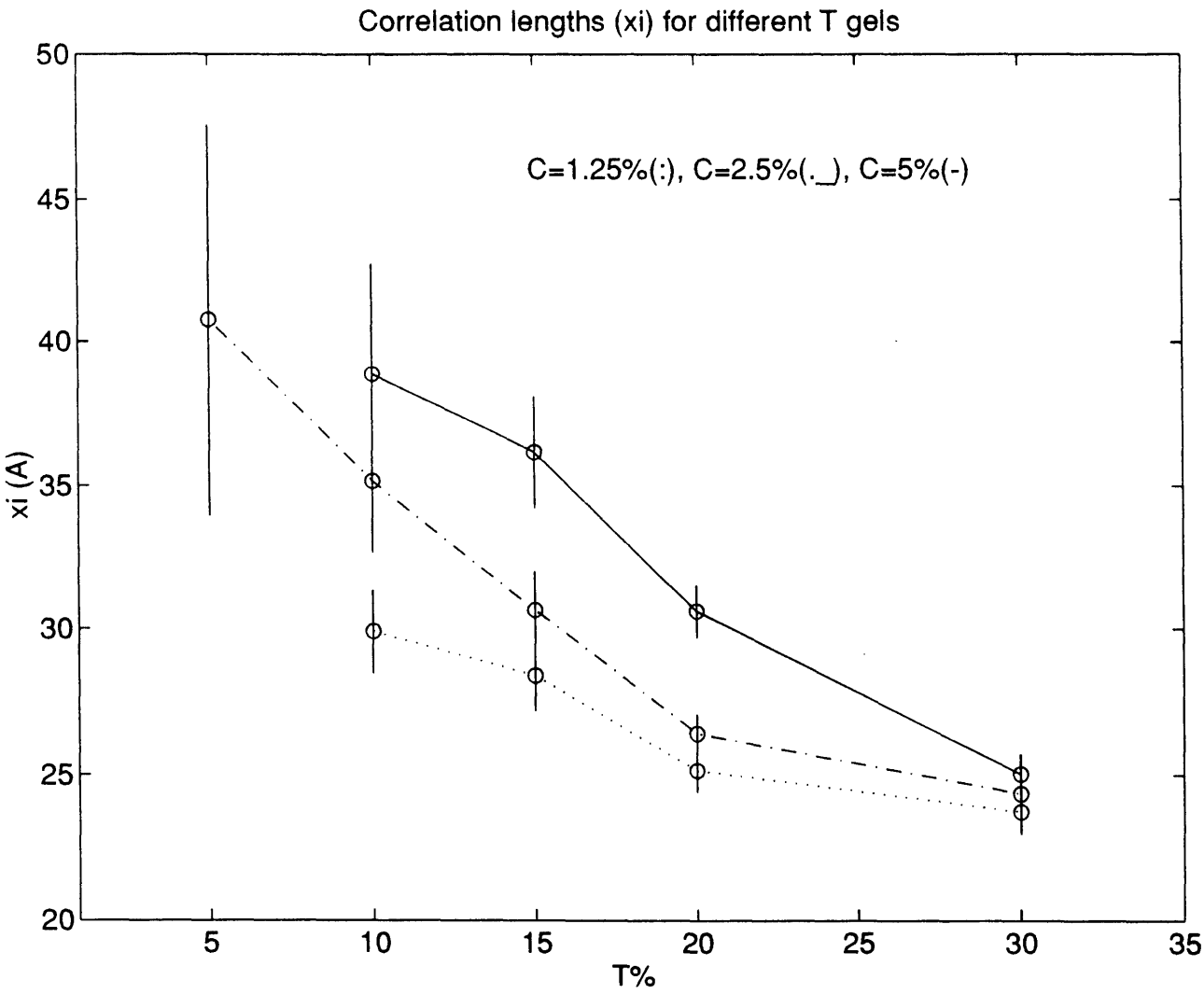

Figure 3-3: Values of ξ'^2 at constant crosslinker concentration C, varying the monomer concentration T.

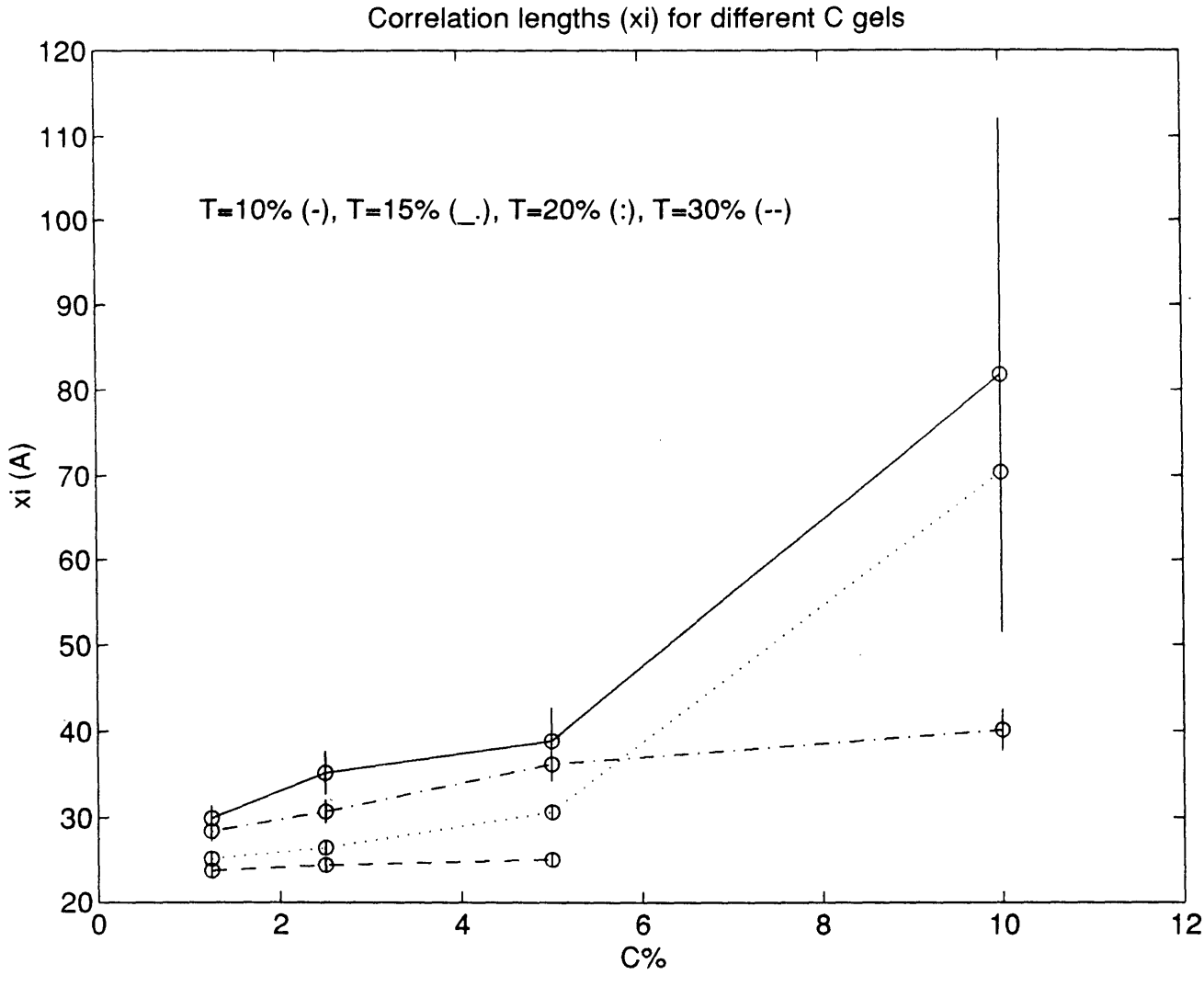

Figure 3-4: Values of ξ'^2 at constant monomer concentration T, varying the crosslinkerer concentration C.

Figure 3-5: Schematic diagram of structure for polyacrylamide gels as presented by Hecht *et. al.*. (a)Gels of low bisacrylamide content show a small correlation length ξ and a small radius of the chain r_o. (b)As bisacrylamide content in the gel increases, the chains become both thicker and denser and the separation ξ between chains increases.

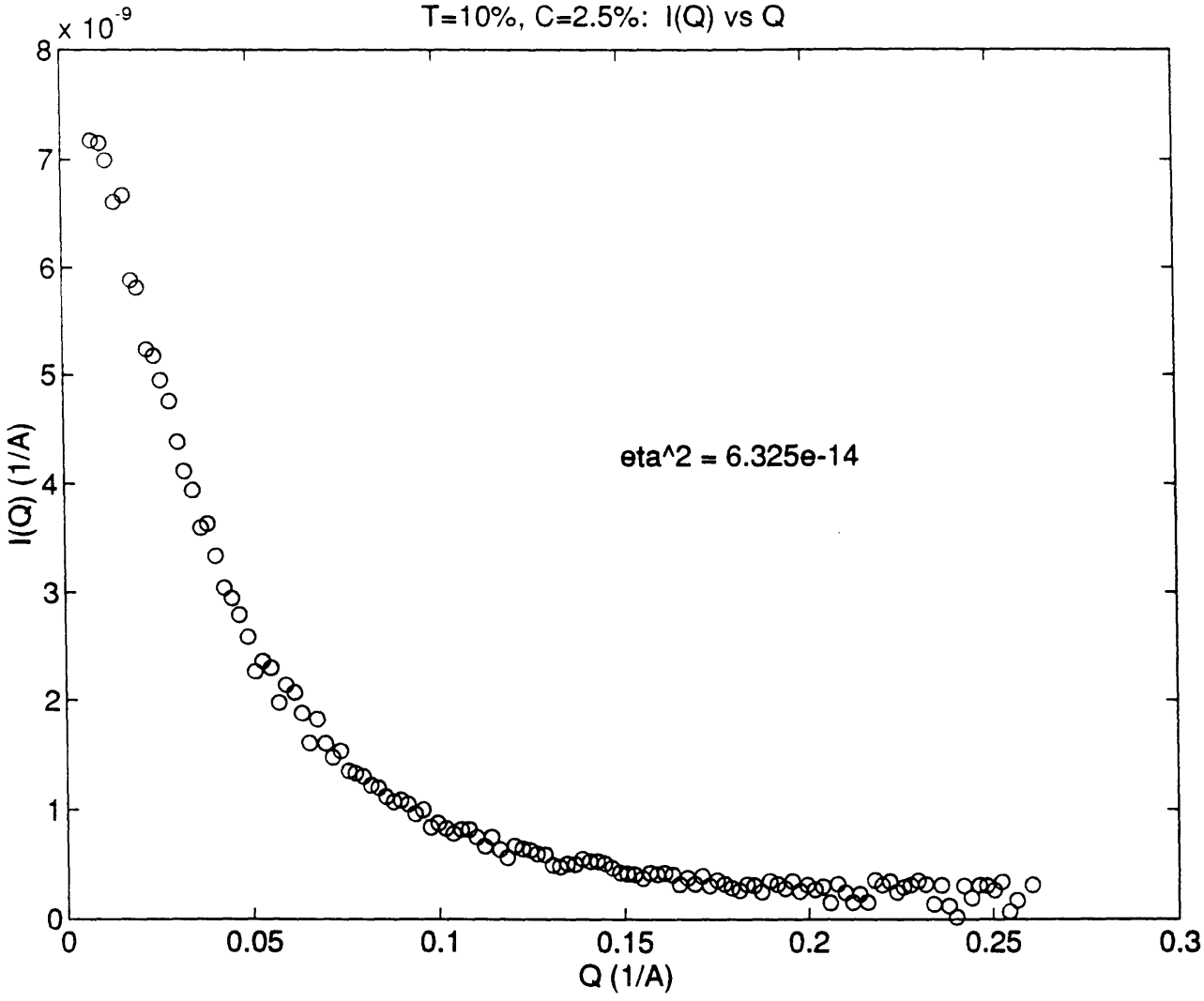

Figure 3-6: $I(Q)$ for T=10%, C=2.5%.

(a)

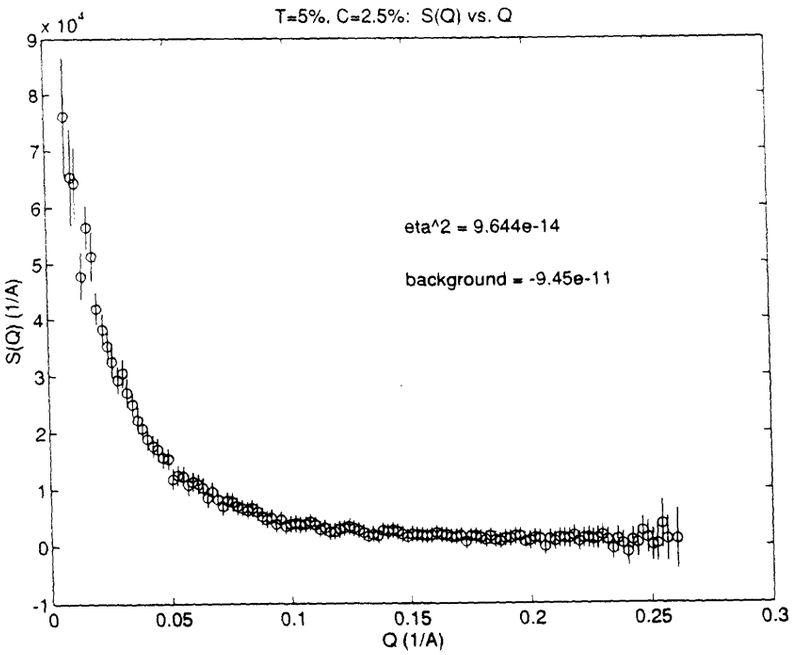

(b)

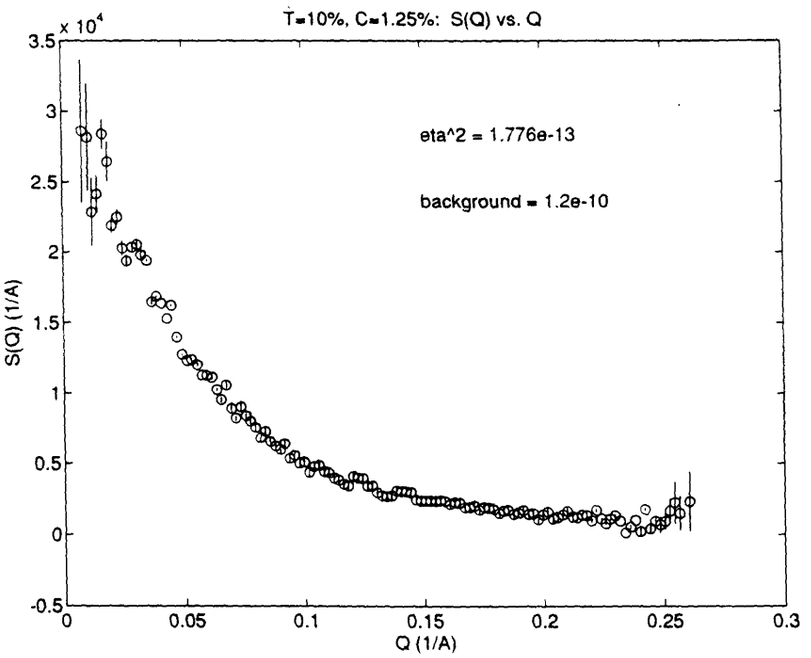

Figure 3-7: Absolute scattering intensity $S(Q)$ profiles for all gels.

(c)

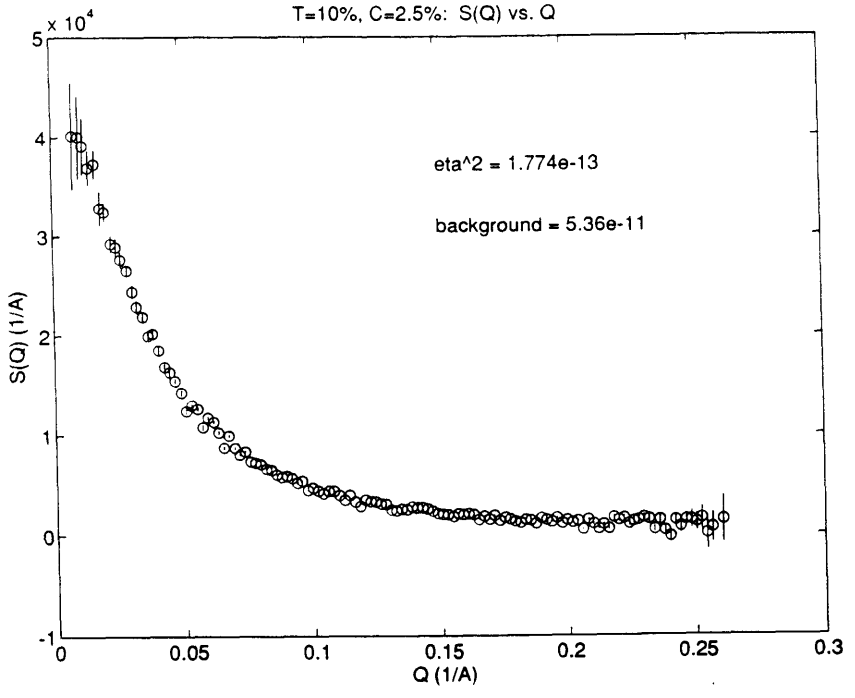
T=10%, C=2.5%: S(Q) vs. Q
x 10^4
eta^2 = 1.774e-13
background = 5.36e-11
S(Q) (1/A)
Q (1/A)

(d)

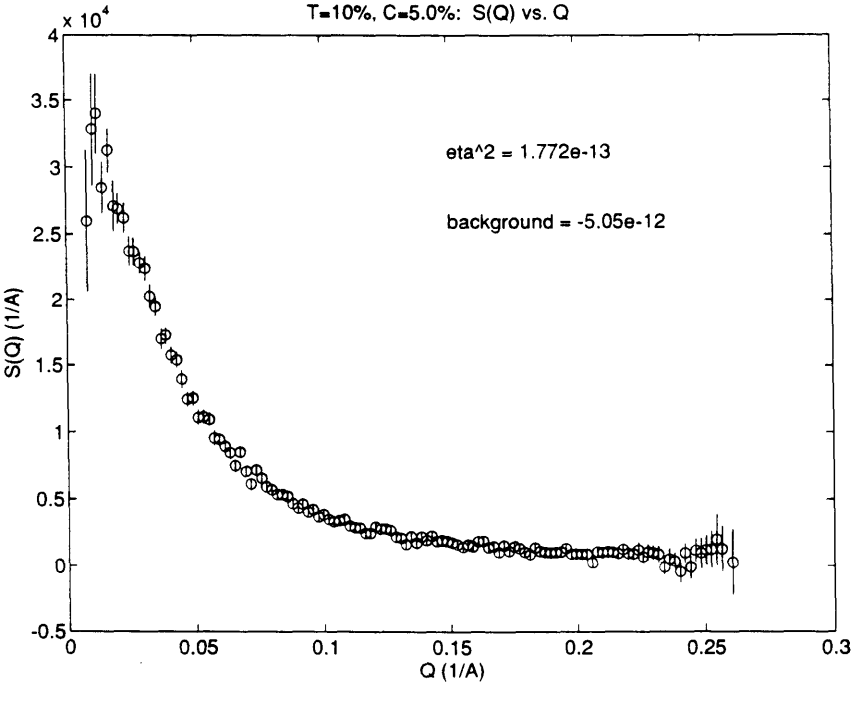
T=10%, C=5.0%: S(Q) vs. Q
x 10^4
eta^2 = 1.772e-13
background = -5.05e-12
S(Q) (1/A)
Q (1/A)

(e)

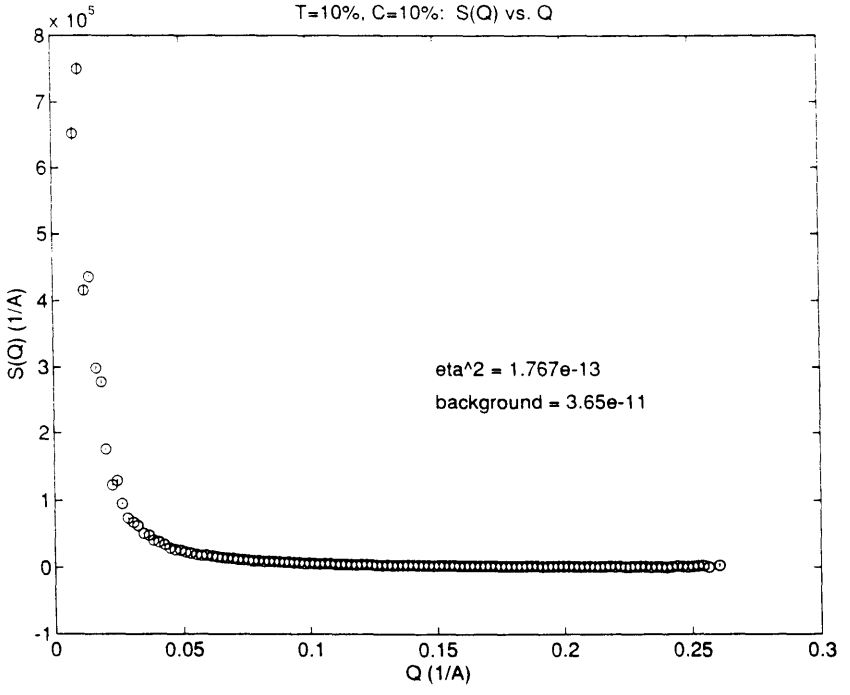
T=10%, C=10%: S(Q) vs. Q
x 10^5
S(Q) (1/A)
Q (1/A)
eta^2 = 1.767e-13
background = 3.65e-11

(f)

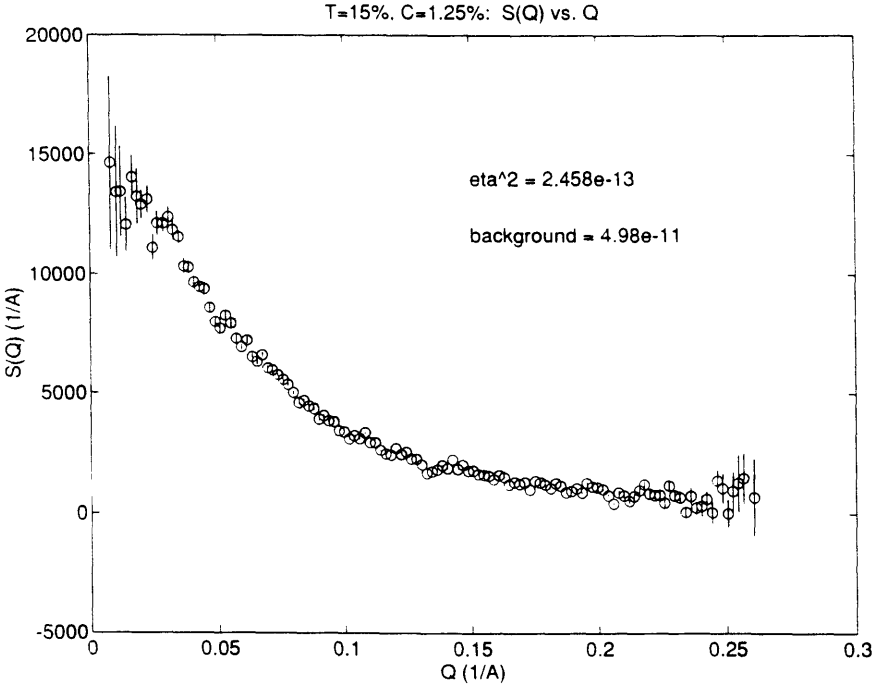
T=15%, C=1.25%: S(Q) vs. Q
S(Q) (1/A)
Q (1/A)
eta^2 = 2.458e-13
background = 4.98e-11

(g)

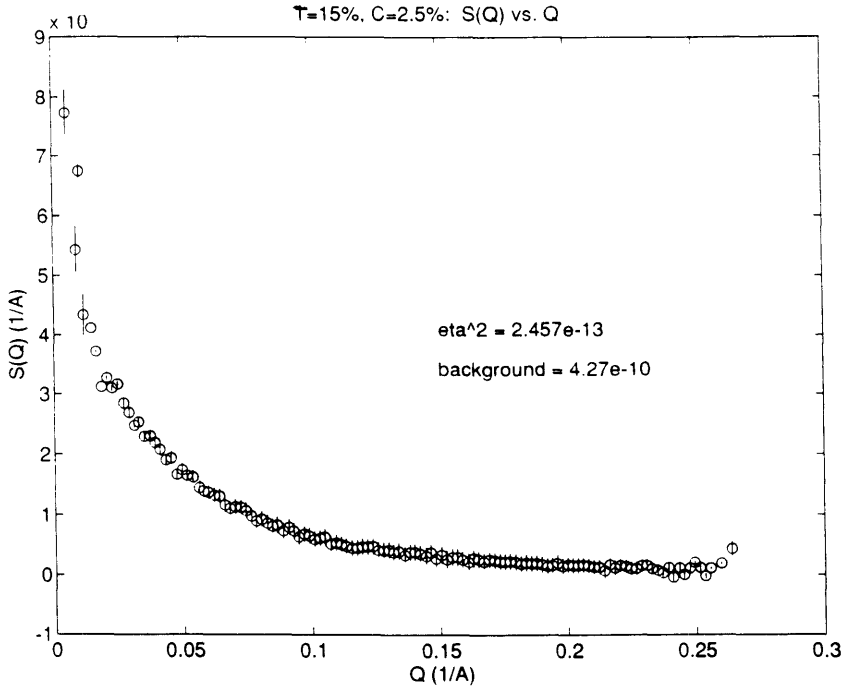
T=15%, C=2.5%: S(Q) vs. Q
x 10
S(Q) (1/A)
Q (1/A)
eta^2 = 2.457e-13
background = 4.27e-10

(h)

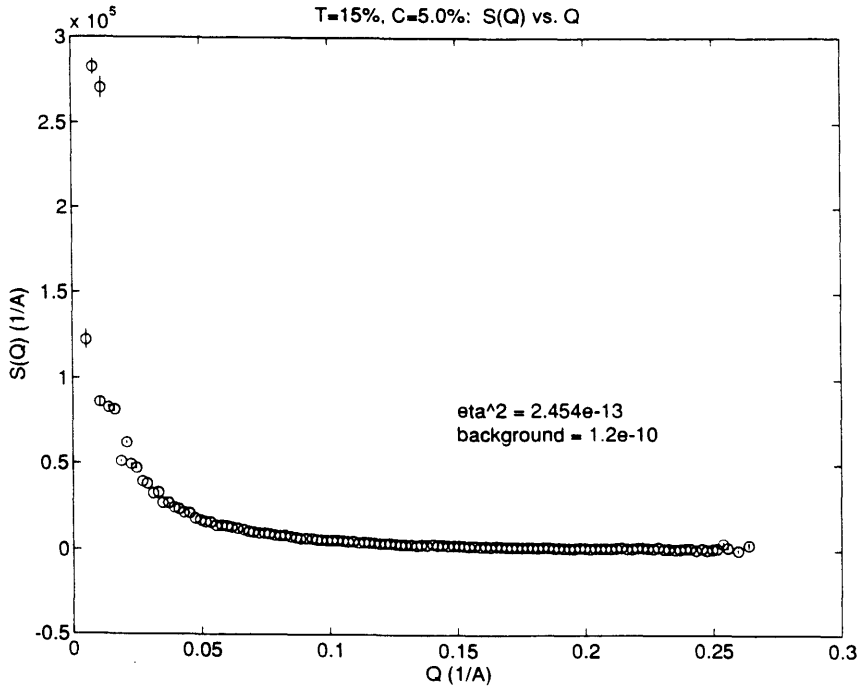
T=15%, C=5.0%: S(Q) vs. Q
x 10^5
S(Q) (1/A)
Q (1/A)
eta^2 = 2.454e-13
background = 1.2e-10

(i)

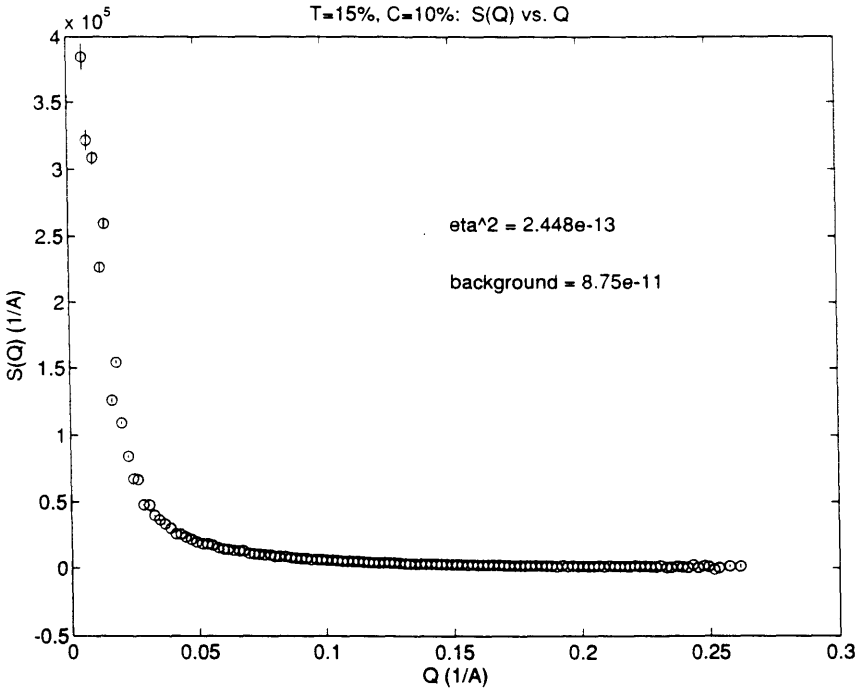
T=15%, C=10%: S(Q) vs. Q
x 10^5
S(Q) (1/A)
Q (1/A)
eta^2 = 2.448e-13
background = 8.75e-11

(j)

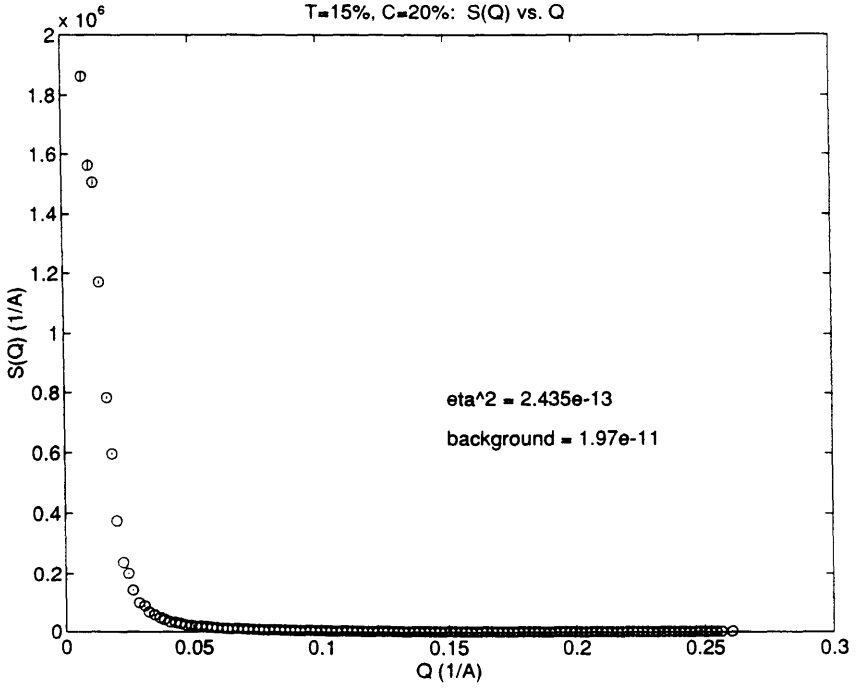
T=15%, C=20%: S(Q) vs. Q
x 10^6
S(Q) (1/A)
Q (1/A)
eta^2 = 2.435e-13
background = 1.97e-11

(k)

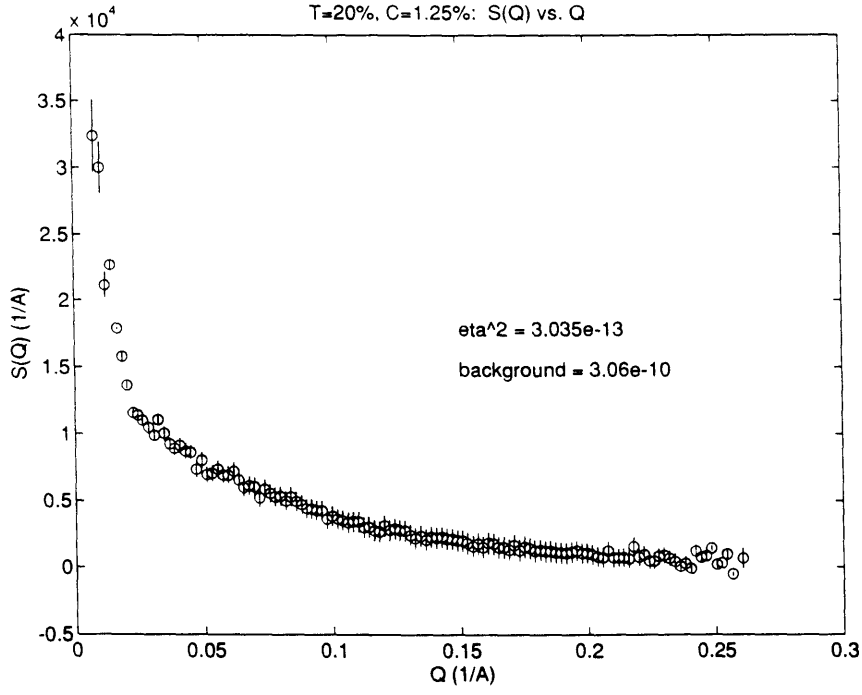
T=20%, C=1.25%: S(Q) vs. Q
x 10^4
S(Q) (1/A)
Q (1/A)
eta^2 = 3.035e-13
background = 3.06e-10

(l)

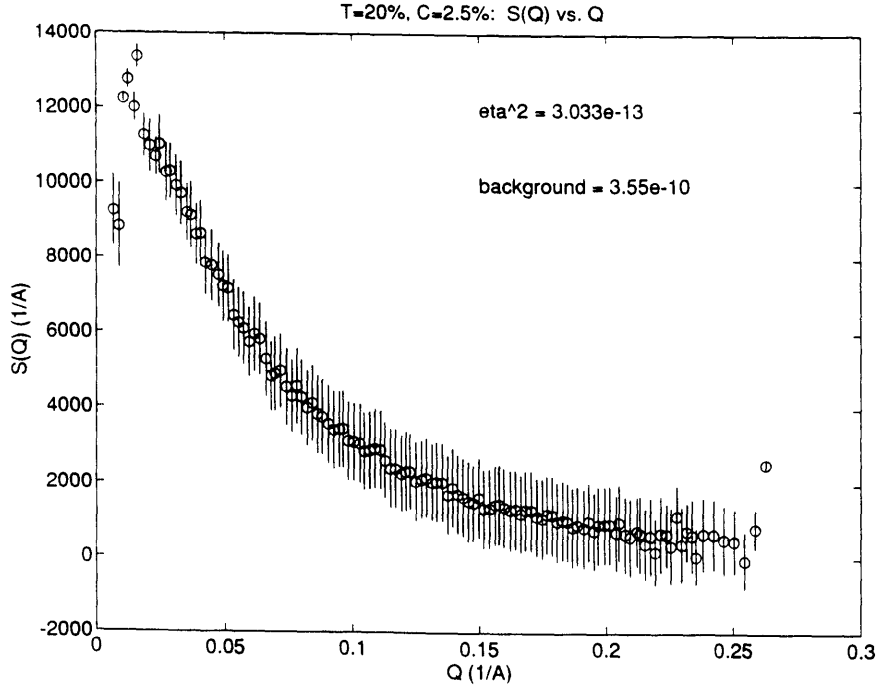
T=20%, C=2.5%: S(Q) vs. Q
S(Q) (1/A)
Q (1/A)
eta^2 = 3.033e-13
background = 3.55e-10

(m)

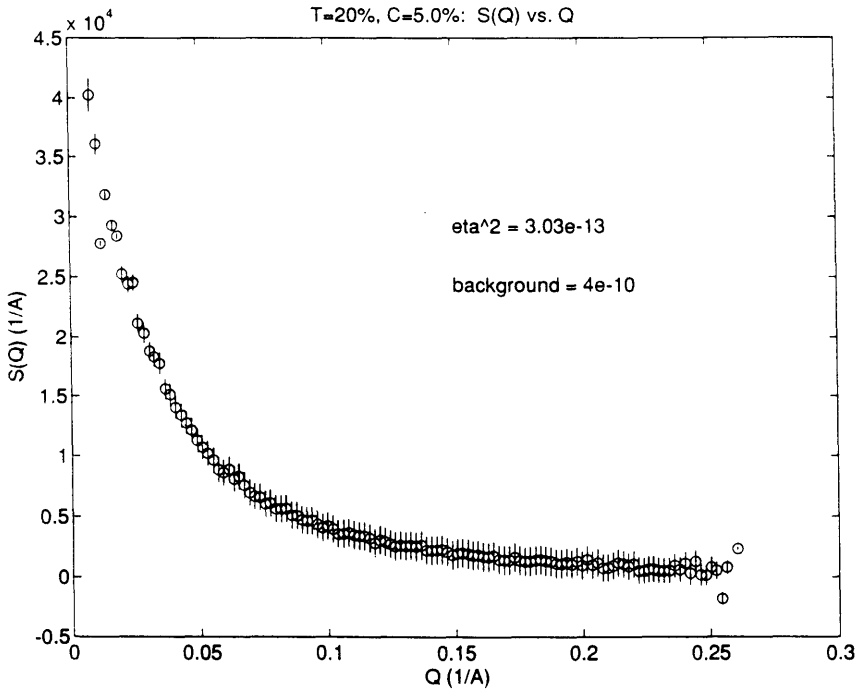
T=20%, C=5.0%: S(Q) vs. Q
x 10^4
4.5
4
3.5
3
2.5
2
1.5
1
0.5
0
-0.5
S(Q) (1/A)
eta^2 = 3.03e-13
background = 4e-10
0
0.05
0.1
0.15
0.2
0.25
0.3
Q (1/A)

(n)

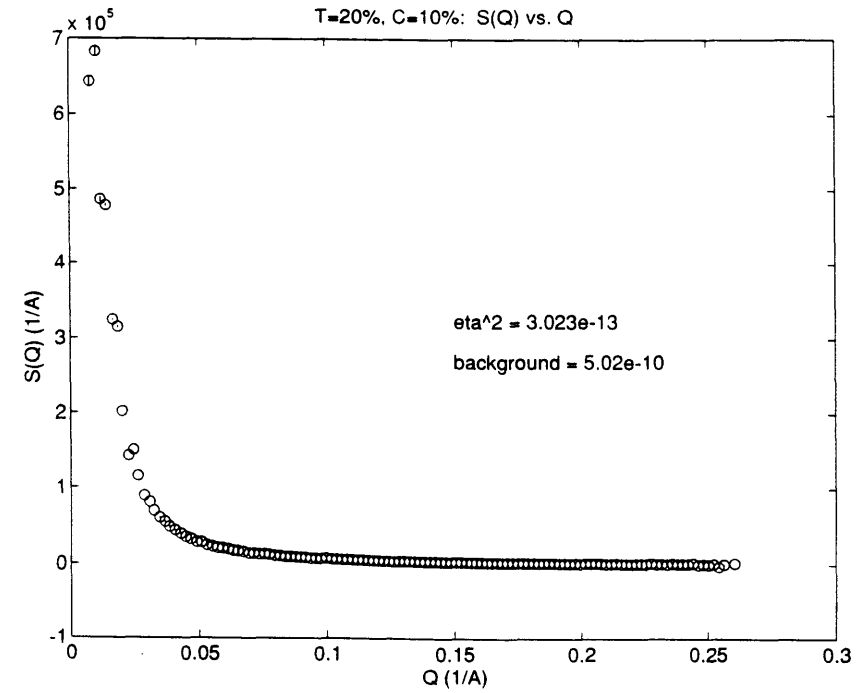
T=20%, C=10%: S(Q) vs. Q
x 10^5
7
6
5
4
3
2
1
0
-1
S(Q) (1/A)
eta^2 = 3.023e-13
background = 5.02e-10
0
0.05
0.1
0.15
0.2
0.25
0.3
Q (1/A)

(p)

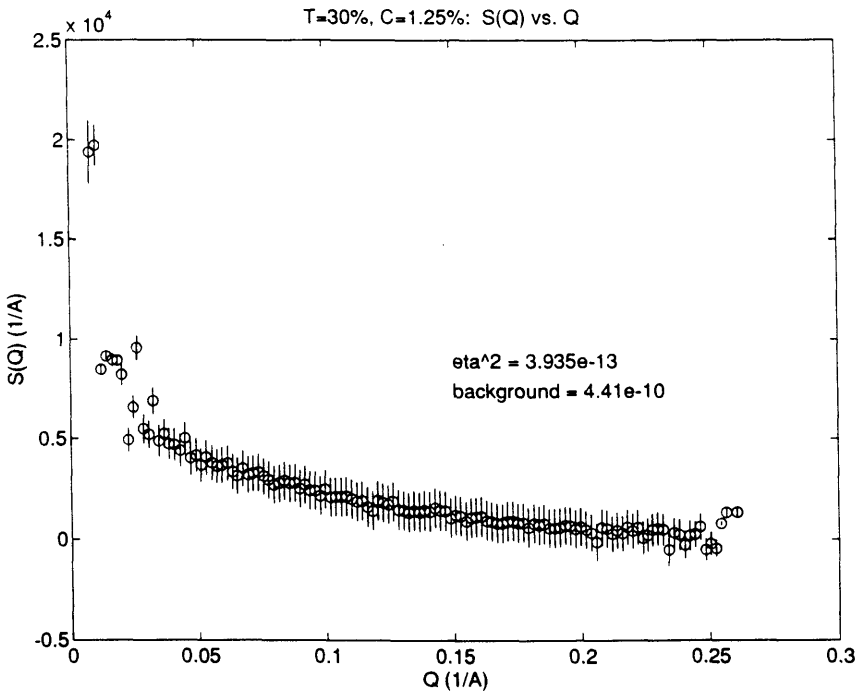
T=30%, C=1.25%: S(Q) vs. Q
x 10^4
S(Q) (1/A)
Q (1/A)
eta^2 = 3.935e-13
background = 4.41e-10

(o)

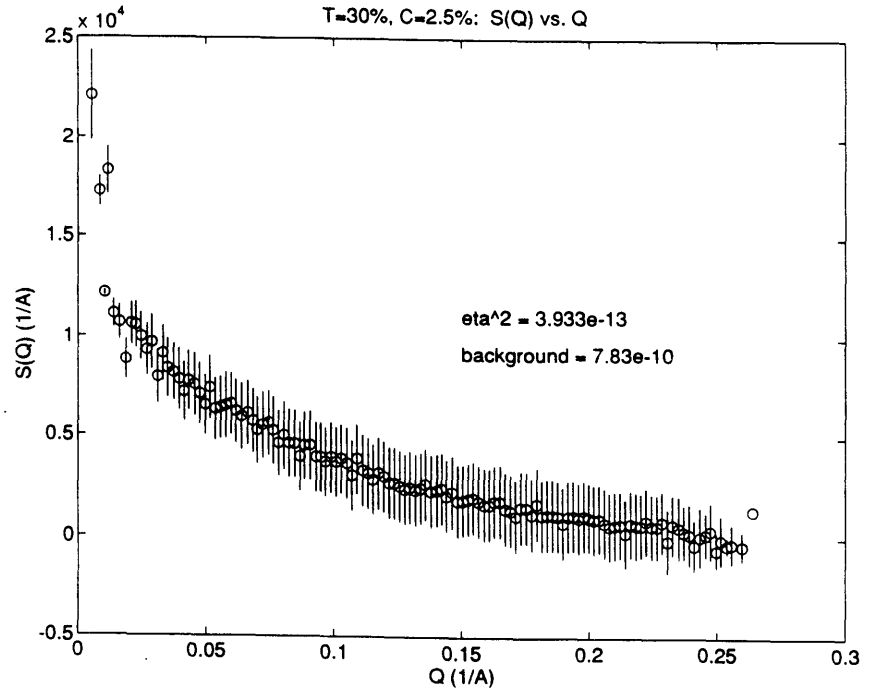
T=30%, C=2.5%: S(Q) vs. Q
x 10^4
S(Q) (1/A)
Q (1/A)
eta^2 = 3.933e-13
background = 7.83e-10

(q)

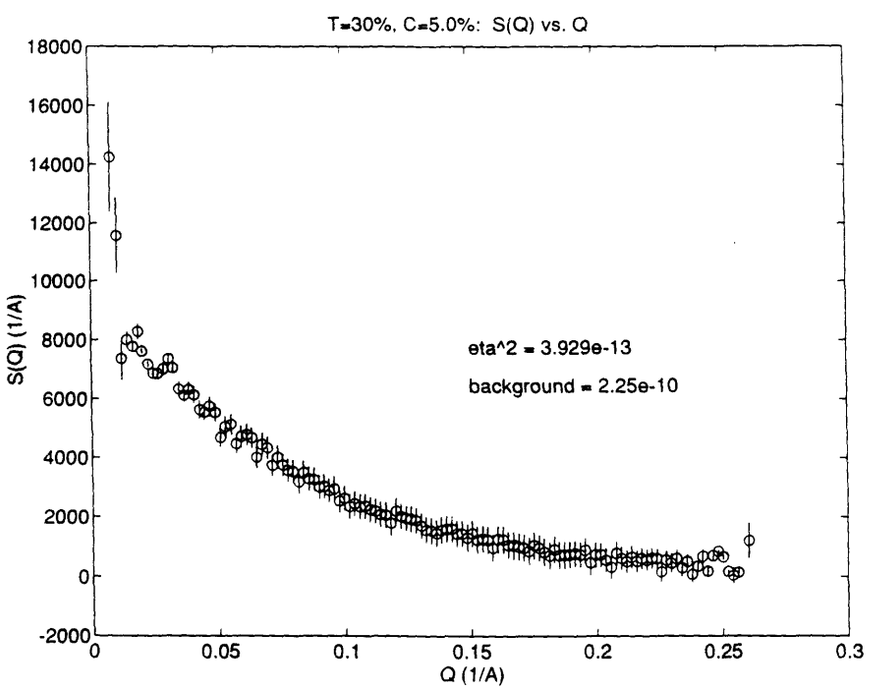
T=30%, C=5.0%: S(Q) vs. Q
S(Q) (1/A)
Q (1/A)
eta^2 = 3.929e-13
background = 2.25e-10
18000
16000
14000
12000
10000
8000
6000
4000
2000
0
-2000
0
0.05
0.1
0.15
0.2
0.25
0.3

sample	T% (mL)	40% solution pH 8.8 (mL)	4×Tris·Cl/SDS (mL)	H_2O
1	5	1.25	2.5	6.25
2	10	2.5	2.5	5.0
3	15	3.75	2.5	3.75
4	20	5.0	2.5	2.5
5	30	7.5	2.5	0

Table 3.1: Using a stock solution of T=40% and respectively, C=1.25, 2.5, 5, and 10%; the stock solutions were diluted in the proportions given above to produce a 10 mL sample of each type of gel. Each monomer solution was degassed in vacuum for 15-20 minutes. 0.025 mL of 10% accelerator (APS) solution and 0.005 mL of initiator (TEMED) were added to the sample solutions just prior to gelation.

	C=1.25%	C=2.5%	C=5%	C=10%
T=5%	none	34.20±12.0Å	none	none
T=10%	42.98±4.8Å	52.20±8.0Å	50.98±10.7Å	349.6±260Å
T=15%	36.78±3.7Å	76.61±7.8Å	91.73±10.5Å	120.5±15.2Å
T=20%	40.52±3.0Å	35.87±2.1Å	60.08±4.1Å	537.0±174Å
T=30%	28.15±2.4Å	48.67±4.0Å	35.73±2.5Å	none

Table 3.2: The effective correlation length ξ'^2 values for gel samples.

Chapter 4

Conclusion

It has been shown that small angle X-ray scattering (SAXS) yields information about the effective pore size and local correlation of pores in polyacrylamide gels of different monomer (T) and crosslinker (C) concentrations. Furthermore, the structural information gained from SAXS is consistent with electrophoretic results from SDS-protein complexes migrating through polyacrylamide gels. In chapter 2, it was found that when the crosslinker concentration C was fixed, and the monomer concentration T was raised, the mobilities of SDS-protein complexes within the gel medium decreased depending on their molecular weights. This indicates that the pore size of the gels decreased as T was incresased. Heavier proteins moved a greater distance in the gels than lighter proteins. Likewise, when the monomer concentration T was fixed, and the crosslinker concentration C was raised, the mobilities of SDS-protein complexes within the gel medium again decreased depending on their molecular weights. This indicates that the pore size decreased as the C is increased.

In chapter 3, the large Q data was fitted to a Tuebner-Strey model of a bicontinuous structure which has been successfully applied to water-oil microemulsion systems. The scattering intensity $I(Q)$ was shown by Debye as

$$I(Q) = (\Delta\rho)^2\phi_p(1-\phi_p)\int_0^\infty dr 4\pi^2 \frac{\sin Qr}{Qr}\Gamma_D(r) \tag{4.1}$$

$$= (\Delta\rho)^2\phi_p(1-\phi_p)S(Q) \tag{4.2}$$

where the Debye correlation function $\Gamma_D(r)$ was found by Teubner and Strey for the case of a bicontinuous structure to be

$$\Gamma_D(r) = \exp^{-r/\xi} \frac{\sin kr}{kr} \tag{4.3}$$

In equation (1.3), $k = 2\pi/d$, where d is the inter-pore distance and ξ is the coherence length which measures the extent of order from a central point. The resulting structure factor $S(Q)$ for the Tuebner-Strey model is

$$S(Q) = \frac{8\pi\xi^3}{(k^2\xi^2+1)^2 + 2(1-k^2\xi^2)\xi^2Q^2 + \xi^4Q^4} \tag{4.4}$$

In the Q region covered by this experiment, the Q^4 term in the Tuebner-Strey model is negligible and the resulting model had a Lorentzian form. From this analysis, the effective Lorentzian length scale $(\xi')^2 = \alpha(\xi)^2$ was determined to have a trend as the T and C of the gel were varied. For a fixed crosslinker concentration C, the ξ' were found to decrease with increasing polymer concentration T. If the Lorentzian length scale is identified with an effective pore size, then the pore size of the gel decreases with larger monomer concentration T. This interpretation is consistent with the electrophoresis results for SDS-protein complexes in polyacrylamide gel which demonstrate that the effective pore size becomes smaller with increasing T.

For a fixed polymer concentration T, the Lorentzian lengths ξ' were found to increase with increasing crosslinker concentration C, and in the case of C=20% the $(\xi')^2$ was found to be negative. The negative value is consistant with the Teubner-Strey model because α is allowed to take both positive and negative values depending on whether $k\xi < 1$ or $k\xi > 1$. At first glance this trend in the Lorentzian length scale appears to contradict electrophoresis results. However, with increasing C, the topology of gels changes in such a way that the effective correlation length ξ' may increase in spite of the fact that the effective correlation length is decreasing. In fact, as the gel structure becomes more regular due to the addition of more crosslinker, the pore size decreases in response to an increasing coherence length. Thus, the effective pore size trends are again in agreement with those expected from electrophoretic

results. In the future, more careful and systematic SAXS measurements will be made, and the entire absolute scattering intensity $S(Q)$ will be analyzed with the Teubner-Strey model to extract d and ξ.

Bibliography

[1] B. Alberts, D. Bray, D. Lewis, J. Raff, K. Roberts, and J. D. Watson. *Molecular Biology of the Cell.* Garland Pub., Inc., New York, 1983.

[2] R. C. Allen, C. A. Saravis, and H. R. Maurer. *Gel Electrophoresis and Isoelectric Focusing of Proteins.* Walter de Gruyter, New York, 1984.

[3] Anthony T. Andrews. *Electrophoresis.* Claridon Press, Oxford, second edition, 1986.

[4] G. A. Banker and C. W. Cotman. *J. Biol. Chem.*, 247, 1972.

[5] H. Benoît, J. F Joanny, G. Hadziioannou, and B. Hammouda. Scattering by linear, branched, and copolymer chain molecules for large scattering vectors. *Macromolecules*, 33, 1993.

[6] H. J. Benoit. *Polym. Sci.*, 11, 1953.

[7] Bio-Rad Laboratories, 2000 Alfred Nobel Drive, Hercules, CA 94547. *Prestained SDS-PAGE Standards, Low, High, and Broad Range.* Catalog number 161-0318.

[8] Bio-Rad Laboratories, 2000 Alfred Nobel Drive, Hercules, CA 94547. *SDS-PAGE Molecular Weight Standards, High, Low and Broad Range.* Catalog number 161-0317.

[9] H. C. Birnboim. *Anal. Biochem.*, 29, 1969.

[10] D. P. Blatter and F. J. Reithel. *J. Chromatogr.*, 34, 1970.

[11] W. S. Bont, J. Geels, and G. Rezelman. *Anal. Biochem.*, 27, 1969.

[12] C. Bordier and A. Crettol-Jarvinen. *J. Biol. Chem.*, 254, 1979.

[13] G. J. Brewer, E. Lopez-Corella, and M. E. Noelken. *Clin. Chim. Acta*, 36, 1972.

[14] W. P. Campbell, C. W. Wrigley, and J. Margolis. *Anal. Biochem.*, 129, 1983.

[15] L. O. Chang, A. M. Srb, and F. C. Steward. *Nature*, 193, 1962.

[16] K. H. Chao, R. G. H. Cotton, and D. M. Danks. *Anal. Biochem.*, 103, 1980.

[17] D. W. Cleveland. *Methods Enzymol.*, 96, 1983.

[18] J. S. Condeelis. *Anal. Biochem.*, 77, 1977.

[19] J. R. Davie. *Anal. Biochem.*, 120, 1982.

[20] B. J. Davis and L. Ronstein. *Ann N. Y. Acad. Sci.*, 121, 1964.

[21] P. J. Debye. *Appl. Phys.*, 68, 1944.

[22] P. G. deGennes. *Scaling Concepts in Polymer Physics.* Cornell University Press, Ithaca, NY, 1979.

[23] M. DeMets, A. Lagosse, and M. Radaey. *J. Chromatogr.*, 43, 1969.

[24] E. J. Devillez. *Anal. Biochem.*, 9, 1964.

[25] R. DeWachter and W. Fiers. *Anal. Biochem.*, 49, 1972.

[26] A. K. Dunker and R. R. Rueckert. *J. Biol. Chem.*, 244, 1969.

[27] E. Epstein, Y. Houvras, and B. Zak. *Clin. Chim. Acta*, 20, 1968.

[28] K. Felgenhauer. *Biochem. Biophys. Acta*, 133, 1967.

[29] G. Ferro-Luzzi-Ames and K. Nikaido. *Biochemistry*, 15, 1976.

[30] Ö. Gaál, G. A. Medgyesi, and L. Vereczkey. *Electrophoresis in the Separation of Biological Macromolecules.* John Wiley and Sons, New York, 1980.

[31] Sean R. Gallagher and John A. Smith. *Current Protocols in Immunology*, chapter Section III, Chapter 8.4. National Institute of Health, 1991.

[32] B. Garfinkle. *Anal. Biochem.*, 38, 1970.

[33] C. Gelfi and P. G. Righetti. *Electrophoresis*, 2, 1981.

[34] I. P. Griffith. *Biochem. J.*, 126, 1972.

[35] Xuan-Hui Guo. *The Structure and Phase Transition of Protein-SDS Complexes in Solution and the Transport Mechanism in SDS-PAGE.* PhD thesis, Massachusetts Institute of Technology, June 1991.

[36] B. D. Hames and D. Rickwood. *Gel Electrophoresis of Proteins: A Practical Approach.* Oxford University Press, New York, second edition, 1990.

[37] Anne-Marie Hecht, Robert Duplessix, and Erik Geissler. Structural inhomogeneities in the range 2.5–2500 å in polyacrylamide gels. *Macromolecules*, 18, 1985.

[38] J. L. Hedrick and A. J. Smith. *Arch. Biochem. Biophys.*, 126, 1968.

[39] S. Hjerten. *J. Cromatogr.*, 11, 1963.

[40] S. Hjerten, S. Jerstedt, and A. Tiselius. *Anal. Biochem.*, 11, 1965.

[41] S. Hjerten, S. Jerstedt, and A. Tiselius. *Anal. Biochem.*, 27, 1969.

[42] S. C. Hodges and A. A. Hirata. *Clin. Chem.*, 30, 1984.

[43] T. Jovin, A. Chrambach, and M. A. Naughton. *Anal. Biochem.*, 9, 1964.

[44] E. Kaltschmidt and H. G. Witmann. *Anal. Biochem.*, 36, 1970.

[45] O. Kratky and G. Porod. *Rec. Trav. Chim. Pays–Bas*, 68, 1949.

[46] H. G. Kunkel and P. J. Slater. *Proc. Soc. Exp. Med.*, 80, 1952.

[47] H. G. Kunkel and A. Tiselius. *J. Gen. Physiol.*, 35, 1951.

[48] K. S. Lam and C. B. Kasper. *Anal. Biochem.*, 108, 1980.

[49] J. V. Maizel, Jr. *Science*, 151, 1966.

[50] J. Margolis and K. G. Kenrick. *Biochem. Biophys. Res. Commun.*, 27, 1967.

[51] J. Margolis and K. G. Kenrick. *Nature*, 221, 1969.

[52] J. Margolis and C. W. Wrigley. *J. Chromatogr.*, 106, 1975.

[53] L. J. Mets and L. Bogorad. *Anal. Biochem.*, 57, 1974.

[54] D. W. Miller and S. C. R. Elgin. *Anal. Biochem.*, 60, 1974.

[55] P. H. O'Farrell. *J. Biol. Chem.*, 250, 1975.

[56] Leonard Ornstein. *Annals of the New York Academy of Sciences*, 121, 1964.

[57] L. R. Orrick, M. O. J. Olson, and H. Busch. *Proc. Nat. Acad. Sci. USA*, 70, 1973.

[58] C. R. Parish and J. J. Marschalonis. *Anal. Biochem.*, 34, 1970.

[59] J. L. Peterson and E. H. McConkey. *J. Biol. Chem.*, 251, 1976.

[60] R. C. Peterson. *J. Pharm. Sci.*, 56, 1967.

[61] S. Raymond. *Clin. Chem.*, 8, 1962.

[62] S. Raymond and M. Nakamichi. *Anal. Biochem.*, 3, 1960.

[63] S. Raymond, M. Nakamichi, and B. Aursell. *Nature*, 195, 1962.

[64] S. Raymond and L. Weintraub. *Science*, 130, 1959.

[65] S. Raymond and Wang Yi-Ju. *Anal. Biochem.*, 1, 1960.

[66] U. Ringborg, E. Egyhazi, B. Daneholt, and B. Lambert. *Nature*, 220, 1968.

[67] J. Rittenhouse and F. Marcus. *Anal. Biochem.*, 138, 1984.

[68] A. L. Shapiro, E. Vinuela, and J. V. Maizel. *Biochem Biophys Res. Commun.*, 28, 1967.

[69] Duncan J. Shaw. *Electrophoresis.* Academic Press, New York, 1969.

[70] Larry R. Sherman and Jamese A. Goodrich. The historical development of sodium dodecyl sulphate-polyacrylamide gell electrophoresis. *Chemical Society Reviews*, 14(3):225–236, 1985.

[71] G. G. Slater. *Anal. Biochem.*, 24, 1968.

[72] I. Smith and J. B. Weiss. *J. Chromatogr.*, 28, 1967.

[73] O. Smithies. *Biochem. J.*, 61, 1955.

[74] O. Smithies. *Biochem. J.*, 71, 1959.

[75] J. T. Stoklosa and H. W. Latz. *Biochem. Biophys. Res. Commun.*, 58, 1974.

[76] M. Teubner and R. Strey. *J. Chem. Phys.*, 87, 1987.

[77] P. Tijssen and E. Kurstak. *Anal. Biochem.*, 128, 1983.

[78] A. Tiselius. *Biochem. J.*, 31, 1937.

[79] A. Tiselius. *Trans. Faraday Soc.*, 33, 1937.

[80] K. Tsujii and T. Takagi. *J. Biochem. (Tokoyo)*, 77, 1975.

[81] J. Vos and H. J. van der Helm. *J. Neurochem.*, 11, 1963.

[82] R. W. Wallace, P. H. Yu, P. J. Dieckert, and W. J. Dieckert. *Anal. Biochem.*, 61, 1974.

[83] K. Weber and M. Osborn. *J. Biol. Chem.*, 244, 1969.

[84] J. Wein. *Anal. Biochem.*, 31, 1969.

[85] D. L. Wilson, M. E. Hall, G. C. Stone, and R. W. Rubin. *Anal. Biochem.*, 83, 1977.

[86] B. J. Zimm. *J. Chem. Phys.*, 16, 1948.

[87] J. Zwaan. *Anal. Biochem.*, 21, 1967.